

Lateral Force Resistance for Shell Foundation

Guangjun Ou

A Thesis

in

The Department

of

Building, Civil and Environmental Engineering

Presented in Fulfillment of the Requirements

for the degree of Master of Applied Science (Civil Engineering) at

Concordia University

Montreal, Quebec, Canada

February 2021

@ Guangjun Ou, 2021

**CONCORDIA UNIVERSITY
SCHOOL OF GRADUATE STUDIES**

This is to certify that the thesis prepared

By: Guang Jun Ou

Entitled: Lateral Force Resistance for Shell Foundation

and submitted in partial fulfillment of the requirements for the degree of

Master of Applied science (CIVIL ENGINEERING)

complies with the regulations of the University and meets the accepted standards with respect to originality and quality.

Signed by the final Examining Committee:

	Chair
Dr. B. Li	
	Examiner
Dr. R. Ganesan	
	Examiner
Dr. G. J. Gouw	
	Supervisor
Dr. A. M. Hanna	

Approved by _____
Dr. M. Nokken Chair of Department or Graduate Program Director

_____ 2021 _____
 Dean of Faculty Dr. Mourad Debbabi

ABSTRACT

Lateral Force Resistance for Shell Foundation

Guangjun Ou

Shell foundation has been increasingly used around the world as an economic alternative to the traditional flat foundation. It provides higher bearing capacity and experience less settlement as compared to its counterpart flat foundation, these beside its high resistance to lateral pressure. The objective of this thesis is to highlight shell foundation superiorities in resisting horizontal loading and accordingly seismic condition.

A comprehensive analytical and numerical investigation were conducted. Analytically, a MATLAB code was generated to calculate the lateral resistance for shell and flat foundations. Numerically, a 2-D finite-element model was developed to examine the governing parameters affecting soil-shell structure interaction, using the commercial software “PLAXIS”. In this analysis the soil was modeled by the Mohr-Coulomb failure criteria, and the elastic perfectly plastic model. Mesh deformations, displacement vectors and failure points diagrams are presented.

The results of this study indicated that shell foundations are superior to resist higher lateral forces than the flat foundations, which may advance its use in seismic zones.

ACKNOWLEDGEMENTS

First and foremost, I appreciate the valuable guidance, understanding, inspiration and feedback from my supervisor, Professor Adel M. Hanna, under his supervision this research work was carried out. Dr. Hanna also provided me with his support and precious advice throughout the years, which helped me to cope with many problems in my life.

The financial supports received from NSERC and Concordia University are gratefully acknowledged.

Also, I wish to thank my friends for their encouragement, inspiration and comfort whenever I feel down.

Last but not least, my special gratitude to my parents and sister for their love, patience, encouragement, support and kindness throughout the course of my academic studies in Canada.

Table of Contents

List of Figures	vii
List of Tables	x
1. Introduction	1
1.1 General	1
1.2 Problem Statement	2
1.3 Aim of the Research	2
1.4 Scope of the Thesis	3
1.5 Organization of the Thesis	3
2. Literature Review	5
2.1 Background	5
2.2 Lateral Force in General	5
2.3 Review of Pervious Work	7
2.3.1 Theoretical and Experimental Investigations on Lateral Resistance	7
2.3.2 Theoretical and Experimental Investigations on Different Types of Shell Foundations.....	11
2.3.3 Finite Element Analysis on Different Types of Shell Foundations	14
2.4 Discussions	17
3. Analytical Study	18
3.1 General	18
3.2 Analytical Study Set Up	18
3.2.1 Comparative Study	18
3.2.2 Analytical Example	20
3.3 Analytical Analysis for the Strip, Pyramidal and Conical Shell Foundation and Flat Foundation	21
3.3.1 Case 1 for $a=0$	22
3.3.1-1 Analytical Analysis	24
3.3.1-2 Analytical Example	27
3.3.2 Case 2 for $0 < a < D$	30
3.3.2-1 Analytical Analysis	31
3.3.2-2 Analytical Example	33
3.3.3 Case 3 for $D < a < H$	40
3.3.3-1 Analytical Analysis for $D < a < h'$	42
3.3.3-2 Analytical Analysis for $h' < a < H$	50
3.3.3-3 Analytical Example	56
4. Numerical Modeling	76
4.1 General	76

4.2 Finite Element Model	76
4.3 Properties of Soil and Footings	77
4.4 Boundary Conditions	78
4.5 Process Calculation	78
4.6 Variables Considered	79
4.6.1 Shell Angle (α)	79
4.6.2 Embedment Ratio (a/D)	79
4.7 Verification of Finite Element Analysis	82
5. Conclusion and Recommendation	98
5.1 Conclusion	98
5.2 Recommendation	100
Reference	102
Appendix	106

List of Figures

Figure 1-1 Strip, Conical and Pyramidal shell footing models (From front to back)	1
Figure 1-2 Hyperbolic Paraboloidal Shell Footing Model	2
Figure 2-1 Failure of Retaining Wall: (a) by overturning; (b) by sliding	6
Figure 2-2 Failure mechanisms for shallow foundation with lateral loading	7
Figure 2-3 Square Footing Model	8
Figure 2-4 Actual Failure Mechanism	8
Figure 2-5 Force acting on the structure	9
Figure 2-6 Modeling an embedding post abutting a slab-on-grade	10
Figure 2-7 Responses of normal and shell foundation with and without reinforcement ..	15
Figure 3-1 Different Angle of Shell Foundation Models (2D & Axisymmetric)	19
Figure 3-2 3D Strip and Pyramidal Footing Models	22
Figure 3-3 3D Conical Shell and Circular Flat Footing Models	22
Figure 3-4 2D Flat and Shell Footing Models on Ground Level	22
Figure 3-5 Typical Values of Unit Weight for Soils	26
Figure 3-6 Lateral Friction Resistance of Conical/Strip/Pyramidal Shell Foundations on Surface of Sand Layer	29
Figure 3-7 Total Lateral Friction Resistance of Conical/Strip/Pyramidal Shell Foundations with Various Shell Angles when $a/B=0$	30
Figure 3-8 2D Flat and Shell Foundation Model when $a=D$	30
Figure 3-9 Passive Earth Pressure with Various Shell Angles when $a<D$	35
Figure 3-10 Overturning Moment Resistance due to Passive Earth Pressure with Various Shell Angles in Different Embedment Ratio when $a<D$	35
Figure 3-11 Total Lateral Friction Resistance of Conical Shell Foundations with Various Shell Angles when $a<D$	36
Figure 3-12 Total Lateral Friction Resistance of Strip Shell Foundations with Various Shell Angles when $a<D$	37
Figure 3-13 Total Lateral Friction Resistance of Pyramidal Shell Foundations with Various Shell Angles when $a<D$	37
Figure 3-14 Total Overturning Moment Resistance with Various Shell Angles in Different Embedment Ratio when $a<D$	38
Figure 3-15 Total Lateral Friction Resistance of Conical/Strip/Pyramidal Shell Foundations with Various Shell Angles when $a/B=1/6$	39
Figure 3-16 Total Lateral Friction Resistance of Conical/Strip/Pyramidal Shell Foundations with Various Shell Angles when $a/B=1/6$	39
Figure 3-17 2D Shell Foundation Model, when $D < a < h'$	40
Figure 3-18 Flat Foundation, Left $D \leq a \leq H$ and Right $0 \leq a \leq D$	41
Figure 3-19 2D Shell foundation Model, when $h' < a < H$	48

Figure 3-20 Passive Earth Pressure of Conical/Pyramidal Shell Foundations with Various Shell Angles in Different Embedment Ratio when $a>D$	62
Figure 3-21 Passive Earth Pressure of Strip Shell Foundations with Various Shell Angles in Different Embedment Ratio when $a>D$	62
Figure 3-22 Passive Earth Pressure of Conical/Pyramidal/Strip Shell Foundations with Various Shell Angles in Different Embedment Ratio when $a>D$	63
Figure 3-23 Total Lateral Friction Resistance of Conical Shell Foundations with Various Shell Angles in Different Embedment Ratio when $a>D$	64
Figure 3-24 Total Lateral Friction Resistance of Strip Shell Foundations with Various Shell Angles in Different Embedment Ratio when $a>D$	64
Figure 3-25 Total Lateral Friction Resistance of Pyramidal Shell Foundations with Various Shell Angles in Different Embedment Ratio when $a>D$	65
Figure 3-26 Total Lateral Friction of Conical/Strip/Pyramidal Shell Foundations with Various Shell Angles in Different Embedment Ratio when $a>D$	65
Figure 3-27 Overturning Moment due to Passive Earth Pressure for Strip Shell Foundations with Various Shell Angles in Different Embedment Ratio when $a>D$	66
Figure 3-28 Overturning Moment due to Passive Earth Pressure for Conical/Pyramidal Shell Foundations with Various Shell Angles in Different Embedment Ratio when $a>D$	67
Figure 3-29 Overturning Moment due to Passive Earth Pressure for Conical /Pyramidal /Strip Shell Foundations with Various Shell Angles in Different Embedment Ratio when $a>D$	68
Figure 3-30 Overturning Moment due to Weight of Footing and Weight of Soil above Footing Conical/Pyramidal/Strip Shell Foundations with Various Shell Angles in Different Embedment Ratio when $a>D$	68
Figure 3-31 Total Overturning Moment Resistance for Conical Shell Foundations with Various Shell Angles in Different Embedment Ratio when $a>D$	70
Figure 3-32 Total Overturning Moment Resistance for Conical Shell Foundations with Various Shell Angles in Embedment Ratio Between 11/15 to 14/15	70
Figure 3-33 Total Overturning Moment Resistance for Strip Shell Foundations with Various Shell Angles in Different Embedment Ratio when $a>D$	71
Figure 3-34 Total Overturning Moment Resistance for Strip Shell Foundations with Various Shell Angles in Embedment Ratio Between 11/15 to 14/15	71
Figure 3-35 Total Overturning Moment Resistance for Pyramidal Shell Foundations with Various Shell Angles in Different Embedment Ratio when $a>D$	72
Figure 3-36 Total Overturning Moment Resistance for Pyramidal Shell Foundations with Various Shell Angles in Embedment Ratio Between 11/15 to 14/15	72
Figure 3-37 Total Overturning Moment Resistance for Conical/Strip/Pyramidal Shell Foundations with Various Shell Angles in Embedment Ratio Between 7/30 to 14/15	73
Figure 3-38 Self-Weight of Shell Foundations with Various Angle	74

Figure 3-39 Weight of Back Filled Soil Below the Footing with Various Angle	74
Figure 3-40 Weight of Back Filled Soil Above the Footing with Various Angle	75
Figure 4-1 Finite Element Meshes for Flat Foundations with Various Embedment Ratio	80
Figure 4-2 Finite Element Meshes for 21.8° Shell Foundation with Various Embedment Ratio	81
Figure 4-3 Finite Element Meshes for 38.66° Shell Foundation with Various Embedment Ratio	81
Figure 4-4 The Comparison Between Analytical and Numerical Models	83
Figure 4-5 Finite Element Displacement Vectors for Flat Foundations with Various with Embedment Ratio	85
Figure 4-6 Finite Element Displacement Vectors for 21.8° Shell Foundations with Various Embedment Ratio	86
Figure 4-7 Finite Element Displacement Vectors for 38.66° Shell Foundations with Various Embedment Ratio	88
Figure 4-8 Finite Element Displacement Vectors for Flat Foundations with Various Embedment Ratio	90
Figure 4-9 Finite Element Displacement Vectors for 21.8° Shell Footings with Various Embedment Ratio	91
Figure 4-10 Finite Element Displacement Vectors for 38.66° Shell Footings with Various Embedment Ratio	92
Figure 4-11 Displacement Vectors at Failure Load (M_{max}) with Zero Horizontal Displacement	93
Figure 4-12 Finite Element Total Displacement Vectors for Various Footings with Embedment Ratio=5/6	94
Figure 4-13 Finite Element Displacement Vectors for Flat Foundations with Various Embedment Ratio	95
Figure 4-14 Finite Element Displacement Vectors for 21.8° Shell Footings with Various Embedment Ratio	96
Figure 4-15 Finite Element Displacement Vectors for 38.66° Shell Footings with Various Embedment Ratio	97

List of Tables

Table 1-1 Content of Thesis	3
Table 3-1 Soil and Foundation Geometrical Data	21
Table 3-2 Results of Sliding and Moment Resistance for Strip/Pyramidal Shell and Square Flat Foundations when $a/B = 0$	27
Table 3-3 Results of Sliding and Moment Resistance for Conical Shell and Circular Flat Foundations when $a/B = 0$	28
Table 3-4 Results of Sliding and Moment Resistance for Strip/Pyramidal Shell and Square Flat foundations when $a/B = 1/6$	33
Table 3-5 Results of Sliding and Moment Resistance for Conical Shell and Circular Flat Foundations when $a/B=1/6$	34
Table 3-6 Results of Sliding and Moment Resistance for Strip/Pyramidal Shell and Square Flat Foundations when $a/B=1/2$	57
Table 3-7 Results of Sliding and Moment Resistance for Conical Shell and Circular Flat Foundations when $a/B=1/2$	58
Table 3-8 Results of Sliding and Moment Resistance for Strip/Pyramidal Shell and Square Flat Foundations when $a/B=11/15$	58
Table 3-9 Results of Sliding and Moment Resistance for Conical Shell and Circular Flat Foundations when $a/B=11/15$	59
Table 3-10 Results of Sliding and Moment Resistance for Strip/Pyramidal Shell and Square Flat Foundations when $a/B=14/15$	60
Table 3-11 Results of Sliding and Moment Resistance for Conical Shell and Circular Flat Foundations when $a/B=14/15$	60
Table 4-1 Material Parameters for PLAXIS 2D	77
Table 4-2 Load Resistance Between Analytical and Numerical Models when $a/B =1/3$..	82
Table 4-3 Load Resistance Between Analytical and Numerical Models when $a/B =1/2$..	82
Table 4-4 Load Resistance Between Analytical and Numerical Models when $a/B =2/3$..	83
Table 4-5 Load Resistance Between Analytical and Numerical Models when $a/B =5/6$..	83

CHAPTER 1

Introduction

1.1 General

Foundation design necessitates two different studies: one deals with the bearing capacity of the soil under the foundation; the second is concerned with the foundation settlements due to soil compressibility. Shell foundations were introduced in early fifties as cost-effective alternatives to plain shallow foundations, which have become more popular in Mexico, China, and several European countries. Compared with conventional flat shallow foundations, shell foundations required less materials to achieve an equivalent ultimate bearing capacity due to its thin structures. Since shells are structurally more efficient, it becomes an advantage in a situation involving heavy superstructure loads transmitted to weaker soils. Moreover, different geometric characteristics enable them to perform more efficiently in different situations. Although shell footings are borrowed from various shell roof designs, only a few geometries and types can be used in foundations.

Figure 1-1 and Figure 1-2 present model shell foundation, which were tested in Concordia University.

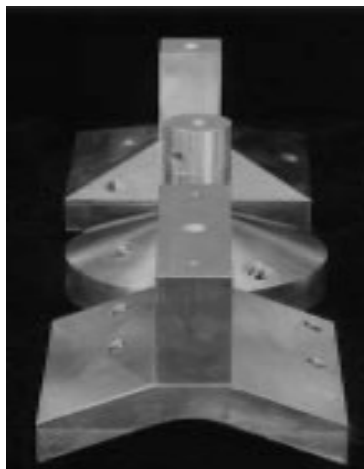


Figure 1-1. Strip, Conical and Pyramidal shell footing models (From front to back), (Hanna & Abdel-Rahman, 1998)

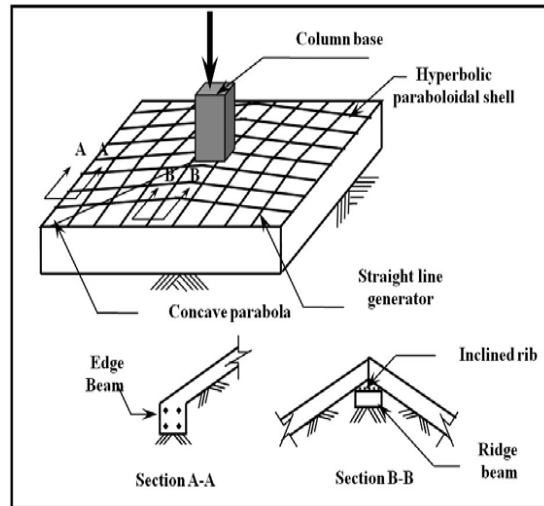


Figure 1-2. Hyperbolic Paraboloidal Shell Footing Model, (Aziz, Al-Azzwai & Al-Ani, 2011)

1.2 Problem Statement

Since Candela poured the first shell foundation on the Mexican soil in 1963, much research was focused on two categories: geotechnical performance and structural performance of shells as foundations. The studies of shell configuration and embedment depth on the ultimate bearing capacity and settlement (Hanna & Abdel-Rahman, 1998) and the contact pressure distribution (Abdel-Rahman & Hanna, 2003) can be categorized as the geotechnical performance. The report of Conical Shell Foundations Composed of Reactive Powder Concrete (Fattah, Waryosh, & Al-Hamdani, 2015), can be categorized as structural performance. However, most of the report found in the literature were considering only the performance of shell foundations subjected to vertical force, ignoring the earth pressure and the horizontal loading from the structure.

1.3 Aim of the research

This thesis presents analytical and numerical models for various shell and flat foundations subjected to lateral loading. The lateral force design on retaining walls, Rankine passive earth pressure, safety against overturning, and sliding-based theories will be presented

herein. Furthermore, comparative analysis demonstrating that shell foundations have higher lateral load and overturning moment resistance than the equivalent flat ones.

1.4 Scope of the thesis

The objectives of this thesis are:

1. To develop analytical models to predict the static lateral force acting on different types of shell foundations, viz strip, pyramidal and conical shell foundation on a homogenous sandy soil.
2. To conduct parametric studies on the factors, govern the performance of these foundation, such as the embedment depth to base width ratio (a/B), the peak angle of shell footing (α), and to investigate the factors, which influence the stability of those footings.
3. To develop a 2-D numerical model to simulate these foundations using the commercial software “PLAXIS”.
4. To conduct comparative analysis with shell and flat foundations subjected to the same conditions, where conclusion was drawn.

1.5 Organization of the thesis

The thesis has been organized in the following Table 1, which outlined sequentially into chapter, titles and descriptions.

Table 1-1. Content of Thesis

Chapter	Titles	Description
1	Introduction	This chapter includes an introduction, problem statement, aim of the research, objective of the research and the structure of the research.

2	Literature Review	This chapter introduces and reviews the research that related to the thesis, provided information on theories, models and technique. Moreover, it also includes some information that relatives to the research relative to bearing capacity on different types of shell foundation.
3	Analytical Study	This chapter presents detail analytical analysis for strip, Pyramidal, and conical shell footings versus flat footing. Analytically, a MATLAB code was generated to calculate the lateral resistance for shell and flat foundations
4	Numerical Model	This chapter presents a 2-D finite-element model developed by the commercial software “PLAXIS” to examine the governing parameters that affect the soil-shell structure interaction.
5	Conclusion and Recommendation	This chapter presents a summary of the results obtain from the present investigation and discussions. This chapter also places recommendations for future work.
	References	List of references
	Appendix	MATLAB code

CHAPTER 2

Literature Review

2.1 Background

In this chapter, a comprehensive review is carried out by gathering past research related to lateral force theory and providing information on theories, models, and techniques. Moreover, this chapter also reviewed the geotechnical and structural properties of various foundations (conventional and alternative foundation) under different circumstances.

2.2 Lateral force in general

The most common types of lateral load are wind load, seismic load, water pressure, and earth pressure. The dynamic effects of wind and seismic load are usually considered equivalent to static loads in most small or medium-size buildings (Luebkeman & Peting, 1995,1996).

Furthermore, underground water and earth pressure can be regarded as either supporting or exerting force on the below-ground structure, such as shallow foundation, and its pressure increase with the depth.

Das (2007, Chapter 8), suggested using Rankine active/passive pressure theory to calculate the magnitude of earth pressure, which causes an overturning moment. These besides, he recommended a minimum value for the safety against overturning and against sliding as 2 to 3 and 1.5 to 2, separately. Moreover, most cases of the range of interface friction angle between concrete and soil are $1/2$ to $2/3$ times of soil friction angle.

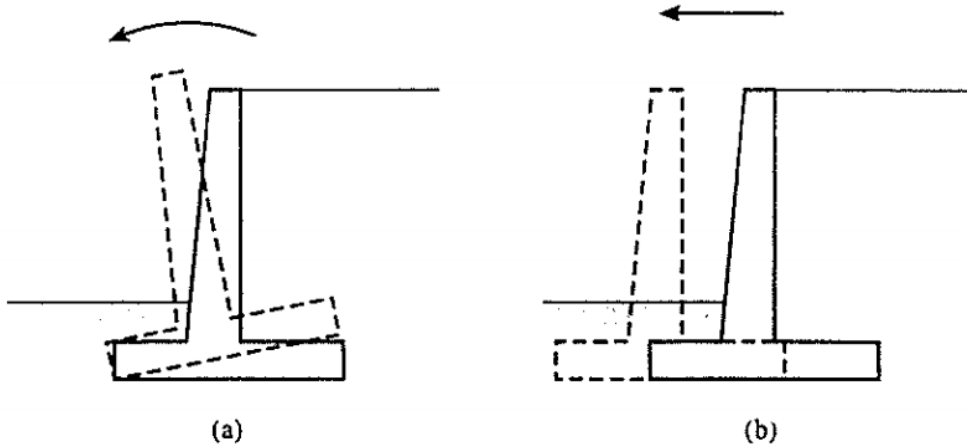


Figure 2-1. Failure of Retaining Wall: (a) by overturning; (b) by sliding (Das, 2007)

Figure 2-1 presents, the mechanisms of lateral load resistance for a shallow foundation are similar to the lateral load resistance mechanisms for retaining wall. Therefore, the methods of calculating the lateral load resistance for retaining wall can be adapted to calculate lateral load resistance for the shallow foundation.

An assumption of lateral load resistance for shallow foundations is commonly considered as the combination of sliding friction along the base of the footing and passive earth pressure acting on the embedded foundation elements. Nevertheless, the actual mechanisms of lateral load resistance for shallow foundations are complex. Clough and Duncan (1991) provided three possible failure mechanisms, viz “Wedge Failure”, “Flow-Under Failure”, and “Tip-to-Top Failure”, as shown in Figure 2-2.

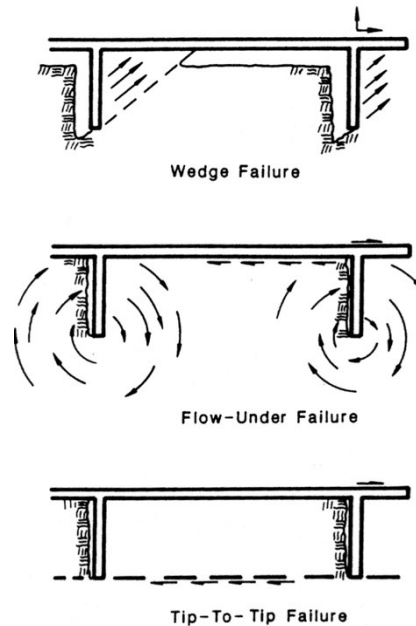


Figure 2-2. Failure mechanisms for shallow foundation with lateral loading (Clough & Duncan, 1991)

According to their study, the “Wedge Failure” is based on the classical Rankine passive earth pressure theory. It also shows the incompatibility between the mechanisms of sliding friction and passive earth resistance. The “Flow-Under Failure” is only suitable for very soft soil, and the “Tip-to-Top Failure” usually occurs when the foundation beams are close together.

2.3 Review of Previous Work

2.3.1 Theoretical and Experimental Investigations on Lateral Resistance

Gadre and Dobry (1998) were interested in how base shear, active/passive forces, and shearing sides influence a square embedded footing's total lateral response. Thus, performed seven cyclic lateral loading centrifuge tests on embedded foundations with different parameters, viz stiffness, damping (both radiation and material damping components), and ultimate lateral capacity, to evaluate the contribution of the base, shearing sides, and active/passive sides of the foundation to the total lateral response. The various forces contributing to the lateral resistance and test model showed in Figure 2-3.

For all the tests, there is little interaction between the stiffness contribution of the base, shearing sides, and active/passive sides of the foundation; additionally, for all parameters measured in these models, the passive side's contribution accounts for more than half of the total.

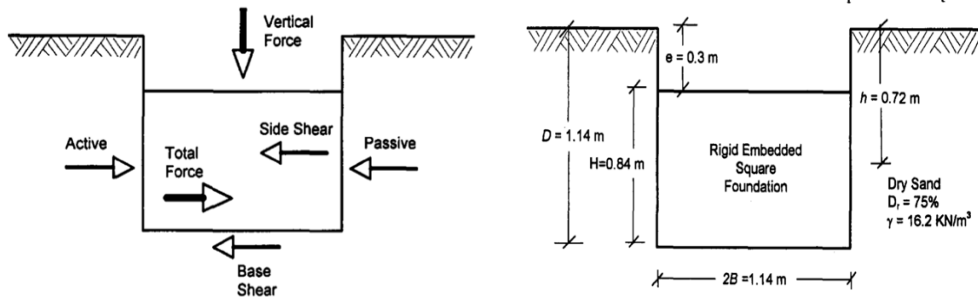


Figure 2-3. Square Footing Model (Gadre & Dobry, 1998)

McManus and Burdon (2001) studied two different combinations of foundations (“slab-on-grade” and “slab built on foundation beam”) to understand the lateral resistance mechanisms of shallow foundations and the interaction between the passive resistance to lateral movement, respectively. The results revealed that the actual failure mechanism under lateral loading was similar to the “Wedge Type” with significant passive pressure against the foundation beams' vertical face, which caused one side of the structure to be lifted vertically, as shown in Figure 2-4. Furthermore, analysis predicted that lateral load capacity was highly sensitive to the eccentricity of the applied lateral load.

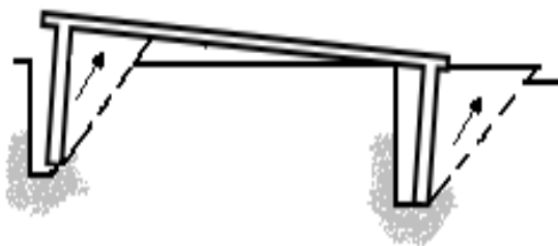


Figure 2-4. Actual Failure Mechanism (McManus & Burdon, 2001)

The formula for calculating passive earth pressure also was given as:

$$R_1 = R_3 = 0.5K_p\gamma h^2 L$$

$$R_2 = R_5 K_p$$

$$R_6 = \frac{(R_1 + R_3)\left(1 + \frac{2h}{3e}\right) - W\left(\frac{o}{e} - \frac{s}{2e} - K_p\left(1 + \frac{h}{2e}\right)\right)}{\frac{s}{e} - \tan\phi_g\left(1 + \frac{h}{e}\right) - \frac{o}{e} + K_p\left(1 + \frac{h}{2e}\right)}$$

Where:

$$W = R_5 + R_6$$

$$R_5 = o = \frac{h}{2} \tan\left(45^\circ + \frac{\phi_b}{2}\right) + \frac{b}{2}$$

$$K_p = \frac{1 + \sin\phi_b}{1 - \sin\phi_b}$$

$$R_4 = R_6 \tan\phi_g$$

ϕ_b is the internal friction angle of backfill material, ϕ_g is the interface friction angle between the base of the foundation beam and subgrade and L is the length of the foundation beam.

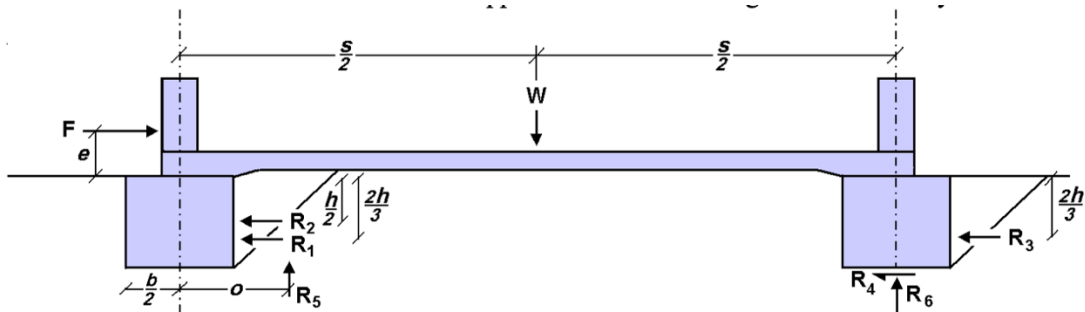


Figure 2-5. Force acting on the structure (McManus & Burdon, 2001)

Bohnhoff (2015) presented the theory and assumptions inherent in developing equations and methods for lateral movement and embedded piers and posts' lateral strength capacity.

Ultimate Lateral Soil Resistance P_u :

$$P_{u,z} = 3\sigma'_{v,z}K_p + \left(2 + \frac{z}{b}\right) cK_p^{0.5} \quad \text{for } 0 \leq z \leq 4b$$

$$P_{u,z} = 3(\sigma'_{v,z}K_p + 2cK_p^{0.5}) \quad \text{for } z \geq 4b$$

Where c is the soil cohesion, b is the face width of foundation at the groundline, $\sigma'_{v,z}$ is the effective vertical stress and K_p is the coefficient of passive earth pressure.

During the developing formula of the bending moment and shear force for embedded post/pier foundation in the universal method, Bohnhoff introduced a model of soil behavior called soil springs, such shown in Figure 2-6.

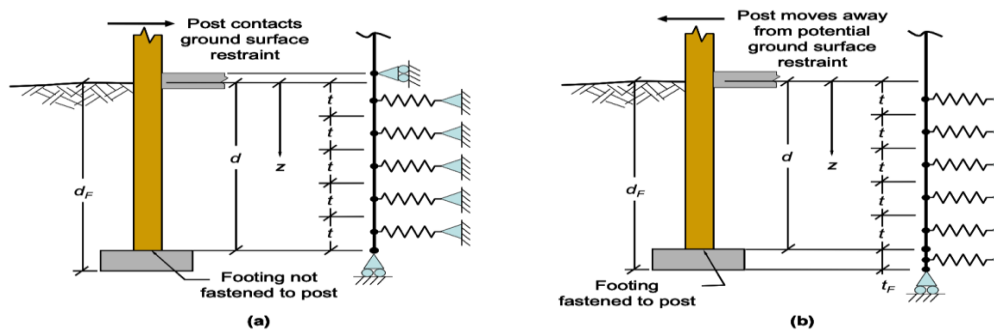


Figure 2-6. Modeling an embedding post abutting a slab-on-grade when the post moves (Bohnhoff, 2015)

Minami (n.d.) used a series of laboratory tests and field tests to investigate the shell foundation's performance under earthquake situation. Based on laboratory tests, results showed that shell foundations have a higher bearing capacity and more economy than a flat foundation; additionally, bearing capacity increased with larger area-ratio or length-ratio. Under the inclined loading, the shell foundation provided more excellent stability to the construction by preventing overturning.

Shoukath and Rajesh (2017) investigated the seismic performance of the inverted spherical and hyperbolic paraboloid shell foundation by varying the shell's rise with different contact conditions. The test is simulated by a finite element software called ANSYS 16.1. The significant conclusions obtained from the study are that shell footings show perfect soil-structure interaction and better performance under seismic conditions. Furthermore, a hyper shell with a 0.5 to 0.6 ratio of f/a and inverted spherical shell with a ratio of less than 0.4 have smaller percentage settlement.

2.3.2 Theoretical and Experimental Investigations on different types of shell foundations

In 1990, Hanna and EI-Rahman adapted the ultimate bearing capacity as function to contain the friction angle of sand ϕ and the peak angle of the foundation θ , and modified bearing capacity coefficients N_{ct} , N_{qt} , and N_{yt} to calculate the ultimate bearing capacity of shell foundations based on the results of laboratory model tests for triangular shell foundations. In 1998, Hanna & Abdel-Rahman investigated various shell foundations' geotechnical performances, which included triangular strip, conical and pyramidal shell foundation, by studying the influence of sand, embedment ratio (D/B), and the rise-to-half width ratio (a/b). The results deduced that shell foundations have better settlement characteristics and higher bearing capacity than the conventional flat ones. Besides, the bearing capacity increases with an increase of shell angle. Furthermore, they also conducted that shell foundations provide higher resistance to lateral loading as compared with flat ones. In 2003, Abdel-Rahman & Hanna extended their work to investigate the contact pressure distribution between soil and various foundations. The results can conclude the following points. First of all, the contact pressure increased almost linearly but has a curvature at the ultimate stage. Besides, the smaller the domain's size, the less the variation of the contact pressures over the footing base. Furthermore, the maximum contact pressure occurs at/or near the edge of the flat strip and triangular shell footings and at the center for the square flat and pyramidal shell footings.

Esmaili & Hataf (2008) introduced a shell factor (SF), representing the effect of shell configuration on ultimate load capacity, to investigate the ultimate bearing capacity of different shell foundations on reinforced and unreinforced sand. In the experimental tests, eight types of footing models, viz three types of conical, pyramidal shell foundations, and two types of flat foundations, were tested to understand the influence of foundation thickness to capacity on reinforced and unreinforced sand. They developed a unique

relation to representing the variations of the ultimate load capacity of shell foundations to their flat counterparts' ratio ($Q_{u\ shell}/Q_{u\ flat}$) for SF.

$$\frac{Q_{u\ shell}}{Q_{u\ flat}} = 0.812SF^2 - 0.0777SF + 1$$

where

$$SF = 1 - \frac{a'}{A'}$$

a' is the area of the flat portion of the base of she and flat foundation

A' is the base area of counterpart circular and square foundation

According to the results, the ultimate load capacity for conical and pyramidal shell foundations on reinforced sand is greater than that for unreinforced sand; additionally, if decreasing the shell factor (SF), the behavior of the shell foundation gets closer to that for flat foundation and the ultimate load capacity decreases.

In 2015, Fattah et al. conducted 38 laboratory tests to investigate the behavior of reactive powder concrete (RPC) conical shell foundation with and without a ring beam by using different fraction values of steel fiber and silica fume. The tests results indicated that adding steel fibers and ring beam would significant enhanced ductility, stiffness and the ability of absorbed energy for RPC footings, respectively. The load carrying capacity of shell footing was found to increase when the content of the steel fibers or silica fume or the ratio of height to radius (f/r_2) was increased. A month later (July 2015), Fattah et al. extended their work from laboratory tests to theoretical study. Based on the membrane theory, they investigated the effect of the ratio of height to the radius, ring beams, and the applied load's eccentricity on shell foundations' behavior. The theoretical results are roughly consistent with the experimental results.

Rinaldi, Abdel-Rahman and Hanna (2017) conducted a laboratory test, which applying monotonic load on scaled models of inverted/upright triangular shells and flat foundation in variable soil conditions and introduced the Shell Efficiency factor (η_{is}) and the

Settlement factor ($F_{\delta(is)}$) to analyze and predict the influence shell angle and the quality of the concrete material to the performance of shell footings.

$$\eta_{is} = \left(\frac{Q_{is} - Q_f}{Q_{us} - Q_f} \right)_u$$

$$F_{\delta(is)} = \left(\frac{\delta \gamma A_p}{Q_u} \right)_u$$

Where:

η_{is} is shell efficiency factor, Q_{is} is failure load for inverted shell model (kN), Q_f is failure load for flat model (kN), Q_{us} is ultimate load for shell model (kN) and $F_{\delta(is)}$ is settlement factor $\delta(is)$'s settlement (mm).

The experiment results showed that shell footings' performance depends on the shape of the shell used, inducing a shell-soil interface primarily based on shell angle and the quality of the concrete material employed. Besides, inverted shells have a higher load-carrying capacity than flat or upright shell foundation. The contact pressure indicates a tendency for edge concentrations in the elastic stages of loading.

Mohammed, Singh and Pandey (2018) designed hyperbolic and conical shell footings to investigate shell foundations' structural efficiency and economy compared with sloped square footing. The problem is analyzed by calculating the size of the concrete mass and reinforcing the steel area according to code IS 9456-1980 and design requirements. The data obtained through this study is analyzed with data from previous studies to illustrate the shell foundation's economic and engineering efficiency. The results found that hyperbolic and conical shell foundations consume fewer materials than the conventional footing, which hyperbolic 48.1%, conical 41%, and gives the greater load capacity and stability over the conventional footing.

2.3.3 Finite element analysis on different types of shell foundations

Huat and Mohammed (2006) used a non-linear finite element analysis code called PLAXIS to investigate the influence of adding various edge beams at the bottom of the footing and depth of embedment of the footings load-carrying capacity of the footing. Since the structures were symmetrical, therefore only one half of the cross-section passing through the axis of symmetry of the footing is considered. Unlike other studies, they employed the Mohr-Coulomb model as a soil model instead of a linear Winker and Pasternak soil model. The soil and the footing were modeled using 15-noded linear strain quadrilateral elements 'LSQ' with quadratic variations for the displacement along the element's sides; the nodes along the bottom and both sides of the section are considered as pinned supports. The FE analysis showed a reasonably good agreement with the experimental laboratory results, with a discrepancy of 11 to 25%. The results found that adding edge beams at the bottom and increasing the embedment ratio would increase the footing's load-carrying capacity.

Azzam and Nasr (2015) conducted laboratory tests using different sand densities and different embedment ratios (a/B) to investigate the geotechnical behavior of strip shell foundation on unreinforced and reinforced sand layers. The model test results (the failure pattern and stress behavior), shown in Figure 2-7, were verified using the plain strain elastoplastic finite element analysis program called PLAXIS. The Shell Efficiency factor (η) and the Settlement factor (F_d) were also introduced. Nevertheless, the equation of the shell efficiency factor was slightly different from the one mentioned above (Rinaldi et al., 2017).

$$\eta = \frac{Q_{us} - Q_{uf}}{Q_{uf}}$$

Where

Q_{us} is ultimate load of shell footing; Q_{uf} is ultimate load of flat footing.

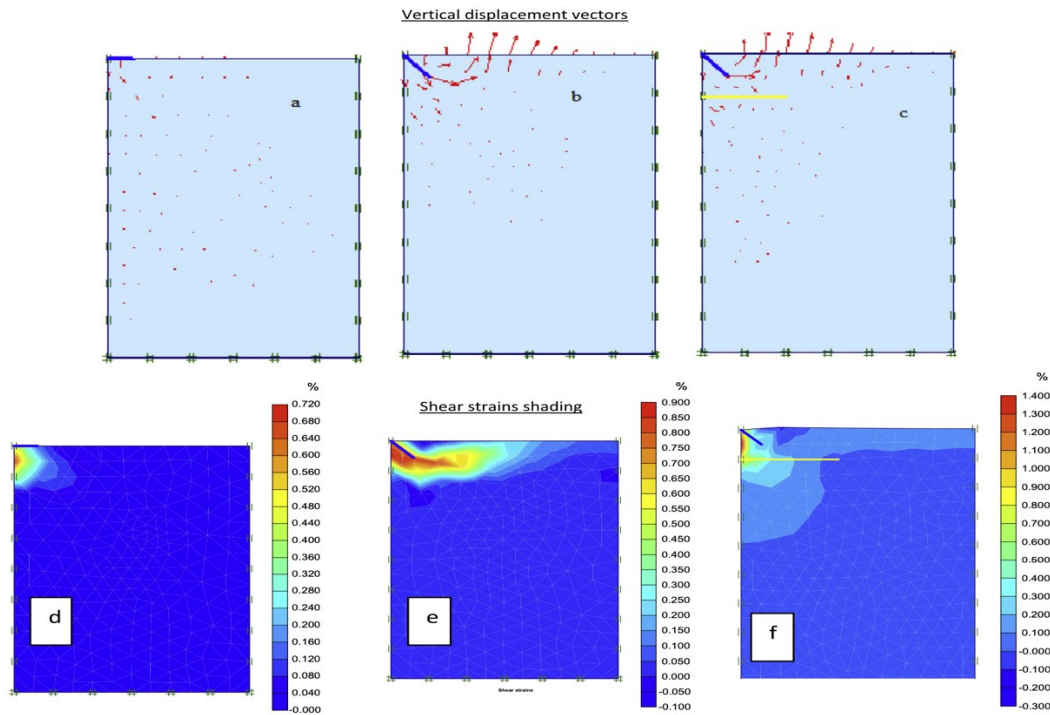


Figure 2-7. Responses of normal and shell foundation with and without reinforcement (Azzam & Nasr, 2015)

The experiment results indicated that the shelling efficiency and bearing capacity increase with the increase of embedment depth. Moreover, the increase in the angle of shear resistance of the subgrade for reinforced shell foundation reduces the settlement and increases shell efficiency. The reinforcement can increase the bearing capacity by significantly changing the collapse pattern's geometry, preventing the mechanism from reaching deep into the soil.

Thilakan and Naik and (2015) used the finite element code, named Optum G2, to simulate shell strip surface footings on single layer sand. They employed the various Mohr-Coulomb model as a soil model, viz MC-Loose, MC-Medium, and MC- dense, to study the strip shell foundation's geotechnical behavior. Two configurations of triangular strip models were considered by varying the rise (a) to half-width (b). Besides, 6-noded triangular Gaussian elements were adopted for the finite element analysis. The results indicated that strip shell footings have higher load carrying capacity and lower settlement than flat footings. The

shell with a higher rise exhibited a higher load-carrying capacity than the shell with a lower rise.

Krishnan, Sivapriya and Nagarajan (2017) used a 2-D finite element code called PLAXIS to simulate the HYPAR shell foundation on medium dense sand and investigate the influence of various edges beams size and embedment ratios to the bearing capacity and settlement of the footing. In this study, the 15-noded meshes were generated under the plane strain model with undrained soil behaving with Mohr-Coulomb properties and the footing behaving as an elastic element. In general, increasing the edge beam width as opposed to depth greatly improves the load bearing and settlement characteristics. The maximum load-bearing characteristics were observed in shells with full embedment, with a reduction in load-bearing ability with a decreasing embedment ratio.

Hassan, Al-Soud and Mohammed (2018) conducted laboratory tests to investigate the influence of various peak angles of pyramidal shell foundation models to capacity on reinforced and unreinforced sand. The experiment results were verified using a computer program named ABAQUS. The soil model has used the Drucker-Prager model with different sand densities, namely 15%, 20% and 30%. The load-settlement curves indicated that the values of numerical analysis are close to those of laboratory test models. In addition, the bearing capacity ratio (BCR), the settlement reduction factor (SRF), the Shell Efficiency factor (η) and the Settlement factor (F_d) were introduced during the comparison.

$$BCR = \frac{q_R}{q}$$
$$SRF = \frac{S_R}{S}$$

Where

q_R is ultimate load for the foundation rest on reinforced layer, q is ultimate load for the foundation rest on unreinforced layer, S_R is the settlement for the foundation rest on reinforced layer and S is the settlement for the foundation rest on unreinforced layer.

The experiment results indicated that the shell efficiency increases with increasing shell angle. Besides, BCR increases and SRF reduces with increasing the top geogrid depth (u).

2.4 Discussions

Despite all the previous work to gain a better understanding of the use of geometric and structural performance on different types of shell foundations, there is less research on the lateral force acting on shell foundations.

According to the literature review, all the previous work supports that embedment depth, peak angle, and thickness of shell footing significantly influence the bearing capacity and settlement of shell foundation. Furthermore, adding beam, using better material or reinforcing soil layer under the shell footing could help shell foundations to gain a higher bearing and lower settlement. Therefore, these factors should be properly taken into consideration when investigating the lateral resistance of the shell foundation.

CHAPTER 3

Analytical Study

3.1 General

A comprehensive analysis of strip, pyramidal and conical shell and flat foundations on a homogenous sand layer was conducted in this chapter. Two factors were employed in the study, viz a variety of peak shell angle of footings and different embedded depths, to investigate how these factors affect the ability of shell foundations to resist lateral forces. Moreover, a MATLAB code was generated to calculate the lateral resistance for 3x3 m and 0.5 m thick of shell and flat foundations as examples to verify the prediction from comparative studies. ($D=0.5\text{m}$, $H=6D$, $B=6D$, $b=D$, $a=y \times D$ where $y=\text{fraction}$)

3.2 Analytical Study Set Up

3.2.1 Comparative Study

A comparative study was conducted based on equations that were used to calculate the sliding resistance and overturning moment of the retaining wall.

The resistance to lateral loading was analyzed for three types of square shell foundation, viz strip, pyramidal and conical shell models. Additionally, the influence of changes in the shell angle (α) from 0 to 90 degrees and the embedment ratio (a/B) on lateral loading resistance was examined. In this research, the flat footing is regarded as a shell footing with a shell angle equal to 0-degree, as the schematic sketch presented in Figure 3-1 (a). In this analysis sliding resistance along the base of the footing, passive earth pressure and overturning moment resistances were determined for surface embedded footings.

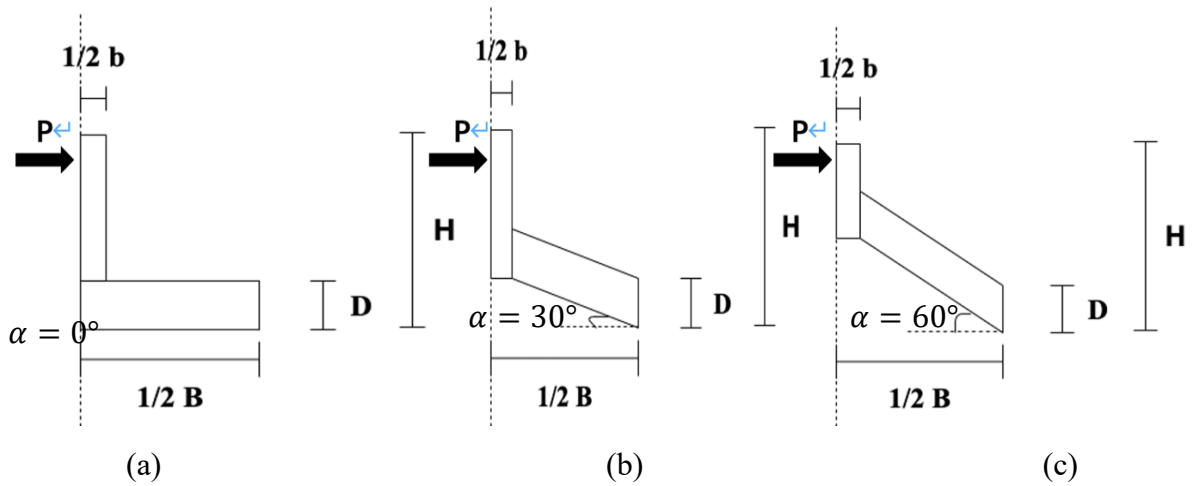


Figure 3-1. Different Angle of Shell Foundation Models (2D & Axisymmetric)

Sliding Resistance

Das (2007) presented a general formula (3-1) that can use to calculate the total resistance of the foundation to sliding.

$$F_f = F_w + F_p \quad (3-1)$$

Where:

F_f : total resistance to sliding

F_w : friction at the base of footing

F_p : passives earth pressure

$$F_w = CB + \sum W \times \tan\phi \quad (3-2)$$

Where:

B : the width of the foundation

C : soil cohesion

ϕ : the angle of friction,

$\sum W$: self-weight of footing plus weight of backfilled soil above and below the footing

Based on Rankine passive earth pressure theory (1857)

$$F_p = P_{passive} \quad (3-3)$$

$$\sigma_h = \sum \sigma_v K_p + 2C\sqrt{K_p} \quad (3-4)$$

$$K_p = \frac{1+\sin\phi}{1-\sin\phi} \quad (3-5)$$

Where:

σ_h : total horizontal stress

σ_v : total vertical stress

C : soil cohesion

K_p : Coefficient of passive earth pressure

Overturning moment due to the horizontal passive earth pressure and self-weight of footing plus the soil's weight above the footing can be written as.

$$RM_1 = P_{passive} \times l_{arm} \quad (3-6)$$

$$M_{self-weight} = (W_{footing} + W_{soil\ above}) \times l_{arm} \quad (3-7)$$

Where:

l_{arm} : the moment arm measured from point C

If the foundation rest on a homogenous non-cohesive soil layer, soil cohesion $C \approx 0$. In this case, formular (3-2) and (3-4) can be simplified as:

$$F_w = \sum W \times \tan\phi \quad (3-8)$$

$$\sigma_h = \sum \sigma_v K_p \quad (3-9)$$

3.2.2 Analytical Example

In order to verify the accuracy of the above analysis, Excel and MATLAB were used to simulate all the scenarios. The following Table 3-1 contains all the soil and foundation geometrical data. The factor of safety for sliding and for overturning moment are equal to 2 and 3, respectively.

$$F_{f\ allow} = \frac{F_{fu}}{\text{Safety Factor}} \quad (3-10)$$

$$RM_{allow} = \frac{RM_u}{\text{Safety Factor}} \quad (3-11)$$

Table 3-1. Soil and Foundation Geometrical Data

Foundation Geometrical Data		Soil Geometrical Data	
Unit Weight of Concrete, γ_c	24 kN/m ³	Unit Weight of Soil, γ_s	17 kN/m ³
Height of Foundation, H	3 m	Friction Angle of soil, ϕ	30 degrees
Thickness of Foundation, D	0.5 m	Soil Cohesion, C	≈ 0 kPa
Width of Foundation, B	3 m	Peak Angle of Shell, α	Various
Width of Column, b	0.5 m	Value of angle α is from 0-63 degrees Value of embedded depth a is from 0-2.8m	
Embedded Depth, a	Various		

According to equation (3-5), $K_p = \frac{1+\sin\phi}{1-\sin\phi} = \frac{1+\sin30}{1-\sin30} = 3$

Furthermore, it was not necessary to display all the datasheets in this chapter. The reason for providing the following scenarios was that these scenarios not only verified the accuracy of the analysis but also indicated that under which circumstances shell foundation was superior to resist lateral loading. Moreover, the peak angle of shell foundation could only be up to 63 degrees in these examples because once the peak angle was over 63 degrees, the height of the shell would exceed 3 meters, exceeding the height of the foundation provided in Table 3-1.

3.3 Analytical Models for the Strip, Pyramidal and Conical Shell and Flat Foundations

During the comparative study, strip, pyramidal and conical shell models were investigated against conventional square and circular flat footing, respectively, as shown in Figures 3-2 and 3-3.

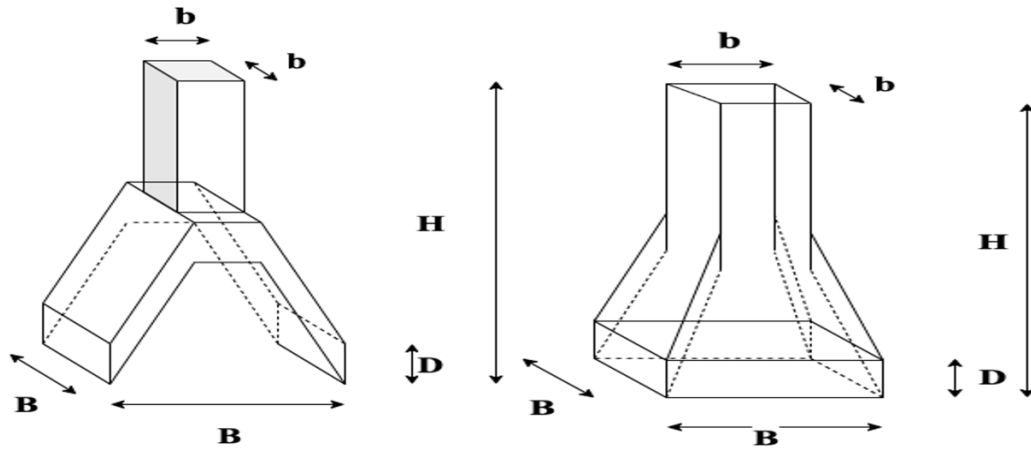


Figure 3-2. 3D Strip and Pyramidal Footing Models

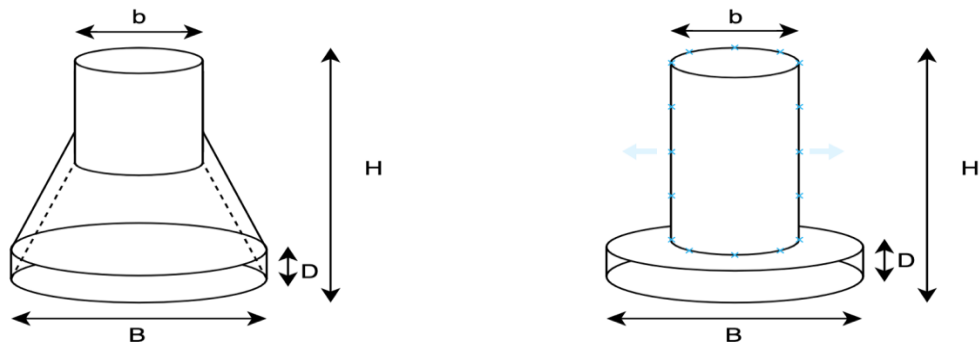


Figure 3-3. 3D Conical Shell and Circular Flat Footing Models

3.3.1 Case 1 ($a = 0\text{m}$)

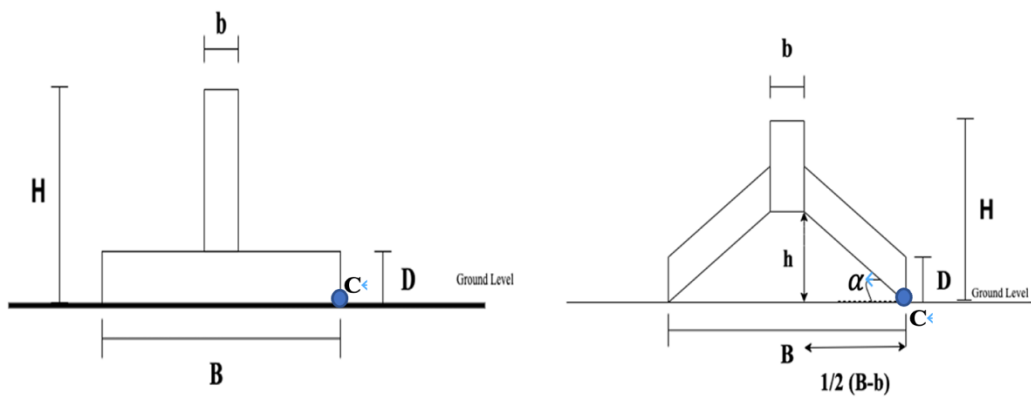


Figure 3-4. 2D Flat and Shell Footing Models on Ground Level

In the case of footing resting on the ground surface ($a=0$), as shown in Figures 3-2 through 3-4, there was no passive earth pressure since passive earth pressure only acts on embedded foundations.

$$\sigma_{h1} = 0 \quad (3-12)$$

$$P_{\text{passive}} = 0 \quad (3-13)$$

For strip and pyramidal shell foundations

$$W_{\text{footing}} = \gamma_{\text{footing}} \left[DB^2 + b^2 \times \left(H - \frac{B-b}{2} \tan\alpha - D \right) \right] \quad (3-14)$$

For the strip shell foundation

$$W_{\text{soil below}} = \gamma_{\text{soil}} \times B \times \frac{B^2 - b^2}{4} \times \tan\alpha \quad (3-15)$$

For the pyramidal shell foundation

$$W_{\text{soil below}} = \frac{1}{6} \gamma_{\text{soil}} \times (B^3 - b^3) \times \tan\alpha \quad (3-16)$$

For the conical shell foundation

$$W_{\text{footing}} = \frac{\pi}{4} \gamma_{\text{footing}} \left[DB^2 + b^2 \times \left(H - \frac{B-b}{2} \tan\alpha - D \right) \right] \quad (3-17)$$

$$W_{\text{soil below}} = \frac{\pi}{12} \gamma_{\text{soil}} (B^3 - b^3) \tan\alpha \quad (3-18)$$

When $\alpha \neq 0$

$$F_w = (W_{\text{footing}} + W_{\text{soil below}}) \times \tan\phi \quad (3-19)$$

When $\alpha = 0$

$$F_w = (W_{\text{footing}} + W_{\text{soil below}}) \times \tan\left(\frac{2}{3}\phi\right) \quad (3-20)$$

$$M_{\text{total}} = W_{\text{footing}} \times \frac{B}{2} \quad (3-21)$$

Where:

b : the width of the column on the foundation

B : the width of the foundation

H : the height of the foundation

D: the thickness of the foundation

α : the angle of shell footing

a: the embedded depth

3.3.1-1 Analytical Analysis

Moment Resistance:

- For strip and pyramidal shell foundations

$$W_{\text{square flat footing}}: W_{\text{strip footing}}: W_{\text{PY footing}}$$
$$DB^2 + b^2H: DB^2 + b^2\left(H - \frac{B-b}{2}\tan\alpha\right): DB^2 + b^2\left(H - \frac{B-b}{2}\tan\alpha\right)$$

Where $B > b$ and $\tan\alpha > 0$

$$H > H - \frac{B-b}{2}\tan\alpha = H - \frac{B-b}{2}\tan\alpha$$

So $W_{\text{strip footing}} = W_{\text{PY footing}} < W_{\text{square flat footing}}$

Since $M_{\text{total}} = W_{\text{footing}} \times \frac{B}{2}$, we could conclude that $M_{\text{self-weight square flat}} >$

$$M_{\text{self-weight strip}} = M_{\text{self-weight PY}}$$

- For the conical shell footing

$$W_{\text{circular flat footing}}: W_{\text{conical shell footing}}$$
$$DB^2 + b^2 \times (H - D): DB^2 + b^2 \times \left(H - \frac{B-b}{2}\tan\alpha - D\right)$$

Where $B > b$ and $\tan\alpha > 0$

$$H > H - \frac{B-b}{2}\tan\alpha$$

Thus $W_{\text{flat footing}} > W_{\text{conical shell footing}}$

Since $M_{total} = W_{footing} \times \frac{B}{2}$, we could conclude that $M_{self-weight circular flat} >$

$M_{self-weight conical}$

Sliding Resistance:

■ For strip and pyramidal shell foundations

$$W_{soil/flat} : W_{soil/strip} : W_{soil/PY}$$

$$0 : \gamma_{soil} B \frac{B^2 - b^2}{4} \tan\alpha : \frac{1}{6} \gamma_{soil} (B^3 - b^3) \tan\alpha$$

$$0 < B^2 + Bb > 2b^2$$

Therefore, $W_{soil/strip} > W_{soil/PY} > W_{soil/flat}$

$$W_{square flat total} : W_{strip total} : W_{PY total}$$

$$\gamma_{footing} \frac{B - b}{2} \tan\alpha : \gamma_{soil} B \frac{B^2 - b^2}{4} \tan\alpha : \frac{1}{6} \gamma_{soil} (B^3 - b^3) \tan\alpha$$

$$\gamma_{footing} b^2 : \gamma_{soil} \frac{B(B + b)}{2} > \gamma_{soil} \frac{(B^2 + b^2 + Bb)}{3}$$

In order to prove that $F_{f shell} > F_{f flat}$, we need only need to prove that $\frac{\gamma_{footing}}{\gamma_{soil}} b^2 <$

$$\frac{(B^2 + b^2 + Bb)}{3}$$

According to Figure 3-5, the smallest dry unit weight of soil was 13 (kN/m³), and the typical unit weight of concrete was 24 (kN/m³). Thus, $\frac{\gamma_{footing}}{\gamma_{soil}} \leq 2$. Under the condition

of $B \geq 2b$, the value of $\gamma_{footing} b^2$ would be always less than the value of $\gamma_{soil} \frac{(B^2 + b^2 + Bb)}{3}$. Moreover, based on the equations (3-19) and (3-20), it resulted in friction

at the base of footing on shell foundation was at least 1.5 times larger than the friction on

a flat foundation because of $\frac{\tan(\phi)}{\tan(\frac{2}{3}\phi)} \geq \frac{1}{\frac{2}{3}} \geq 1.5$. Thus, it could be concluded as

$$F_{f \text{ strip total}} > F_{f \text{ PY total}} > F_{f \text{ square flat total}}$$

Type of soil	γ_{sat} (kN/m ³)	γ_{d} (kN/m ³)
Gravel	20 - 22	15 - 17
Sand	18 - 20	13 - 16
Silt	18 - 20	14 - 18
Clay	16 - 22	14 - 21

Figure 3-5. Typical Values of Unit Weight for Soils (Unit Weights and Densities of Soil, Reviewed at MATHalino, 2020)

■ For the conical shell foundation

$$W_{\text{soil/flat}} : W_{\text{soil/conical}}$$

$$0 : \frac{\pi}{12} \gamma_{\text{soil}} (B^3 - b^3) \tan \alpha$$

So $W_{\text{soil/conical}} > W_{\text{soil/flat}}$

As mentioned above, $\frac{\tan(\phi)}{\tan(\frac{2}{3}\phi)} \geq 1.5$, $B \geq 2b$ and $\frac{\gamma_{\text{footing}}}{\gamma_{\text{soil}}} \leq 2$

$$F_{f \text{ circular flat total}} : F_{f \text{ conical total}}$$

$$\frac{\pi}{4} \gamma_{\text{footing}} b^2 H : \frac{3}{2} \left[\frac{\pi}{4} \gamma_{\text{footing}} b^2 \left(H - \frac{B-b}{2} \tan \alpha \right) + \frac{\pi}{12} \gamma_{\text{soil}} (B^3 - b^3) \tan \alpha \right]$$

To prove:

$$\frac{\pi}{8} \gamma_{\text{soil}} (B^3 - b^3) \tan \alpha + \frac{\pi}{8} \gamma_{\text{footing}} b^2 H - \frac{3\pi}{8} \gamma_{\text{footing}} b^2 \left(\frac{B-b}{2} \tan \alpha \right) > 0$$

Additionally, $B \geq 2b$ and $\frac{\gamma_{\text{footing}}}{\gamma_{\text{soil}}} \leq 2$

If $B = 2b$ and $\gamma_{\text{footing}} = 2\gamma_{\text{soil}}$

$$\frac{2\pi}{16} \gamma_{\text{soil}} B^3 \tan \alpha - \frac{3\pi}{16} \gamma_{\text{footing}} b^2 B \tan \alpha = \frac{\pi}{16} B \gamma_{\text{soil}} (8b^3 - 6b^2) \tan \alpha > 0$$

$$-\frac{2\pi}{16}\gamma_{soil}b^3\tan\alpha + \frac{3\pi}{16}\gamma_{footing}b^3\tan\alpha = \frac{\pi}{16}b^3\gamma_{soil}(-2 + 6)\tan\alpha > 0$$

Thus $F_{f\text{conical total}} > F_{f\text{circular flat total}}$

The analysis revealed that the shell foundation model had larger sliding resistances. Nevertheless, the flat shallow foundation model had the highest overturning moment resistance when the foundation rested on the surface. Moreover, the analysis also indicated that the strip shell foundation model had the largest sliding resistances. To verify the accuracy of this prediction, an analytical example would be provided in the following sections.

3.3.1-2 Analytical Example

According to formulas 3-12 through 3-21, MATLAB code was used to compute the sliding resistance and moment resistance of foundations on the surface. The values were shown in Tables 3-2 and 3-3.

Table 3-2. Results of Sliding and Moment Resistance for Strip/Pyramidal Shell and Square Flat Foundations when $a/B = 0$.

Alpha (α) ($^{\circ}$)	0	10	20	30	40	50	60
Square Flat Foundation							
Total Friction Resistance, F_f (kN)	44.77						
Total Moment Resistance, RM_u (kN.m)	184.5						
Allowable Total Friction Resistance, $F_{f\text{ allow}}$ (kN)	22.39						
Allowable Total Moment Resistance, RM_{allow} (kN.m)	61.5						
Strip Shell Foundation							
Total Friction Resistance, F_f (kN)		81.61	92.9	105.71	121.42	142.62	175.06
Total Moment Resistance, RM_u (kN.m)		182.52	180.45	178.02	175.05	171.09	164.97
Allowable Total Friction Resistance, $F_{f\text{ allow}}$ (kN)		40.81	46.45	52.86	60.71	71.31	87.53

Allowable Total Moment Resistance, RM_{allow} (kN.m)		60.84	60.15	59.34	58.35	57.03	54.99
Pyramidal Shell Foundation							
Total Friction Resistance, F_f (kN)		78.01	85.45	93.9	104.26	118.25	139.64
Total Moment Resistance, RM_u (kN.m)		182.52	180.45	178.02	175.05	171.09	164.97
Allowable Total Friction Resistance, $F_{f\ allow}$ (kN)		39.01	42.73	46.95	52.13	59.13	69.82
Allowable Total Moment Resistance, RM_{allow} (kN.m)		60.84	60.15	59.34	58.35	57.03	54.99

Table 3-3. Results of Sliding and Moment Resistance for Conical Shell and Circular Flat Foundations, when $a/B = 0$.

Alpha (α) (°)	0	10	20	30	40	50	60
Circular Flat Foundation							
Total Friction Resistance, F_f (kN)	35.16						
Total Moment Resistance, RM_u (kN.m)	144.9						
Allowable Total Friction Resistance, $F_{f\ allow}$ (kN)	17.58						
Allowable Total Moment Resistance, RM_{allow} (kN.m)	48.3						
Conical Shell Foundation							
Total Friction Resistance, F_f (kN)		67.35	79.68	93.69	110.86	134.02	169.48
Total Moment Resistance, RM_u (kN.m)		174.99	207.02	243.41	288.03	348.2	440.33
Allowable Total Friction Resistance, $F_{f\ allow}$ (kN)		33.68	39.84	46.85	55.43	67.01	84.74
Allowable Total Moment Resistance, RM_{allow} (kN.m)		58.33	69.01	81.14	96.01	116.07	146.78

Figures 3-6 and 3-7 were highly consistent with the prediction from the analysis. Figure 3-6 showed that on the surface ($a/B=0$), when shell angle increased by 1 degree, the sliding resistance for strip, pyramidal, and conical would increase by approximately 1.4% to 2.6%, 1% to 2.1%, and 1.9% to 2.9%, respectively. In other words, as the shell angle increased, this increasing trend would become more and more steep. This was why the conical shell foundation had a lower sliding resistance than the pyramidal shell

foundation initially, but after the shell angle reached 30 degrees, the conical shell foundation had a higher sliding resistance than the pyramidal shell foundation. As shown in Figure 3-7, with shell angle increased by 1 degree, the total overturning moment resistance for strip, pyramidal, and conical would decrease by approximately 0.1% to 0.6%.

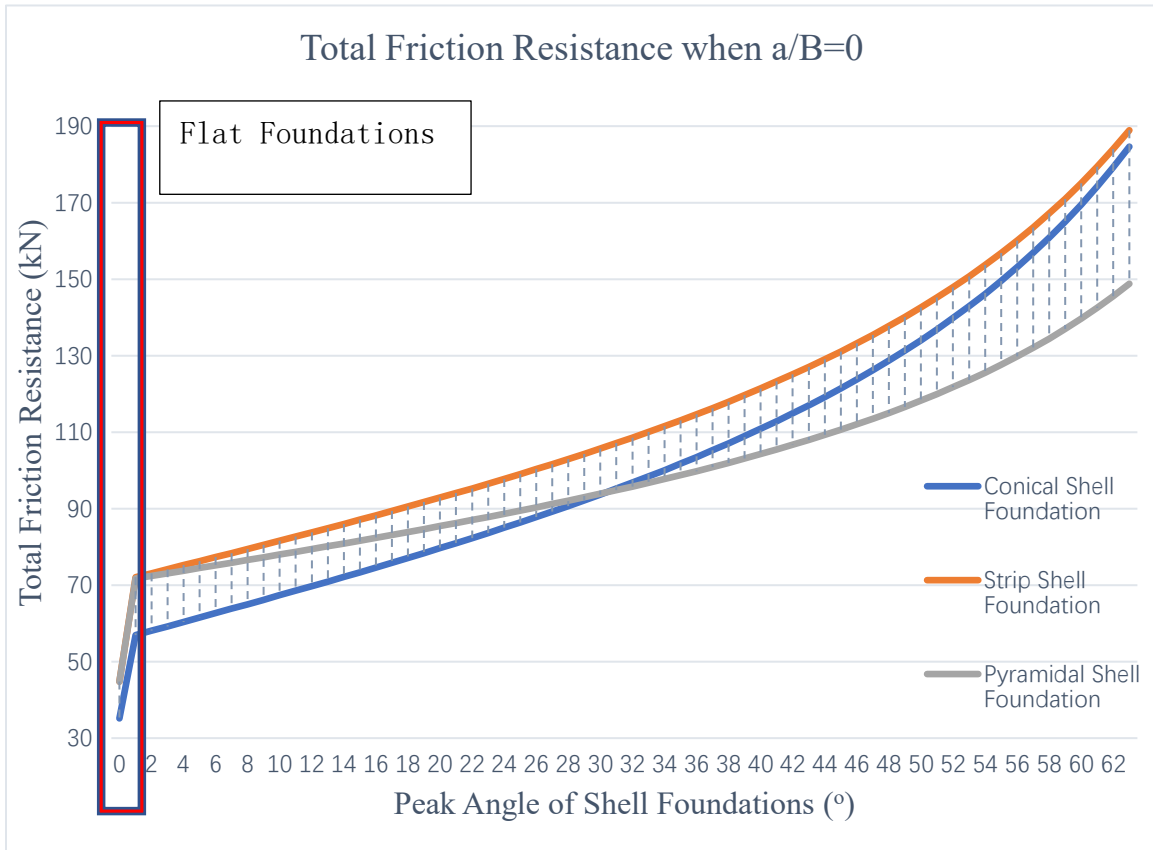


Figure 3-6. Lateral Friction Resistance of Conical/Strip/Pyramidal Shell Foundations on Surface of Sand Layer (0° Shell Foundations = Flat Foundations)

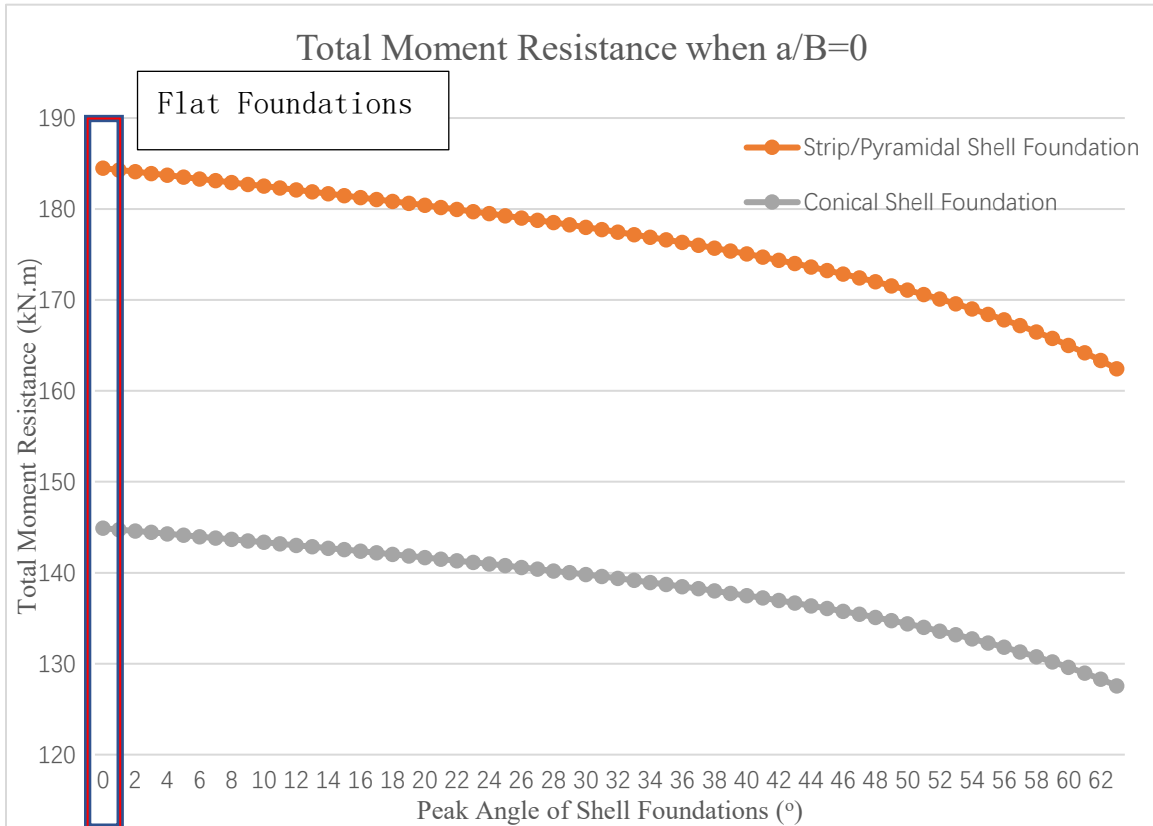


Figure 3-7. Total Moment Resistance of Conical/Strip/Pyramidal Shell Foundations with Various Shell Angles when $a/B=0$ (0° Shell Foundations = Flat Foundations)

3.3.2 Case 2 ($0 < a \leq D$)

In the case of embedded depth equal or less than the thickness of the footing ($0 < a \leq D$), as shown in Figure 3-8.

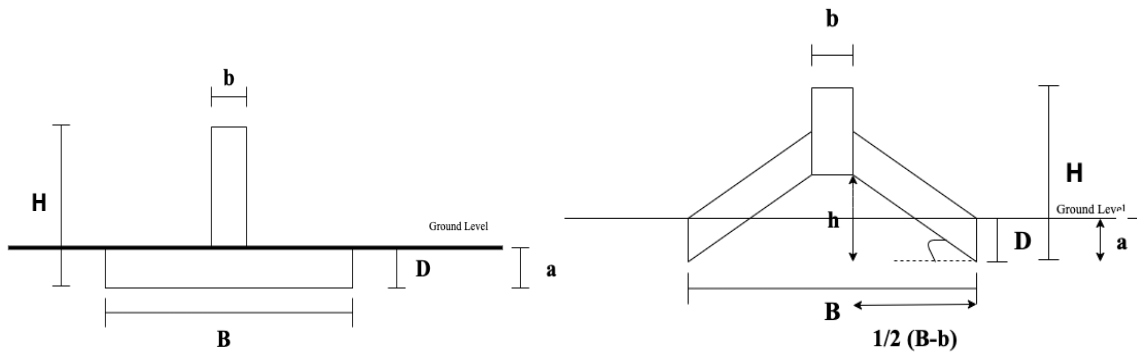


Figure 3-8. 2D Flat and Shell Foundation Model when $a=D$

Compared with Case 1, the only difference in this case was that since the soil on the right side of the footing was compressed laterally, the shell foundation would bear horizontal passive earth pressure. Nonetheless, the weight of the footing and the weight of the backfilled soil below footing were the same as in Case 1. Therefore, the weight of the footing and the backfilled soil below the footing would use equations (3-14) to (3-18). Moreover, the equations (3-19) and (3-20) were used for the sliding friction at the bottom caused by the weight of the footing and the backfilled soil below the footing.

$$P_{passive} = \frac{1}{2} \gamma_{soil} \times a^2 \times K_p \times B \quad (3-22)$$

$$F_f = F_w + P_{passive} \quad (3-23)$$

$$RM_1 = P_{passive} \times \frac{1}{3} a \quad (3-24)$$

$$M_{total} = W_{footing} \times \frac{B}{2} + RM_1 \quad (3-25)$$

3.3.2-1 Analytical Analysis

Moment Resistance:

The previous analysis from case 1 revealed that:

- $M_{self-weight\ square\ flat} > M_{self\ weight\ strip} = M_{self\ weight\ PY}$
- $M_{self\ weight\ circular\ flat} > M_{self\ weight\ conical}$
- $F_w\ strip > F_w\ PY > F_w\ square\ flat$
- $F_w\ conical > F_w\ circular\ flat$

$$RM_{1square\ flat} : RM_{1strip} : RM_{1PY}$$

$$P_{passive} \times \frac{1}{3} a : P_{passive} \times \frac{1}{3} a : P_{passive} \times \frac{1}{3} a$$

Since $RM_{1\text{ square flat}} = RM_{1\text{ strip}} = RM_{1\text{ PY}}$ and $M_{\text{self weighth of suqare flat}} > M_{\text{self weighths trip}} = M_{\text{self weighth PY}}$, it could be summarized as $M_{\text{total square flat}} > M_{\text{total strip}} = M_{\text{total PY}}$.

Additionally,

$$RM_{1\text{ flat}}:RM_{1\text{ conical}}$$

$$P_{\text{passive}} \times \frac{1}{3}a : P_{\text{passive}} \times \frac{1}{3}a$$

Since $RM_{1\text{ circular flat}} = RM_{1\text{ conical}}$ and $M_{\text{self weighth of circular flat}} > M_{\text{self weighth conical}}$. It could be summarized as $M_{\text{total circular flat}} > M_{\text{total conical}}$.

Sliding Resistance:

$$F_{p\text{ square flat}}:F_{p\text{ strip}}:F_{p\text{ PY}}$$

$$\frac{1}{2}\gamma_{\text{soil}}a^2K_pB = \frac{1}{2}\gamma_{\text{soil}}a^2K_pB = \frac{1}{2}\gamma_{\text{soil}}a^2K_pB$$

Since $F_{p\text{ square flat}} = F_{p\text{ strip}} = F_{p\text{ PY}}$ and $F_{w\text{ strip}} > F_{w\text{ PY}} > F_{w\text{ square flat}}$, it could be summarized that $F_{f\text{ strip}} > F_{f\text{ PY}} > F_{f\text{ flat}}$.

Additionally,

$$F_{p\text{ flat}}:F_{p\text{ conical}}$$

$$\frac{1}{2}\gamma_{\text{soil}}a^2K_pB = \frac{1}{2}\gamma_{\text{soil}}a^2K_pB$$

Since $F_{p\text{ circular flat}} = F_{p\text{ conical}}$ and $F_{w\text{ conical}} > F_{w\text{ flat}}$, it could be summarized that $F_{f\text{ conical}} > F_{f\text{ circular flat}}$.

The analysis revealed that Case 2 had the same conclusion as Case 1. The followed section took a foundation with a buried depth of 0.5 m as an example to illustrate the change of the resistance force of shell foundations when the embedded depth is $0 < a \leq D$.

3.3.2-2 Analytical Example

According to formulas 3-12 to 3-20 and 3-22 to 3-25, MATLAB code was used to compute the total sliding resistance and total moment resistance of foundations with embedment ratios (a/B) of 1/30 to 1/6. The results for the embedment ratio of 1/6 were shown in Tables 3-4 and 3-5.

Table 3-4. Results of Sliding and Moment Resistance for Strip/Pyramidal Shell and Square Flat foundations when $a/B=1/6$

Alpha (α) ($^\circ$)	0	10	20	30	40	50	60
Square Flat Foundation							
Total Friction Resistance, F_f (kN)	63.9						
Total Moment Resistance, RM_u (kN.m)	187.69						
Allowable Total Friction Resistance, $F_{f\ allow}$ (kN)	31.95						
Allowable Total Moment Resistance, RM_{allow} (kN.m)	62.59						
Strip Shell Foundation							
Total Friction Resistance, F_f (kN)		100.74	112.03	124.84	140.55	161.75	194.19
Total Moment Resistance, RM_u (kN.m)		185.71	183.64	181.21	178.24	174.28	168.16
Allowable Total Friction Resistance, $F_{f\ allow}$ (kN)		50.37	56.02	62.42	70.28	80.88	97.1
Allowable Total Moment Resistance, RM_{allow} (kN.m)		61.9	61.21	60.4	59.41	58.09	56.05
Pyramidal Shell Foundation							
Total Friction Resistance, F_f (kN)		97.14	104.58	113.03	123.39	137.38	158.77
Total Moment Resistance, RM_u (kN.m)		185.71	183.64	181.21	178.24	174.28	168.16
Allowable Total Friction Resistance, $F_{f\ allow}$ (kN)		48.57	52.29	56.52	61.7	68.69	79.39
Allowable Total Moment Resistance, RM_{allow} (kN.m)		61.9	61.21	60.4	59.41	58.09	56.05

Table 3-5. Results of Sliding and Moment Resistance for Conical Shell and Circular Flat Foundations when $a/B=1/6$

Alpha (α) ($^{\circ}$)	0	10	20	30	40	50	60
Circular Flat Foundation							
Total Friction Resistance, F_f (kN)	54.29						
Total Moment Resistance, RM_u (kN.m)	148.09						
Allowable Total Friction Resistance, $F_{f\ allow}$ (kN)	27.15						
Allowable Total Moment Resistance, RM_{allow} (kN.m)	49.36						
Conical Shell Foundation							
Total Friction Resistance, F_f (kN)		86.48	98.81	112.82	129.99	153.15	188.61
Total Moment Resistance, RM_u (kN.m)		146.55	144.91	143.01	140.68	137.56	132.76
Allowable Total Friction Resistance, $F_{f\ allow}$ (kN)		43.24	49.41	56.41	65	75.58	94.31
Allowable Total Moment Resistance, RM_{allow} (kN.m)		48.85	48.3	47.67	46.89	45.85	44.25

As shown in Figures 3-9 and 3-10, as long as the embedment depth did not exceed the thickness of the foundation, the increase of passive earth pressure and the increase of overturning moment caused by passive earth pressure were only affected by the change of embedment ratio. It had nothing to do with the increase in shell angle. Additionally, as the embedment ratio increases, this increasing trend would become increasingly steep.

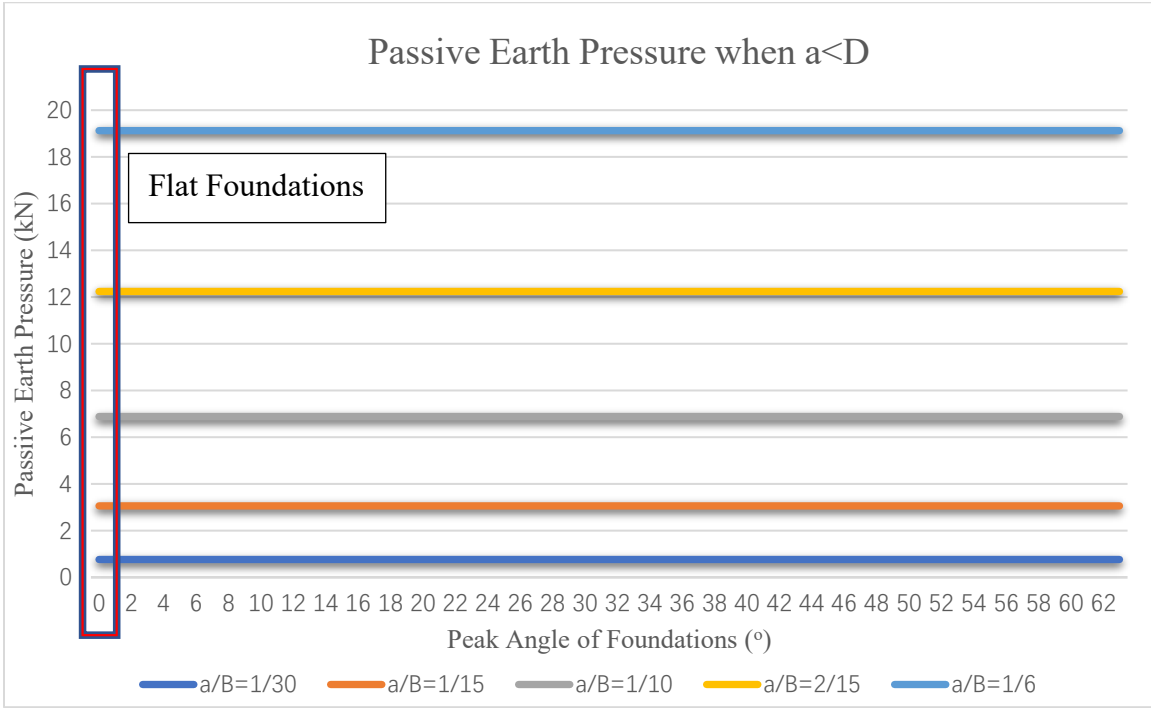


Figure 3-9. Passive Earth Pressure with Various Shell Angles when a < D (0° Shell Foundations = Flat Foundations)

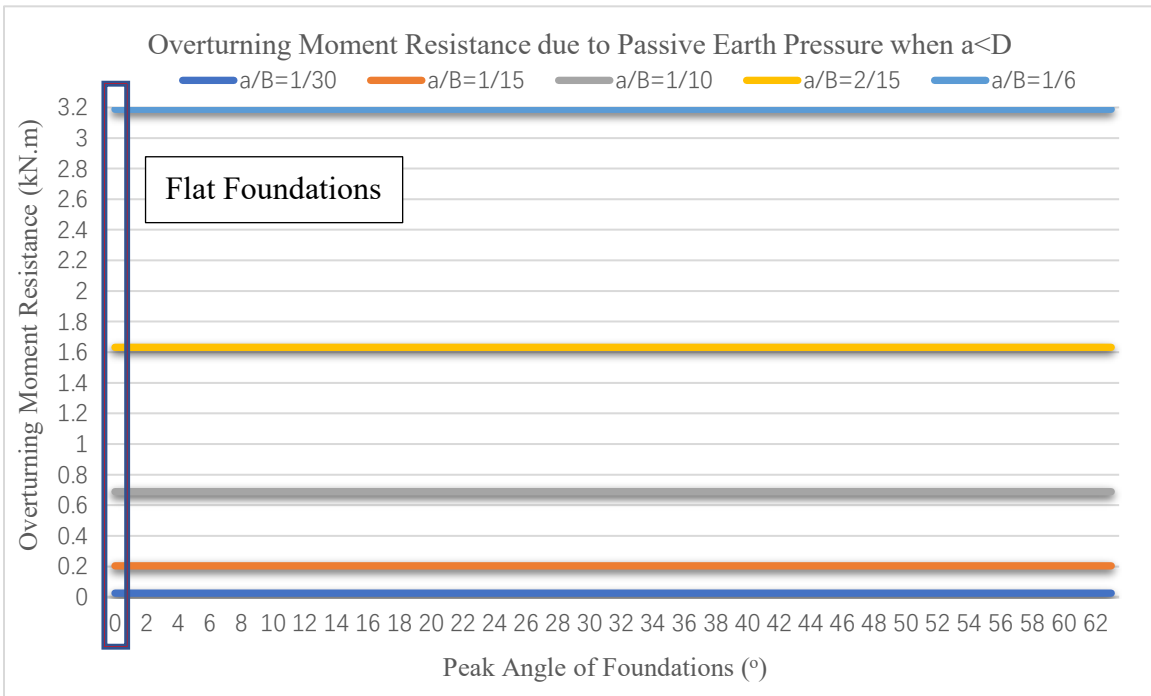


Figure 3-10. Overturning Moment Resistance due to Passive Earth Pressure with Various Shell Angles in Different Embedment Ratio when a < D (0° Shell Foundations = Flat Foundations)

The total friction resistance of conical, strip and pyramidal shell foundations with various shell angles in the situation of $a < D$ was shown in Figures 3-11, 3-12, and 3-13, respectively. These figures indicated that the increased magnitude of resistance was proportional to the rise of shell foundation angles and the increase in embedment ratio. As the shell angle and embedment ratio increased, the increase rate of resistance increased slowly at first, only about 4%, and then increased rapidly, reaching 9% or more.

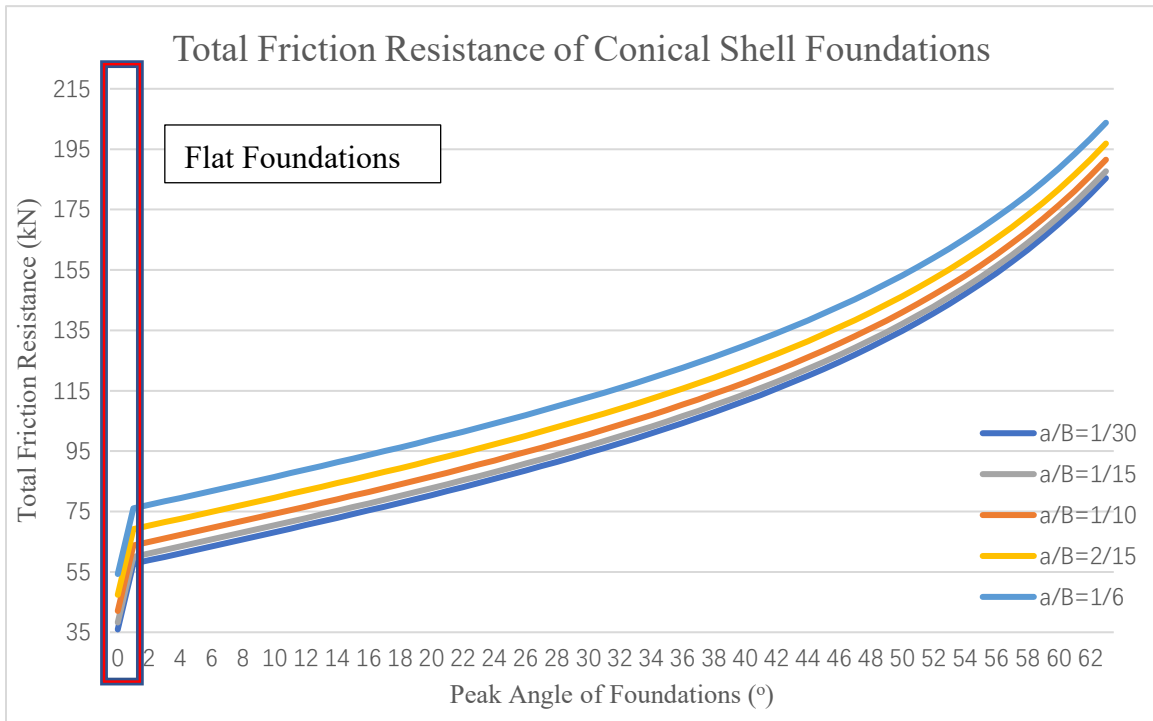


Figure 3-11. Total Lateral Friction Resistance of Conical Shell Foundations with Various Shell Angles when $a < D$ (0° Shell Foundations = Flat Foundations)

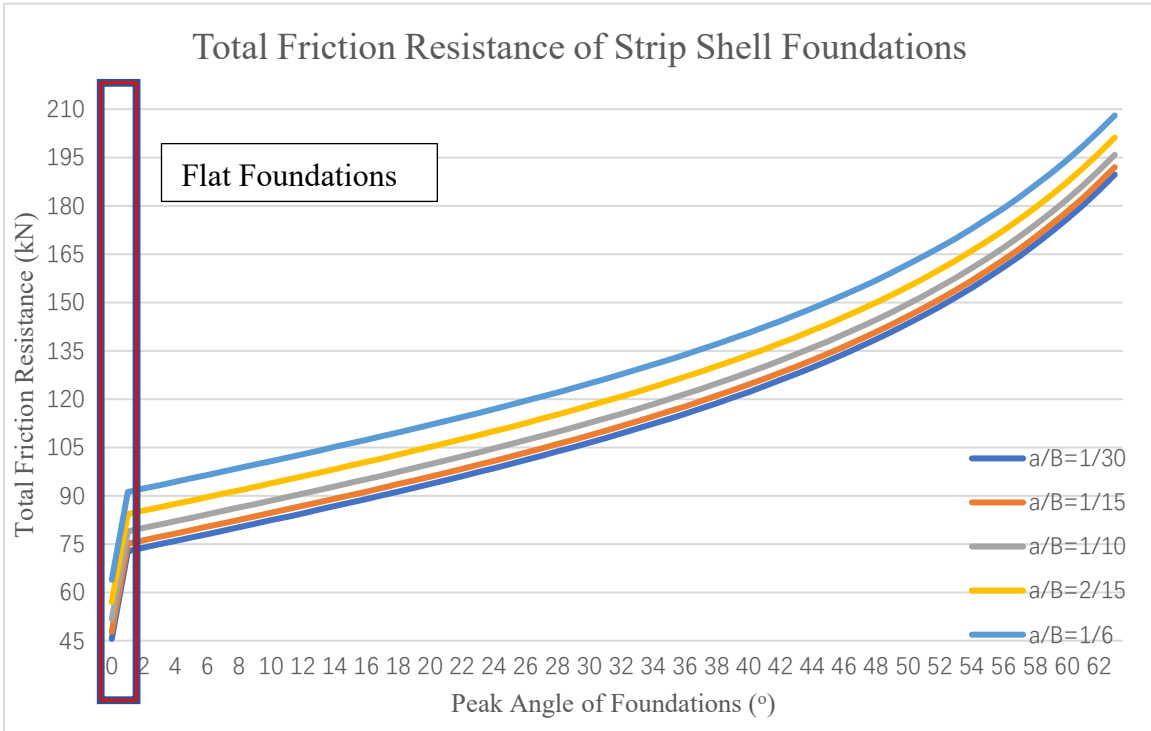


Figure 3-12. Total Lateral Friction Resistance of Strip Shell Foundations with Various Shell Angles when $a < D$ (0° Shell Foundations = Flat Foundations)

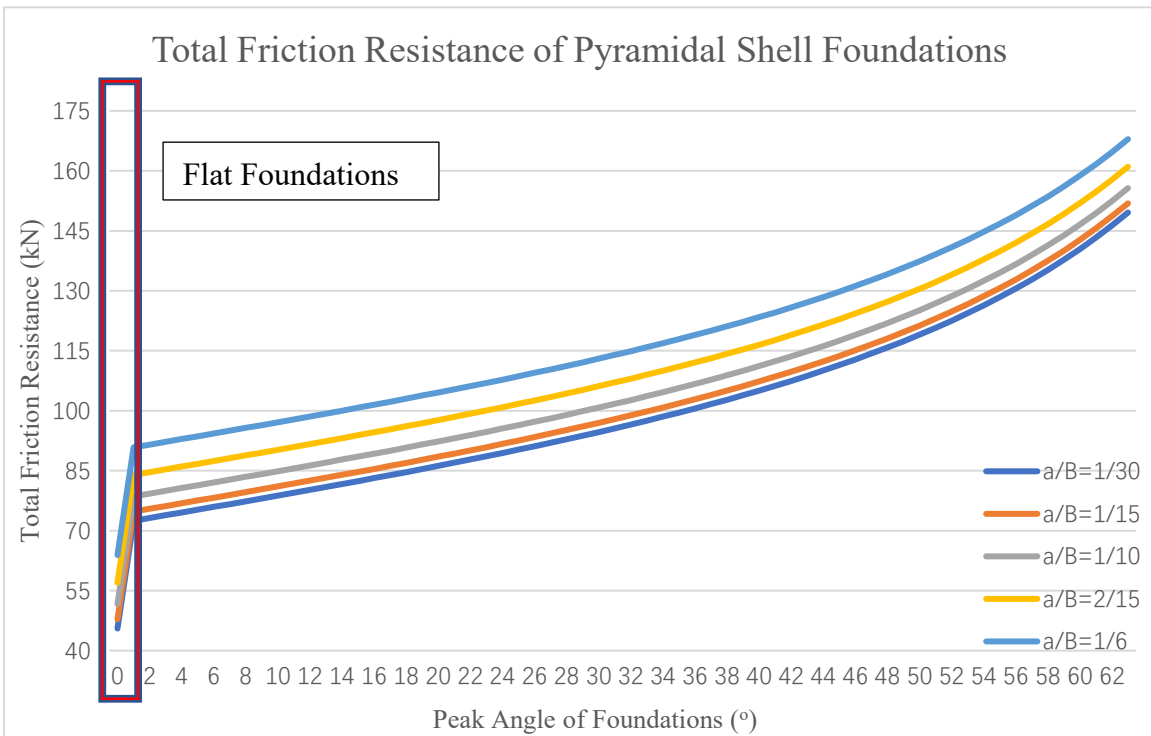


Figure 3-13. Total Lateral Friction Resistance of Pyramidal Shell Foundations with Various Shell Angles When $a < D$ (0° Shell Foundations = Flat Foundations)

Figure 3-14 revealed that square flat foundations had the highest overturning moment resistance, followed by strip and pyramidal shell foundations and flat circular foundations. The conical shell foundations were minimal. Unlike the total overturning moment resistance increased with the increase of embedment ratio, it decreased with the increase of the shell foundation angle. The figure also shows that the rate at which the total overturning moment resistance increases with the increase in buried ratio is much lower than the rate at which friction increases with the increase in buried ratio. For example, increasing from a buried ratio of 1/30 to 1/6, the overturning moment resistance increases by only 1.7%, approximately.

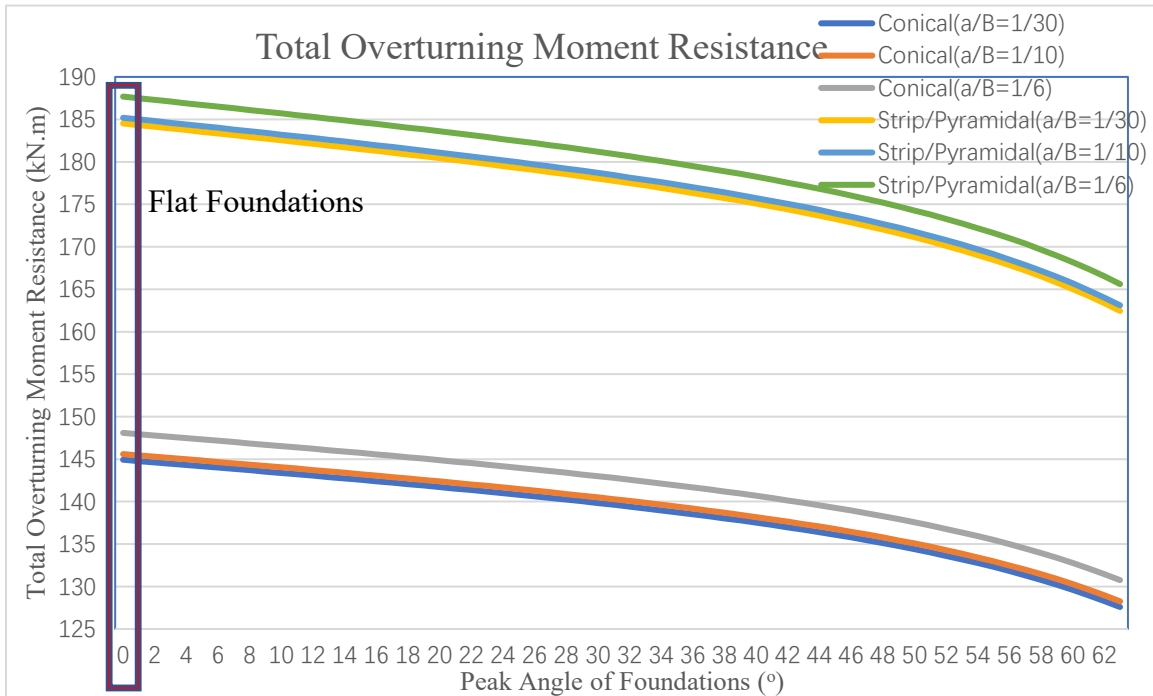


Figure 3-14. Total Overturning Moment Resistance with Various Shell Angles in Different Embedment Ratio when $a < D$ (0° Shell Foundations = Flat Foundations)

The results showed on Figures 3-15 and 3-16 were highly agreed with the prediction from the Case 2. Moreover, compared with Figures 3-6 and 3-7, it could be concluded that the sliding resistance and anti-overturning moment of shell foundations of Case 1 and Case 2 had the same increasing trend. For instance, in both cases, the sliding resistance of pyramidal shell foundations was greater than that of conical shell foundations before 31

degrees, but the sliding resistance of conical shell surpassed that of pyramidal foundations after 31 degrees.

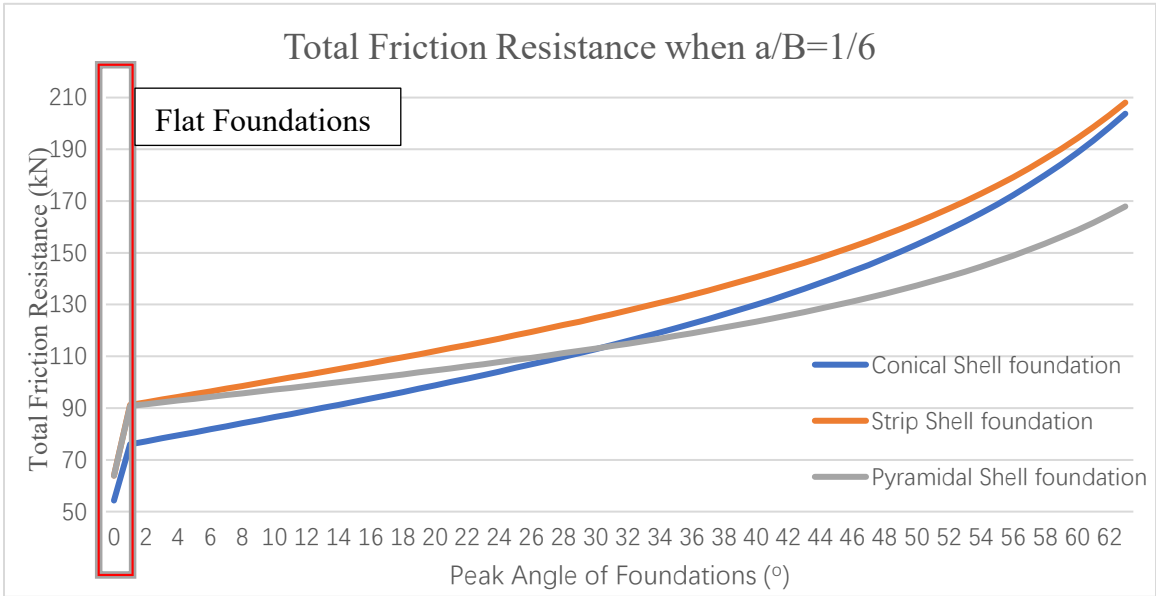


Figure 3-15. Total Lateral Friction Resistance of Conical/Strip/Pyramidal Shell Foundations with Various Shell Angles when $a/B=1/6$ (0° Shell Foundations = Flat Foundations)

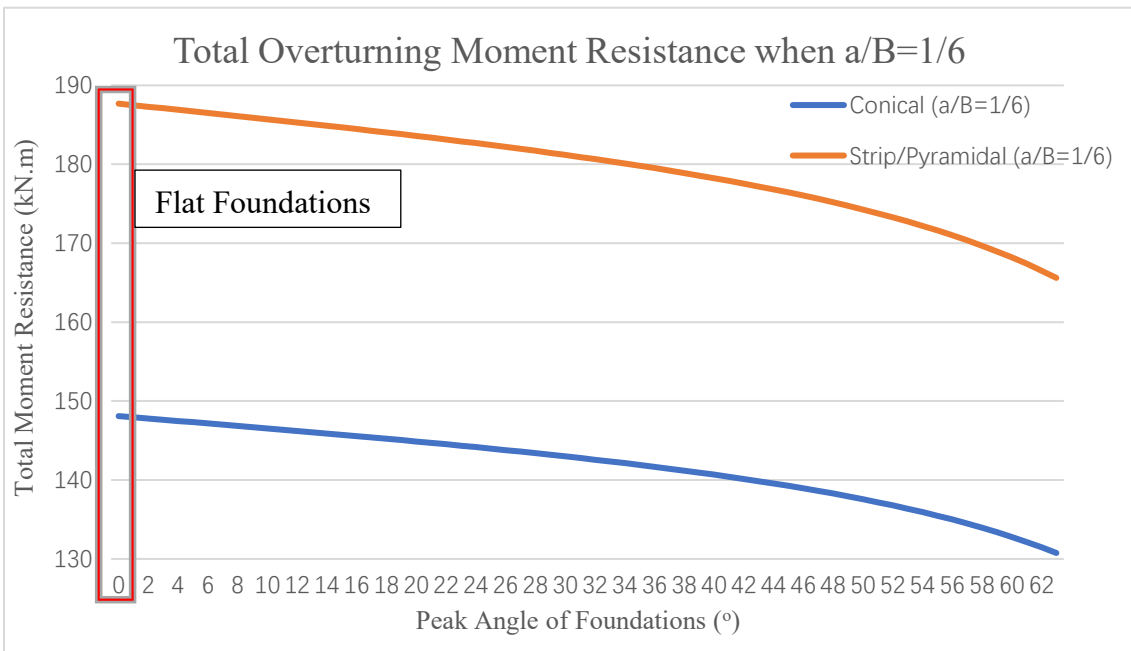


Figure 3-16. Total Lateral Friction Resistance of Conical/Strip/Pyramidal Shell Foundations with Various Shell Angles when $a/B=1/6$ (0° Shell Foundations = Flat Foundations)

3.3.3 Case 3 ($D < a \leq H$)

In the case of embedded depth in range from D to h' ($D < a < h'$), as shown in Figure 3-17, where $h' = h + D$.

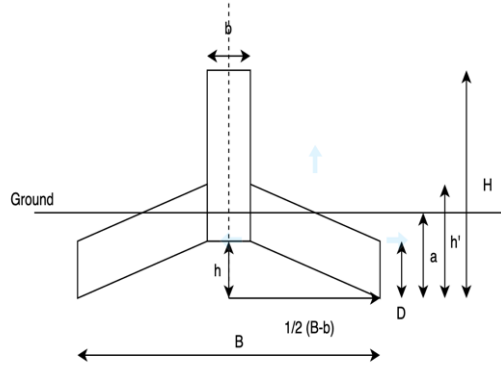


Figure 3-17. 2D Shell Foundation Model, when $D < a < h'$

For strip shell foundation:

$$W_{soil\ above} = \gamma_{soil} \times \frac{(a-D)^2}{\tan\alpha} \times B \quad (3-26)$$

The passive earth pressure could be calculated by using equation (3-22), and the resisting moment due to the horizontal passive earth pressure could be calculated by using equation (3-23).

For pyramidal shell foundation:

$$W_{soil\ above} = \gamma_{soil} \times \frac{(a-D)^2}{\tan\alpha} \times \left(2B - \frac{3}{4} \frac{a-D}{\tan\alpha}\right) \quad (3-27)$$

For conical shell foundation:

$$W_{soil\ above} = \frac{\pi}{3} \gamma_{soil} \frac{(a-D)^2}{\tan\alpha} \left(\frac{3}{2} B - \frac{a-D}{\tan\alpha}\right) \quad (3-28)$$

For pyramidal and conical shell foundation:

$$P_{passive} = \frac{1}{2} \gamma_{soil} a^2 K_p \times \left[B - \frac{a-D}{\tan\alpha}\right] \quad (3-29)$$

$$RM_1 = P_{passive} \times \frac{1}{3} a \quad (3-30)$$

In this case, the weight of the footing and the backfilled soil below the shell footing remained the same weight as in Case 1, thus equations (3-14) to (3-18) would be used.

$$F_w = (W_{footing} + W_{soil\ below} + W_{soil\ above}) \times \tan\phi \quad (3-31)$$

$$F_f = F_w + F_p \quad (3-32)$$

$$M_{total} = (W_{footing} + W_{soil\ above}) \times \frac{B}{2} + RM_1 \quad (3-33)$$

For square flat foundation:

$$W_{soil\ above} = \gamma_{soil}(a - D)(B^2 - b^2) \quad (3-34)$$

For circular flat foundation:

$$W_{soil\ above} = \frac{\pi}{4} \gamma_{soil}(a - D)(B^2 - b^2) \quad (3-35)$$

As shown in Figure 3-18, unlike the shell foundation, the flat foundation did not have to be divided into two cases: $D \leq a \leq h'$ and $h' \leq a \leq H$ to discuss its influence on the change of the lateral resistance.

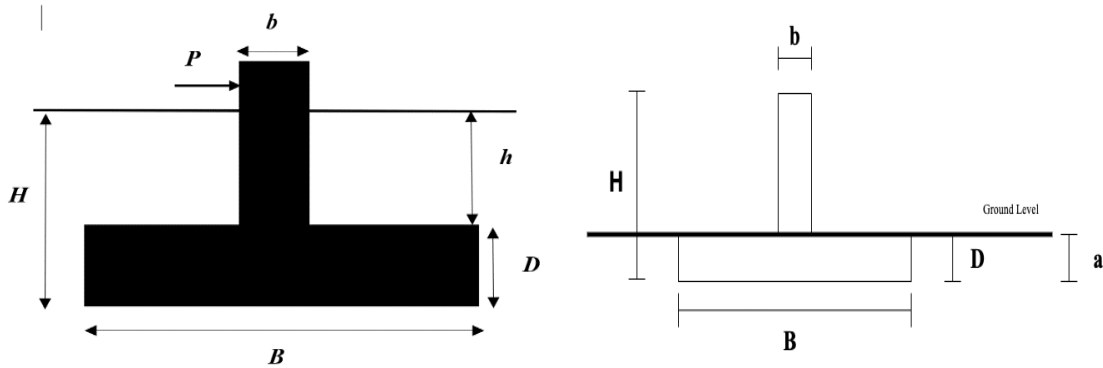


Figure 3-18. Flat Foundation, Left $D \leq a \leq H$ and Right $0 \leq a \leq D$

For square and circular flat foundation:

$$F_1 = \frac{1}{2} \gamma_{soil} K_p b \times (a - D)^2 \quad (3-36)$$

$$RM_1 = F_1 \times \left[\frac{1}{3} (a - D) + D \right] \quad (3-37)$$

$$F_2 = \frac{1}{2} \gamma_{soil} K_p B D \times (2a - D) \quad (3-38)$$

$$RM_2 = \frac{1}{6} \gamma_{soil} K_p B D^2 \times (3a - 2D) \quad (3-39)$$

$$F_w = (W_{footing} + W_{soil\ above}) \times \tan \left(\frac{2}{3} \phi \right) \quad (3-40)$$

$$F_f = F_w + F_1 + F_2 \quad (3-41)$$

$$M_{total} = (W_{footing} + W_{soil\ above}) \times \frac{B}{2} + RM_1 + RM_2 \quad (3-42)$$

3.3.3-1 Analytical analysis for $D < a < h'$

Moment Resistance

■ For strip and pyramidal shell foundations

$$W_{soil\ above\ square\ flat} : W_{soil\ above\ PY}$$

$$\gamma_{soil} (B^2 - b^2) (a - D) : \gamma_{soil} \frac{(a - D)^2}{\tan \alpha} \left(2B - \frac{3a - D}{4 \tan \alpha} \right)$$

Since $a < h'$, if $a = h'$, $a - D = \frac{1}{2} (B - b) \tan \alpha$

$$(B^2 - b^2) : \frac{1}{2} (B - b) \left[2B - \frac{3}{8} (B - b) \right]$$

$$B + b > \frac{13}{16} B + \frac{3}{16} b$$

So $W_{soil\ above\ square\ flat} > W_{soil\ above\ PY}$

$$W_{soil\ above\ strip} : W_{soil\ above\ PY}$$

$$\gamma_{soil} \frac{(a - D)^2}{\tan \alpha} B : \gamma_{soil} \frac{(a - D)^2}{\tan \alpha} \left(2B - \frac{3a - D}{4 \tan \alpha} \right)$$

$$B < \left(2B - \frac{3a - D}{4 \tan \alpha}\right)$$

So $W_{soil \text{ above square flat}} > W_{soil \text{ above PY}} > W_{soil \text{ above strip}}$

According to equations $M_{footing+soil} = (W_{footing} + W_{soil \text{ above}}) \times \frac{B}{2}$ and

$$W_{strip \text{ footing}} = W_{PY \text{ footing}} < W_{square \text{ flat footing}}$$

Thus, $M_{footing+soil \text{ square flat}} > M_{footing+soil \text{ PY}} > M_{footing+soil \text{ strip}}$

$$F_p \text{ square flat} : F_p \text{ strip}$$

$$\frac{1}{2} \gamma_{soil} K_p b (a - D)^2 + \frac{1}{2} \gamma_{soil} K_p B D (2a - D) : \frac{1}{2} \gamma_{soil} a^2 K_p B$$

$$b(a - D)^2 : B(a^2 - 2aD + D^2)$$

$$b(a - D)^2 < B(a - D)^2$$

$$RM_{square \text{ flat}} : RM_{strip}$$

$$\frac{1}{6} \gamma_{soil} K_p b (a - D)^2 (a + 2D) + \frac{1}{6} \gamma_{soil} K_p B D^2 (3a - 2D) : \frac{1}{6} \gamma_{soil} a^3 K_p B$$

$$b(a^3 - 3aD^2 + 2D^2) < B(a^3 - 3aD^2 + 2D^2)$$

So $F_p \text{ strip} > F_p \text{ square flat}$ and $RM_{strip} > RM_{square \text{ flat}}$

Since $RM_{strip} > RM_{square \text{ flat}}$ and $M_{footing+soil \text{ square flat}} > M_{footing+soil \text{ strip}}$, there is a chance that the total moment resistance of strip footings will be greater than that of flat foundations.

$$F_p \text{ strip} : F_p \text{ PY}$$

$$a^2 B > a^2 \left[B - \frac{a - D}{\tan \alpha} \right]$$

$$RM_{strip} : RM_{PY}$$

$$F_p \text{ strip} \times \frac{1}{3} a < F_p \text{ PY} \times \frac{1}{3} a$$

So $F_p \text{ strip} > F_p \text{ PY}$ and $RM_{strip} > RM_{PY}$

$RM_{PY}: RM_{square\ flat}$

$$\begin{aligned} & RM_{PY} - RM_{square\ flat} \\ &= \frac{1}{6}\gamma_{soil}K_p a^3 \left[B - \frac{a-D}{\tan\alpha} \right] - \frac{1}{6}\gamma_{soil}K_p a^3 b - \frac{1}{6}\gamma_{soil}K_p (B-b)(3aD^2 - 2D^3) \\ &= \frac{1}{6}\gamma_{soil}K_p (B-b)(a^3 - 3aD^2 + 2D^3) - \frac{1}{6}\gamma_{soil}K_p a^3 \left(\frac{a-D}{\tan\alpha} \right) \end{aligned}$$

Since $D < a < h + D$, if $a = h'$, $a - D = \frac{1}{2}(B - b)\tan\alpha$

$$RM_{PY} - RM_{square\ flat} = \frac{1}{6}\gamma_{soil}K_p (B-b) \left[\frac{1}{2}h^3 + \frac{3}{2}h^2D - \frac{3}{2}hD^2 - \frac{1}{2}D^3 \right]$$

If $h \leq D$

$RM_{PY} - RM_{square\ flat} \leq 0$, which means $RM_{square\ flat} \geq RM_{PY}$.

Thus $RM_{strip} > RM_{square\ flat} > RM_{PY}$.

Since $RM_{square\ flat} > RM_{PY}$ and $M_{footing+soil\ square\ flat} > M_{footing+soil\ PY}$, we can conduct that $M_{total\ square\ flat} > M_{total\ PY}$.

If $h > D$, $RM_{PY} > RM_{square\ flat}$. Since $M_{footing+soil\ square\ flat} > M_{footing+soil\ PY}$, it was difficult to determine whether the pyramidal shell foundation or the flat foundation had the higher ability to resist the total overturning moment. Nonetheless, there was a chance that the total moment resistance of pyramidal shell foundations would be greater than that of square flat foundations.

■ For the conical shell foundation

$W_{soil\ above\ circular\ flat}: W_{soil\ above\ conical}$

$$\frac{\pi}{4}(a-D)(B^2 - b^2): \frac{\pi}{3} \frac{(a-D)^2}{\tan\alpha} \left(\frac{3}{2}B - \frac{a-D}{\tan\alpha} \right)$$

Since $a < h'$, if $a = h'$, $a - D = \frac{1}{2}(B - b)\tan\alpha$

$$3(B+b)(B-b): 2(B-b) \left[\frac{3}{2}B - \frac{1}{2}(B-b) \right]$$

$$3(B+b) > 2\left(B + \frac{1}{2}b\right)$$

So $W_{soil\ above\ circular\ flat} > W_{soil\ above\ conical}$,

$$\begin{aligned} & RM_{conical} - RM_{flat} \\ &= \frac{1}{6} \gamma_{soil} K_p a^3 \left[B - \frac{a-D}{\tan \alpha} \right] - \frac{1}{6} \gamma_{soil} K_p a^3 b - \frac{1}{6} \gamma_{soil} K_p (B-b)(3aD^2 - 2D^3) \\ &= \frac{1}{6} \gamma_{soil} K_p (B-b)(a^3 - 3aD^2 + 2D^3) - \frac{1}{6} \gamma_{soil} K_p a^3 \left(\frac{a-D}{\tan \alpha} \right) \end{aligned}$$

Since $D < a < h + D$, if $a = h'$, $a - D = \frac{1}{2}(B - b)\tan \alpha$

$$RM_{conical} - RM_{flat} = \frac{1}{6} \gamma_{soil} K_p (B-b) \left[\frac{1}{2}(h+D)^3 - 3(h+D)D^2 + 2D^3 \right]$$

If $h \leq D$

$RM_{conical} - RM_{circular\ flat} < 0$, which means $RM_{circular\ flat} > RM_{conical}$.

Since $RM_{circular\ flat} > RM_{conical}$, $W_{self\ weight\ circular\ flat} > W_{self\ weight\ conical}$ and $W_{soil\ above\ circular\ flat} > W_{soil\ above\ conical}$. We can conduct that $M_{total\ circular\ flat} > M_{total\ conical}$.

If $h \geq D$, $RM_{conical} > RM_{circular\ flat}$. However, $M_{footing+soil\ circular\ flat} > M_{footing+soil\ conical}$, it was difficult to determine whether the conical shell foundation or the flat foundation had the higher ability to resist the total overturning moment. But there was a chance that the total moment resistance of conical shell footings would be bigger than that of circular flat foundations.

Sliding Resistance

■ For strip and pyramidal shell foundations

As mentioned in Case 1, $\frac{\tan(\phi)}{\tan(\frac{2}{3}\phi)} \geq 1.5$. $\sum W$ included the weight of footing, the weight of soil below and above the footing.

$$F_w\ square\ flat: F_w\ strip$$

To proof that $1.5(W_{soil\ above\ strip} + W_{soil\ below\ strip}) - W_{soil\ above\ square\ flat} > 0$

$$\gamma_{soil} \left\{ \frac{3}{2} B \frac{(a-D)^2}{\tan\alpha} + B^2 \left[\frac{3}{4} \left(\frac{1}{2} (B-b) \tan\alpha \right) - (a-D) \right] + b^2 (a-D) \right\} > 0$$

Since $h = \frac{1}{2}(B-b)\tan\alpha$, $h' = h + D$, and $D < a < h'$

If assume $a = h'$, $B \geq 2b$

$$\begin{aligned} & \gamma_{soil} \left\{ \frac{3}{2} \frac{Bh^2}{\tan\alpha} - \frac{1}{4} B^2 h + b^2 h \right\} \\ & \gamma_{soil} \left[Bh \left(\frac{3}{4} B - \frac{3}{4} b - \frac{1}{4} B \right) + b^2 h \right] \\ & \gamma_{soil} \left[Bh \left(\frac{1}{2} (2b) - \frac{3}{4} b \right) + b^2 h \right] \\ & \gamma_{soil} \left[Bh \left(\frac{1}{4} b \right) + b^2 h \right] > 0 \end{aligned}$$

Thus, $F_w\ strip > F_w\ square\ flat$.

Since $F_p\ strip > F_p\ square\ flat$, $F_f\ strip > F_f\ square\ flat$.

Similarly, $W_{soil\ above\ PY} > W_{soil\ above\ strip}$ and $W_{footing\ PY} = W_{footing\ strip}$, we could conclude that $F_w\ PY > F_w\ square\ flat$.

To prove that $F_p\ PY > F_p\ square\ flat$

$$F_p\ square\ flat - F_p\ PY = \frac{1}{2} \gamma_{soil} K_p (B-b) (a^2 - 2aD + D^2) - \frac{1}{2} \gamma_{soil} K_p a^2 \left(\frac{a-D}{\tan\alpha} \right)$$

Since $D < a < h + D$, if $a = h'$, $a - D = \frac{1}{2}(B-b)\tan\alpha$

$$F_p\ square\ flat - F_p\ PY = \frac{1}{2} \gamma_{soil} K_p (B-b) \left(\frac{1}{2} h^2 - hD - \frac{1}{2} D^2 \right)$$

If $h > (1 + \sqrt{2})D$, $F_p\ PY > F_p\ square\ flat$ and $F_f\ PY > F_f\ square\ flat$.

Nevertheless, if $h \leq (1 + \sqrt{2})D$, $F_p\ square\ flat > F_p\ PY$. In this situation, it was difficult to tell whether the sliding resistance of pyramidal shell footing was higher than that of flat footings, since $F_w\ PY > F_w\ square\ flat$.

■ For conical shell foundations

$$F_{p \text{ conical}} - F_{p \text{ circular flat}} = \frac{1}{2}\gamma_{soil}K_p(B-b)(a^2 - 2aD + D^2) - \frac{1}{2}\gamma_{soil}K_p a^2 \left(\frac{a-D}{\tan\alpha}\right)$$

Since $D < a < h + D$, if $a = h'$, $a - D = \frac{1}{2}(B - b)\tan\alpha$

$$F_{p \text{ conical}} - F_{p \text{ circular flat}} = \frac{1}{2}\gamma_{soil}K_p(B-b)\left(\frac{1}{2}h^2 - hD - \frac{1}{2}D^2\right)$$

If $h > (1 + \sqrt{2})D$, $F_{p \text{ conical}} > F_{p \text{ circular flat}}$

As mentioned in Case 1, $\frac{\tan(\phi)}{\tan(\frac{2}{3}\phi)} \geq 1.5$, $B \geq 2b$ and $\frac{\gamma_{footing}}{\gamma_{soil}} \leq 2$

Since $a < h'$, if $a = h'$, $a - D = \frac{1}{2}(B - b)\tan\alpha$

$$W_{soil \text{ above circular flat}} - \frac{3}{2}W_{soil \text{ above conical}} = \frac{\pi}{4}\gamma_{soil}(a - D)(B^2 - b^2) -$$

$$\frac{2\pi}{4}\gamma_{soil}\frac{(a-D)^2}{\tan\alpha}\left(\frac{3}{2}B - \frac{a-D}{\tan\alpha}\right) = \frac{\pi}{4}\gamma_{soil}(a - D)\left(\frac{1}{2}Bb - \frac{1}{2}b^2\right)$$

$$\text{Besides, } \frac{\pi}{8}\gamma_{soil}(B^3 - b^3)\tan\alpha + \frac{\pi}{8}\gamma_{footing}b^2H - \frac{3\pi}{8}\gamma_{footing}b^2\left(\frac{B-b}{2}\tan\alpha\right) > 0$$

To Prove that $\frac{\pi}{8}\gamma_{soil}(B^3 - b^3)\tan\alpha + \frac{\pi}{8}\gamma_{footing}b^2H - \frac{3\pi}{8}\gamma_{footing}b^2\left(\frac{B-b}{2}\tan\alpha\right) -$

$$\frac{\pi}{8}\gamma_{soil}\left(\frac{B-b}{2}\tan\alpha\right)(Bb - b^2) > 0$$

If $B = 2b$ and $\gamma_{footing} = 2\gamma_{soil}$

$$\frac{2\pi}{16}\gamma_{soil}B^3\tan\alpha - \frac{3\pi}{16}\gamma_{footing}b^2B\tan\alpha - \frac{\pi}{16}\gamma_{soil}(B^2b - 2Bb^2)$$

$$= \frac{\pi}{16}B\gamma_{soil}(8b^2 - 6b^2 - 2b^2 + 2b^2)\tan\alpha > 0$$

$$- \frac{2\pi}{16}\gamma_{soil}b^3\tan\alpha + \frac{3\pi}{16}\gamma_{footing}b^3\tan\alpha - \frac{\pi}{16}\gamma_{soil}b^3\tan\alpha = \frac{\pi}{16}b^3\gamma_{soil}(-2 + 6 -$$

$$1)\tan\alpha > 0$$

Thus $F_{w \text{ conical}} > F_{w \text{ circular flat}}$.

To sum up, $F_f \text{ conical} > F_f \text{ circular flat}$

If $h \leq (1 + \sqrt{2})D$, $F_p \text{ conical} < F_p \text{ circular flat}$.

Additionally, $F_w \text{ conical} > F_w \text{ circular flat}$.

In this situation, it was difficult to tell if the sliding resistance of the conical shell foundation was higher than the flat foundation.

The analysis revealed that the strip shell foundation model had the largest sliding resistances. There was a chance that the moment resistance of shell footing would be higher than the moment resistance for the flat foundation.

For the case of embedded depth in range from h' to H ($h' < a < H$), as shown in Figure 3-19.

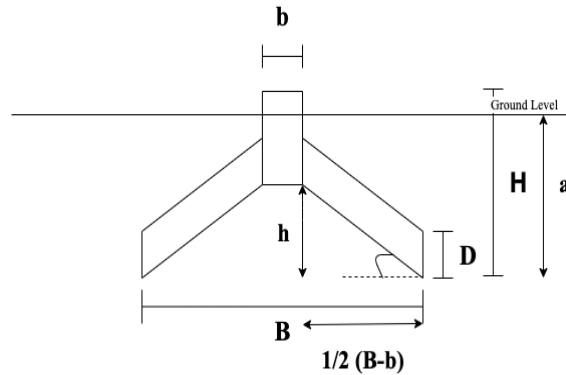


Figure 3-19. 2-D Shell foundation Model when $h' < a < H$

For the strip shell foundation

$$W_{soil\ above} = \gamma_{soil} \times \left[\frac{1}{4} B \times (B - b)^2 \tan \alpha + (a - h') \times (B^2 - b^2) \right] \quad (3-43)$$

where $h' = \frac{1}{2} (B - b) \tan \alpha + D$

$$F_1 = \frac{1}{2} \gamma_{soil} \times K_p \times b \times (a - h')^2 \quad (3-44)$$

$$RM_1 = F_1 \times \left[\frac{1}{3}(a - h') + h' \right] \quad (3-45)$$

$$F_2 = \frac{1}{2} \gamma_{soil} \times K_p \times B \times h' \times (2a - h') \quad (3-46)$$

$$RM_2 = \frac{1}{6} \gamma_{soil} \times K_p \times B \times h'^2 \times (3a - 2h') \quad (3-47)$$

For the pyramidal shell foundation

$$W_{soil\ above} = \gamma_{soil} \times \left[\frac{1}{6}(2B^3 - 3B^2b + b^3) \tan \alpha + (a - h') \times (B^2 - b^2) \right] \quad (3-48)$$

For the conical shell foundation

$$W_{soil\ above} = \frac{\pi}{12} \gamma_{soil} \left(\frac{B-b}{2} \tan \alpha \right) (2B^2 - Bb - b^2) + \frac{\pi}{4} \gamma_{soil} (a - h')(B^2 - b^2) \quad (3-49)$$

For conical and pyramidal shell foundations

$$F_1 = \frac{1}{2} \gamma_{soil} \times K_p \times b \times (a - h')^2 \quad (3-50)$$

$$RM_1 = F_1 \times \left[\frac{1}{3}(a - h') + h' \right] \quad (3-51)$$

$$F_2 = \frac{1}{2} \gamma_{soil} \times K_p \times \frac{B+b}{2} \times h' \times (2a - h') \quad (3-52)$$

$$RM_2 = \frac{1}{12} \gamma_{soil} \times K_p \times (B + b) \times h'^2 \times (3a - 2h') \quad (3-53)$$

According to Figure 3-17, equations (3-36) to (3-42) still used to calculate the circular and square flat foundations under the situation of $D < a < H$.

3.3.3-2 Analytical Analysis for $h' < a < H$

Moment Resistance

■ For strip and pyramidal shell foundations

$$W_{soil\ above\ square\ flat} : W_{soil\ above\ strip} : W_{soil\ above\ PY}$$

$$(a - D) \times (B^2 - b^2): \frac{1}{4}B \times (B - b)^2 \tan \alpha + \left(a - \frac{1}{2}(B - b) \tan \alpha - D \right) \times (B^2 - b^2):$$

$$\frac{1}{6}(2B^3 - 3B^2b + b^3) \tan \alpha + \left(a - \frac{1}{2}(B - b) \tan \alpha - D \right) \times (B^2 - b^2)$$

$$W_{soil \text{ above square flat}}: W_{soil \text{ above strip}}$$

$$2(B - b)(B^2 - b^2): B \times (B - b)^2$$

$$2(B + b) > B$$

$$W_{soil \text{ above square flat}}: W_{soil \text{ above PY}}$$

$$3(B - b)(B^2 - b^2): (2B^3 - 3B^2b + b^3)$$

$$B^3 + 2b^3 > 3Bb^2$$

$$W_{soil \text{ above strip}}: W_{soil \text{ above PY}}$$

$$3B \times (B - b)^2: 2(2B^3 - 3B^2b + b^3)$$

$$b^3 < B^3$$

So $W_{soil \text{ above square flat}} > W_{soil \text{ above PY}} > W_{soil \text{ above strip}}$

The previous analysis from case 1 revealed that $W_{strip \text{ footing}} = W_{PY \text{ footing}} < W_{square \text{ flat footing}}$.

$$M_{square \text{ flat footing}} > M_{PY \text{ footing}} > M_{strip \text{ footing}}$$

If the total moment resistance of the shell footing was greater than that of the flat foundation, it required $RM_{2 \text{ shell}} - RM_{2 \text{ square flat}} > (M_{square \text{ flat footing}} - M_{shell \text{ footing}}) + (RM_{1 \text{ square flat}} - RM_{1 \text{ shell}})$.

To prove that $RM_{1 \text{ strip}} + RM_{2 \text{ strip}} - RM_{1 \text{ square flat}} + RM_{2 \text{ square flat}} > 0$

Since $h' = h + D$, $h'^2 = h^2 + 2hD + D^2$ and $h'^3 = h^3 + 3h^2D + 3hD^2 + D^3$

$$\frac{1}{6} \gamma_{soil} K_p \{ B[3a(h'^2 - D^2) - 2(h'^3 - D^3)] - b[2(D^3 - h'^3) - a(D^2 - h'^2)] \} > 0$$

$$\frac{1}{2} \gamma_{soil} K_p a (h^2 + 2Dh)(B - b) - \left[\frac{1}{3} \gamma_{soil} K_p (h^3 + 3h^2D + 3hD^2) \right] (B - b) > 0$$

$$\gamma_{soil} K_p (B - b) \left[\frac{1}{2} ah^2 + aDh - \frac{1}{3} h^3 - h^2D - hD^2 \right] > 0$$

Since $a > h + D$, assume $a = h + D$

$$\frac{1}{6}h^3 + \frac{1}{2}hD^2 > 0$$

Also $M_{square\ flat\ footing} - M_{strip\ footing} = \gamma_{footing}h\left(\frac{B^2b}{2}\right) + \frac{1}{4}\gamma_{soil}hB(B^2 - b^2)$

$$\gamma_{soil}K_p\left(\frac{1}{6}h^3 + \frac{1}{2}hD^2\right) : \gamma_{footing}h\left(\frac{B^2b}{2}\right) + \frac{1}{4}\gamma_{soil}hB(B^2 - b^2)$$

Therefore, there was a chance that the total overturning moment resistance of strip shell footings would be higher than that of flat foundations when $a > h'$.

Similarly, if the total moment resistance of the pyramidal shell footing was greater than that of the square flat foundation, it required that $RM_{1PY} + RM_{2PY} - RM_{1square\ flat} - RM_{2square\ flat} > 0$

$$\begin{aligned} RM_{1PY} + RM_{2PY} - RM_{1square\ flat} - RM_{2square\ flat} &= \frac{1}{6}\gamma_{soil}K_p b(a^3 - 3ah'^2 + \\ &2h'^3) + \frac{1}{12}\gamma_{soil}K_p(B + b)(3ah'^2 - 2h'^3) - \frac{1}{6}\gamma_{soil}K_p b(a^3 - 3aD^2 + 2D^3) - \\ &\frac{1}{6}\gamma_{soil}K_p B(3aD^2 - 2D^3) = \frac{1}{12}\gamma_{soil}K_p(B - b)[3ah'^2 - 2h'^3 - 6aD^2 + 4D^3] \end{aligned}$$

Since $a > h + D$, assume $a = h + D$,

$$= \frac{1}{12}\gamma_{soil}K_p(B - b)[(h^3 - D^3) + (3h^2D - 3hD^2)]$$

If $h > D$, $RM_{PY} - RM_{square\ flat} > 0$

Therefore, there was a chance that the total moment resistance of pyramidal shell footings would be bigger than the moment resistance of flat foundation when $h > D$.

If $h < D$, $M_{total\ square\ flat\ footing} > M_{total\ PY\ shell\ footing}$

To sum up, there was a chance that the moment resistance of strip/ pyramidal footing would be bigger than that of square flat foundations when $a > h'$; furthermore, M_{strip} was always bigger than M_{py} when $a > h'$.

■ For the conical shell foundation

$$W_{soil \text{ above circular flat}} : W_{soil \text{ above conical}}$$

$$\frac{\pi}{4} \gamma_{soil} (a - D)(B^2 - b^2) : \frac{\pi}{12} \gamma_{soil} \left(\frac{B - b}{2} \tan \alpha \right) (2B^2 - Bb - b^2) + \frac{\pi}{4} \gamma_{soil} (a - h')(B^2 - b^2)$$

$$3(B^2 - b^2) > (2B^2 - Bb - b^2)$$

Thus $W_{soil \text{ above circular flat}} > W_{soil \text{ above conical}}$

To determine whether $RM_{conical} - RM_{circular \text{ flat}}$ large than 0 or less than 0

$$RM_{conical} - RM_{circular \text{ flat}} = \frac{1}{6} \gamma_{soil} K_p b (a^3 - 3ah'^2 + 2h'^3) + \frac{1}{12} \gamma_{soil} K_p (B + b)(3ah'^2 - 2h'^3) - \frac{1}{6} \gamma_{soil} K_p b (a^3 - 3aD^2 + 2D^3) - \frac{1}{6} \gamma_{soil} K_p B (3aD^2 - 2D^3)$$

$$= \frac{1}{12} \gamma_{soil} K_p (B - b) [3ah'^2 - 2h'^3 - 6aD^2 + 4D^3]$$

Since $a > h + D$, assume $a = h + D$,

$$= \frac{1}{12} \gamma_{soil} K_p (B - b) [(h^3 - D^3) + (3h^2D - 3hD^2)]$$

If $h > D$, $RM_{conical} - RM_{circular \text{ flat}} > 0$

Therefore, there was a chance that the total moment resistance of conical shell footings will be higher than that of flat foundation when $h > D$.

If $h < D$, $M_{total \text{ circular flat footing}} > M_{total \text{ conical shell footing}}$

Sliding Resistance:

■ For strip and pyramidal shell foundations

As mentioned in case 1, $\frac{\tan(\phi)}{\tan(\frac{2}{3}\phi)} \geq 1.5$.

$$F_{w \text{ square flat}}: F_{w \text{ strip}}$$

$$W_{\text{footing square flat}} + W_{\text{soil below square flat}} + W_{\text{soil above square flat}}$$

$$: 1.5 (W_{\text{footing strip}} + W_{\text{soil below strip}} + W_{\text{soil above strip}})$$

$$W_{\text{soil below square flat}} + W_{\text{soil above square flat}}: 1.5(W_{\text{soil below strip}} + W_{\text{soil above strip}})$$

$$\gamma_{\text{soil}} \left[\frac{3}{8}B(B-b)^2 \tan\alpha + \frac{3}{2} \left(a - \frac{1}{2}(B-b) \tan\alpha - D \right) (B^2 - b^2) + \frac{3}{2}B \frac{B^2 - b^2}{4} \tan\alpha \right. \\ \left. - (a - D)(B^2 - b^2) \right] > 0$$

$$\left[\frac{3}{8}B(B-b)^2 \tan\alpha + \left(\frac{1}{2}a - \frac{3}{4}(B-b) \tan\alpha - \frac{1}{2}D \right) (B^2 - b^2) + \frac{3}{2}B \frac{B^2 - b^2}{4} \tan\alpha \right] > 0$$

Since $a > h'$, assume $a = h'$

$$\frac{3}{8}B(B-b)^2 \tan\alpha + \left(-\frac{1}{2}(B-b) \tan\alpha \right) (B^2 - b^2) + \frac{3}{2}B \frac{B^2 - b^2}{4} \tan\alpha > 0$$

$$\frac{3}{8}B(B-b)(B+b) \tan\alpha - (B-b)^2 \tan\alpha \left(\frac{1}{8}B + \frac{1}{2}b \right) > 0$$

$$(B-b) \tan\alpha \left[\frac{1}{4}B^2 + \frac{1}{2}b^2 \right] > 0$$

$$1.5W_{\text{footing strip}} - W_{\text{footing square flat}} = \gamma_{\text{footing}} \left[\frac{1}{2}DB^2 + \frac{1}{2}Hb^2 - \frac{3}{4}b^2(B-b) \tan\alpha \right] = \frac{1}{2}DB^2 + \frac{1}{2}b^2(H-h) > 0$$

As mentioned in Case 1, $\frac{\gamma_{\text{footing}}}{\gamma_{\text{soil}}} < 2$. Under the condition of $B \geq 2b$, the value of

$$F_{w \text{ strip}} - F_{w \text{ square flat}} = \gamma_{\text{footing}} \left(\frac{1}{2}DB^2 + \frac{1}{2}Hb^2 \right) + \frac{3}{2}\gamma_{\text{soil}}(B-b) \tan\alpha -$$

$$\frac{3}{4}\gamma_{\text{footing}}b^2(B-b) \tan\alpha > 0$$

$$\text{Moreover, } F_{1 \text{ strip}} + F_{2 \text{ strip}} - F_{1 \text{ square flat}} - F_{2 \text{ square flat}} = \frac{1}{2}\gamma_{\text{soil}}K_p(B+b)(h^2 +$$

$$2hD) + \frac{1}{2}\gamma_{\text{soil}}K_p(B-b)(2ah) > 0$$

Therefore, $F_{f \text{ strip}} > F_{f \text{ square flat}}$.

Similarly, $W_{soil\ above\ PY} > W_{soil\ above\ strip}$ and $W_{footing\ PY} = W_{footing\ strip}$, we can conclude that $F_{w\ PY} > F_{w\ square\ flat}$.

Furthermore,

$$\begin{aligned}
 & F_{1\ strip} : F_{1\ PY} \\
 & \frac{1}{2} \gamma_{soil} \times K_p \times b \times (a - h')^2 = \frac{1}{2} \gamma_{soil} \times K_p \times b \times (a - h')^2 \\
 & F_{1\ square\ flat} : F_{1\ strip} \\
 & \frac{1}{2} \gamma_{soil} \times K_p \times b \times (a - D)^2 : \frac{1}{2} \gamma_{soil} \times K_p \times b \times (a - h')^2 \\
 & (a - D)^2 > \left(a - \frac{1}{2}(B - b)\tan\alpha - D \right)^2
 \end{aligned}$$

So $F_{1\ square\ flat} > F_{1\ strip} = F_{1\ PY}$

$$F_{2\ square\ flat} : F_{2\ PY}$$

When $\tan\alpha \left(a - \frac{B-b}{4}\tan\alpha - D \right) > \frac{1}{2}$, $F_{2\ square\ flat} < F_{2\ PY}$, otherwise $F_{2\ square\ flat} > F_{2\ PY}$

Under the condition of $\tan\alpha \left(a - \frac{B-b}{4}\tan\alpha - D \right) > \frac{1}{2}$, $F_{1\ PY} + F_{2\ PY} - F_{1\ square\ flat} - F_{2\ square\ flat} > 0$ and $F_{f\ PY} > F_{f\ square\ flat}$. When $\tan\alpha \left(a - \frac{B-b}{4}\tan\alpha - D \right) < \frac{1}{2}$, $F_{1\ PY} + F_{2\ PY} - F_{1\ square\ flat} - F_{2\ square\ flat} < 0$.

In this situation, it could not confirm whether the sliding resistance of the pyramidal shell foundation was higher than that of the flat foundation.

Moreover, to prove $F_{p\ PY} - F_{p\ square\ flat} < 0$

$$\begin{aligned}
 & \frac{1}{2} \gamma_{soil} K_p b (a - h')^2 + \frac{1}{4} \gamma_{soil} K_p (B + b) (2ah' - h'^2) - \frac{1}{2} \gamma_{soil} K_p b (a - D)^2 - \\
 & \frac{1}{2} \gamma_{soil} K_p B (2aD - D^2) < 0
 \end{aligned}$$

Since $a > h + D$, assume $a = h + D$,

$$= \frac{1}{4}\gamma_{soil}K_p(B-b)(h^2 - 2hD - D^2)$$

If $h > (1 + \sqrt{2})D$, $F_{p PY} > F_{p squareflat}$ and $F_{f PY} > F_{f square flat}$.

Nevertheless, if $h \leq (1 + \sqrt{2})D$, $F_{p squareflat} > F_{p PY}$. In this situation, it was difficult to tell whether the sliding resistance of pyramidal shell footing was higher than that of flat footings, since $F_{w PY} > F_{w square flat}$.

■ For the conical shell foundation

$$F_{p conical} - F_{p flat} < 0$$

$$\frac{1}{2}\gamma_{soil}K_p b(a - h')^2 + \frac{1}{4}\gamma_{soil}K_p(B + b)(2ah' - h'^2) - \frac{1}{2}\gamma_{soil}K_p b(a - D)^2 - \frac{1}{2}\gamma_{soil}K_p B(2aD - D^2) < 0$$

Since $a > h + D$, assume $a = h + D$,

$$= \frac{1}{4}\gamma_{soil}K_p(B-b)(h^2 - 2hD - D^2)$$

If $h > (1 + \sqrt{2})D$, $F_{p flat} < F_{p conical}$

$$\text{Moreover, } \frac{\pi}{8}\gamma_{soil}(B^3 - b^3)\tan\alpha + \frac{\pi}{8}\gamma_{footing}b^2H - \frac{3\pi}{8}\gamma_{footing}b^2\left(\frac{B-b}{2}\tan\alpha\right) > 0$$

Thus,

$$\frac{\pi}{8}\gamma_{soil}(B^3 - b^3)\tan\alpha + \frac{\pi}{8}\gamma_{footing}b^2H - \frac{3\pi}{8}\gamma_{footing}b^2\left(\frac{B-b}{2}\tan\alpha\right) - \frac{\pi}{8}\gamma_{soil}\left(\frac{B-b}{2}\tan\alpha\right)(B^2 + Bb - b^2) + \frac{\pi}{8}\gamma_{soil}(a - D)(B^2 - b^2) > 0$$

If $B = 2b$ and $\gamma_{footing} = 2\gamma_{soil}$

$$\frac{2\pi}{16}\gamma_{soil}B^3\tan\alpha - \frac{3\pi}{16}\gamma_{footing}b^2B\tan\alpha - \frac{\pi}{16}\gamma_{soil}B(B^2 + Bb - b^2)\tan\alpha + \frac{\pi}{16}\gamma_{soil}B(B^2 - b^2)\tan\alpha = \frac{\pi}{16}B\gamma_{soil}(8b^2 - 6b^2 - 5b^2 + 3b^2)\tan\alpha > 0$$

$$-\frac{2\pi}{16}\gamma_{soil}b^3\tan\alpha + \frac{3\pi}{16}\gamma_{footing}b^3\tan\alpha + \frac{\pi}{16}\gamma_{soil}b(B^2 + Bb - b^2)\tan\alpha - \frac{\pi}{16}\gamma_{soil}b(B^2 - b^2) = \frac{\pi}{16}b^3\gamma_{soil}(-2 + 6 + 5 - 3)\tan\alpha > 0$$

Thus $F_w\ conical > F_w\ flat$

Since $F_p\ conical > F_p\ flat$, $F_w\ conical > F_w\ flat$, $F_f\ conical > F_f\ flat$.

If $h \leq (1 + \sqrt{2})D$, $F_p\ conical < F_p\ circular\ flat$.

Additionally, $F_w\ conical > F_w\ circular\ flat$.

In this situation, it was difficult to tell if the sliding resistance of the conical shell foundation was higher than the flat foundation.

In summary, the analysis revealed that the strip shell foundation model had the largest sliding resistances. There was a chance that the moment resistance of shell footing would be bigger than that of flat foundation. For a clearer understanding, the following section provided several examples of foundations when the embedded depth is $D < a < H$.

3.3.3-3 Analytical Example

Since the above analytical studies could not clearly indicate in which circumstances the shell foundation was superior to resist lateral load, MATLAB coding was used to simulate all the scenarios where the embedded ratio (a/B) was from 1/5 to 1.

As shown in Tables 3-6 to 3-11, these shell foundation models had higher resistance to sliding friction than that of flat foundation models. According to Table 3-8 and Table 3-9, some of strip shell foundation models began to show superiority in the total moment resistance when the embedded ratio reached 11/15; nevertheless, pyramidal and conical shell foundation models' total moment resistance were still smaller than that of flat

foundations. When the buried ratio reached 14/15, all strip shell foundation models appeared the superiority in the total moment resistance; additionally, some pyramidal and conical shell foundation models also show the superiority in the total moment resistance, as shown in Table 3-10 and Table 3-11.

Table 3-6. Results of Sliding and Moment Resistance for Strip/Pyramidal Shell and Square Flat Foundations when $a/B=1/2$

Alpha (α) ($^{\circ}$)	0	10	20	30	40	50	60
Flat Foundation							
Total Friction Resistance, F_f (kN)	207.29						
Total Moment Resistance, RM_u (kN.m)	440.57						
Allowable Total Friction Resistance, $F_{f\ allow}$ (kN)	103.65						
Allowable Total Moment Resistance, RM_{allow} (kN.m)	146.86						
Strip Shell Foundation							
Total Friction Resistance, F_f (kN)		290.05	309.72	323.45	328.64	339.45	364.19
Total Moment Resistance, RM_u (kN.m)		425.69	410.89	389.01	352.29	321.35	295.2
Allowable Total Friction Resistance, $F_{f\ allow}$ (kN)		145.03	154.86	161.73	164.32	169.73	182.1
Allowable Total Moment Resistance, RM_{allow} (kN.m)		141.9	136.96	129.67	117.43	107.12	98.4
Pyramidal Shell Foundation							
Total Friction Resistance, F_f (kN)		237.73	247.65	254.23	259.61	282.43	308.28
Total Moment Resistance, RM_u (kN.m)		418.2	405.29	387.11	360.99	337.53	311.47
Allowable Total Friction Resistance, $F_{f\ allow}$ (kN)		118.87	123.83	127.12	129.81	141.22	154.14
Allowable Total Moment Resistance, RM_{allow} (kN.m)		139.4	135.1	129.04	120.33	112.51	103.82

Table 3-7. Results of Sliding and Moment Resistance for Conical Shell and Circular Flat Foundations when $a/B=1/2$

Alpha (α) ($^{\circ}$)	0	10	20	30	40	50	60
Circular Flat Foundation							
Total Friction Resistance, F_f (kN)	186.06						
Total Moment Resistance, RM_u (kN.m)	353.09						
Allowable Total Friction Resistance, $F_{f\ allow}$ (kN)	93.03						
Allowable Total Moment Resistance, RM_{allow} (kN.m)	117.7						
Conical Shell Foundation							
Total Friction Resistance, F_f (kN)		210.19	226.55	240.62	255.14	289.58	331.76
Total Moment Resistance, RM_u (kN.m)		335.17	326.73	314.11	294.66	278.4	259.55
Allowable Total Friction Resistance, $F_{f\ allow}$ (kN)		105.1	113.28	120.31	127.57	144.79	165.88
Allowable Total Moment Resistance, RM_{allow} (kN.m)		111.72	108.91	104.7	98.22	92.8	86.52

Table 3-8. Results of Sliding and Moment Resistance for Strip/Pyramidal Shell and Square Flat Foundations when $a/B=11/15$

Alpha (α) ($^{\circ}$)	0	10	20	30	40	50	60
Flat Foundation							
Total Friction Resistance, F_f (kN)	322.84						
Total Moment Resistance, RM_u (kN.m)	638.82						
Allowable Total Friction Resistance, $F_{f\ allow}$ (kN)	161.42						
Allowable Total Moment Resistance, RM_{allow} (kN.m)	212.94						
Strip Shell Foundation							
Total Friction Resistance, F_f (kN)		447.44	487.65	525.47	559.18	582.93	594.45
Total Moment Resistance, RM_u (kN.m)		635.92	638.24	642.53	644.32	626.13	564.14
Allowable Total Friction Resistance, $F_{f\ allow}$ (kN)		223.72	243.83	262.74	279.59	291.47	297.23

Allowable Total Moment Resistance, RM_{allow} (kN.m)		211.97	212.75	214.18	214.77	208.71	188.05
Pyramidal Shell Foundation							
Total Friction Resistance, F_f (kN)		363	383.17	401.81	418.37	430.06	465.59
Total Moment Resistance, RM_u (kN.m)		616.88	612.52	607.42	599.56	579.19	547.27
Allowable Total Friction Resistance, $F_{f\ allow}$ (kN)		181.5	191.59	200.91	209.19	215.03	232.8
Allowable Total Moment Resistance, RM_{allow} (kN.m)		205.63	204.17	202.47	199.85	193.06	182.42

Table 3-9. Results of Sliding and Moment Resistance for Conical Shell and Circular Flat Foundations when a/B=11/15

Alpha (α)	0	10	20	30	40	50	60
Circular Flat Foundation							
Total Friction Resistance, F_f (kN)	293.48						
Total Moment Resistance, RM_u (kN.m)	517.82						
Allowable Total Friction Resistance, $F_{f\ allow}$ (kN)	146.74						
Allowable Total Moment Resistance, RM_{allow} (kN.m)	172.61						
Conical Shell Foundation							
Total Friction Resistance, F_f (kN)		322.56	394.17	375.31	401.02	424.97	478.94
Total Moment Resistance, RM_u (kN.m)		500.32	500.45	500.91	499.78	488.26	469.03
Allowable Total Friction Resistance, $F_{f\ allow}$ (kN)		161.28	174.59	187.66	200.51	212.49	239.47
Allowable Total Moment Resistance, RM_{allow} (kN.m)		166.77	166.82	166.97	166.59	162.75	156.34

Table 3-10. Results of Sliding and Moment Resistance for Strip/Pyramidal Shell and Square Flat Foundations when a/B=14/15

Alpha (α) ($^{\circ}$)	0	10	20	30	40	50	60
Flat Foundation							
Total Friction Resistance, F_f (kN)	431.82						
Total Moment Resistance, RM_u (kN.m)	830.31						
Allowable Total Friction Resistance, $F_{f\ allow}$ (kN)	215.91						
Allowable Total Moment Resistance, RM_{allow} (kN.m)	138.38						
Strip Shell Foundation							
Total Friction Resistance, F_f (kN)		592.3	650.11	708.58	767.53	824.95	864.6
Total Moment Resistance, RM_u (kN.m)		837.67	854.7	881.38	918.13	959.54	957.88
Allowable Total Friction Resistance, $F_{f\ allow}$ (kN)		296.15	325.06	354.29	383.77	412.48	432.3
Allowable Total Moment Resistance, RM_{allow} (kN.m)		139.61	142.45	146.9	153.02	159.92	159.65
Pyramidal Shell Foundation							
Total Friction Resistance, F_f (kN)		480.31	509.29	538.25	567.43	595.96	615.24
Total Moment Resistance, RM_u (kN.m)		808.7	811.7	817.79	827.42	836.87	818.11
Allowable Total Friction Resistance, $F_{f\ allow}$ (kN)		240.16	254.65	269.13	283.72	297.98	307.62
Allowable Total Moment Resistance, RM_{allow} (kN.m)		134.78	135.28	136.3	137.9	139.48	136.35

Table 3-11. Results of Sliding and Moment Resistance for Conical Shell and Circular Flat Foundations when a/B=14/15

Alpha (α) ($^{\circ}$)	0	10	20	30	40	50	60
Circular Flat Foundation							
Total Friction Resistance, F_f (kN)	395.49						
Total Moment Resistance, RM_u (kN.m)	680.56						
Allowable Total Friction Resistance, $F_{f\ allow}$ (kN)	197.75						

Allowable Total Moment Resistance, RM_{allow} ($kN.m$)	226.85						
Conical Shell Foundation							
Total Friction Resistance, F_f (kN)		428.8	464.23	500.68	539.02	579.81	617.98
Total Moment Resistance, RM_u ($kN.m$)		663.4	670.91	682.54	698.92	717.22	712.32
Allowable Total Friction Resistance, $F_{f\ allow}$ (kN)		214.4	232.12	250.34	269.51	289.91	308.99
Allowable Total Moment Resistance, RM_{allow} ($kN.m$)		221.13	223.64	227.51	232.97	239.07	237.44

In general, with the embedment ratio growth, the passive earth pressure grows rapidly, as shown in Figures 3-20 and 3-21. For example, when the embedding ratio increased from 7/30 to 1/3, 1/3 to 11/15 and 11/15 to 14/15, the sliding resistance caused by passive pressure of a conical shell foundation at the angle of 10° increased by about 45%, 70%, and 30%, respectively. These two figures showed that the embedment ratio from 1/6 to 1/3, the passive earth pressure of different shell angles was almost the same, especially for strip shell foundations. However, the embedment ratio starting from 8/15, the differences in passive earth pressure at different shell angles became obvious.

Moreover, according to Figure 3-20, the passive earth pressure of conical or pyramidal shell foundation had a lower passive earth pressure than that of flat foundations when shell angle below 30 degrees. In the shell angle range of 30 to 40 degrees, the passive earth pressure of shell footings would eventually exceed that of flat footings as the embedment ratio rise. When the shell angle over 50 degrees, the passive earth pressure of shell footings would always be higher than that of flat footings. The reason was that in the range of 0 to 20 degrees, the passive earth pressure decreased as the shell angle increased. Once the shell angle exceeded 20 degrees, the passive earth pressure would increase with the increase of the shell angle, as shown in Figure 3-22. However, flat foundations' passive earth pressure was the smaller than that of any shell angle of a foundation at any shell angle, as shown in Figure 3-21.

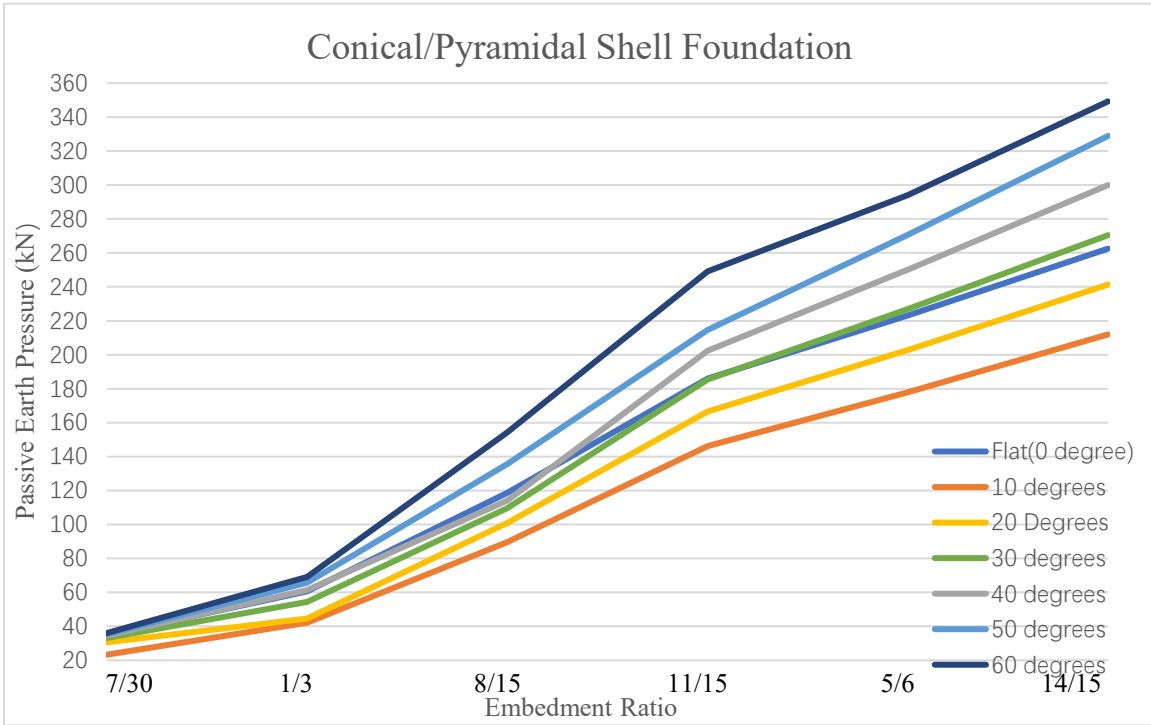


Figure 3-20. Passive Earth Pressure of Conical/Pyramidal Shell Foundations with Various Shell Angles in Different Embedment Ratio when $a > D$

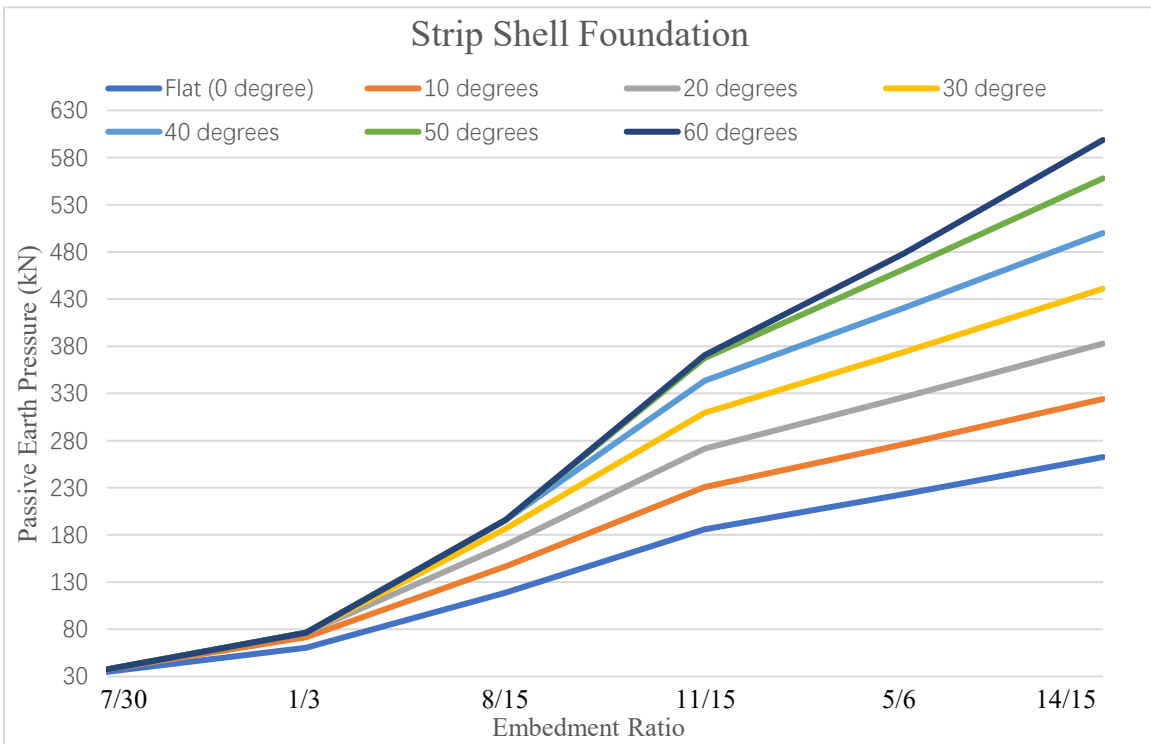


Figure 3-21. Passive Earth Pressure of Strip Shell Foundations with Various Shell Angles in Different Embedment Ratio when $a > D$

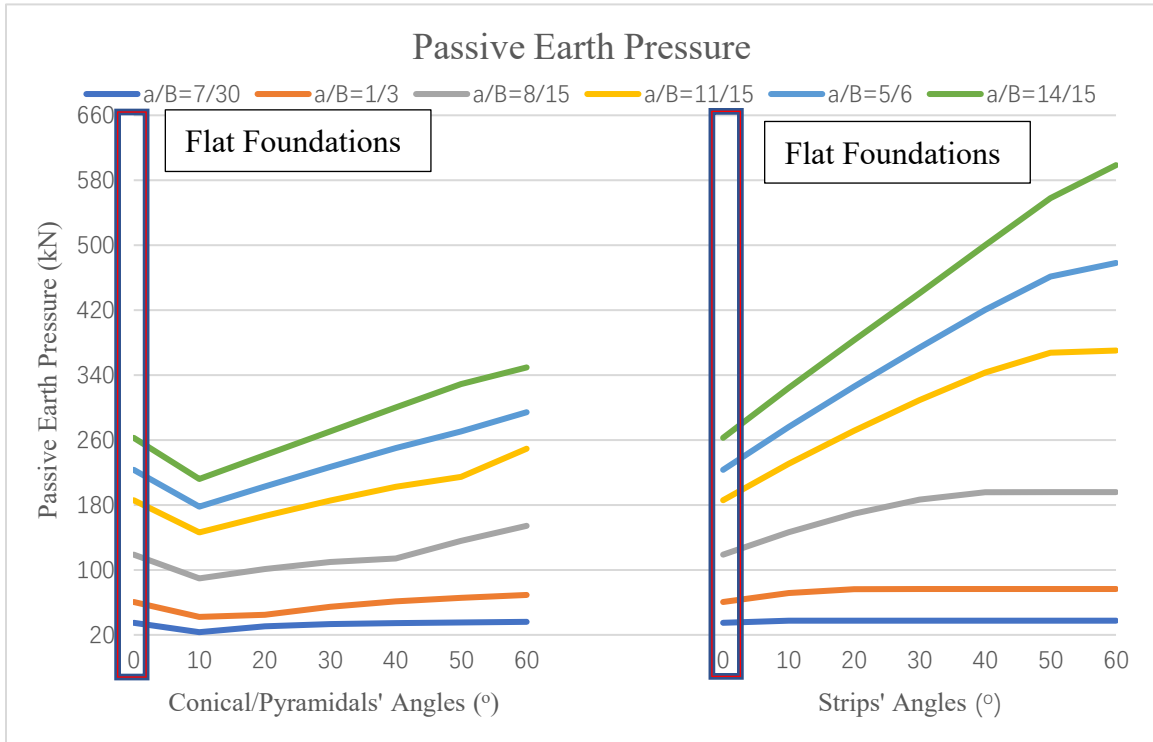


Figure 3-22. Passive Earth Pressure of Conical/Pyramidal/Strip Shell Foundations with Various Shell Angles in Different Embedment Ratio when $a > D$ (0° Shell Foundations = Flat Foundations)

Figures 3-23 to 4-25 had similar upward trends as Figures 3-20 and 3-21. However, unlike Figure 3-20, the line of the flat foundation always remains at the bottom, regardless of the embedded ratio. In summary, under the situation of $a > D$, the total sliding resistance of shell foundations were always larger than that of flat foundation.

Figure 3-26 exhibited that the total sliding resistance of shell foundations showed a linear upward trend when the embedment ratio was between 11/15 to 14/15. On the other hand, when the embedment ratio was from 7/30 to 8/15, the total sliding resistance of shell foundations revealed a concave upward trend with the increase of the shell angle. Moreover, the total sliding resistance of strip shell foundations increased much more rapidly than others when the embedment ratio was between 11/15 to 14/15.

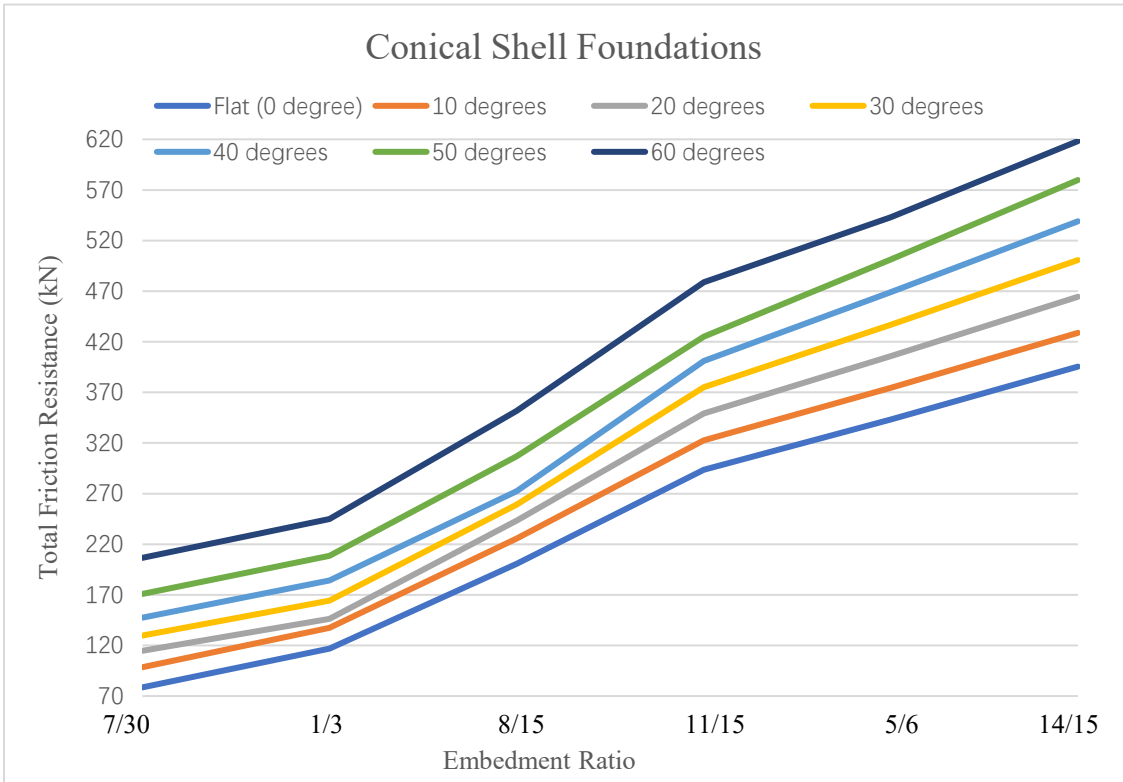


Figure 3-23. Total Lateral Friction Resistance of Conical Shell Foundations with Various Shell Angles in Different Embedment Ratio when $a > D$

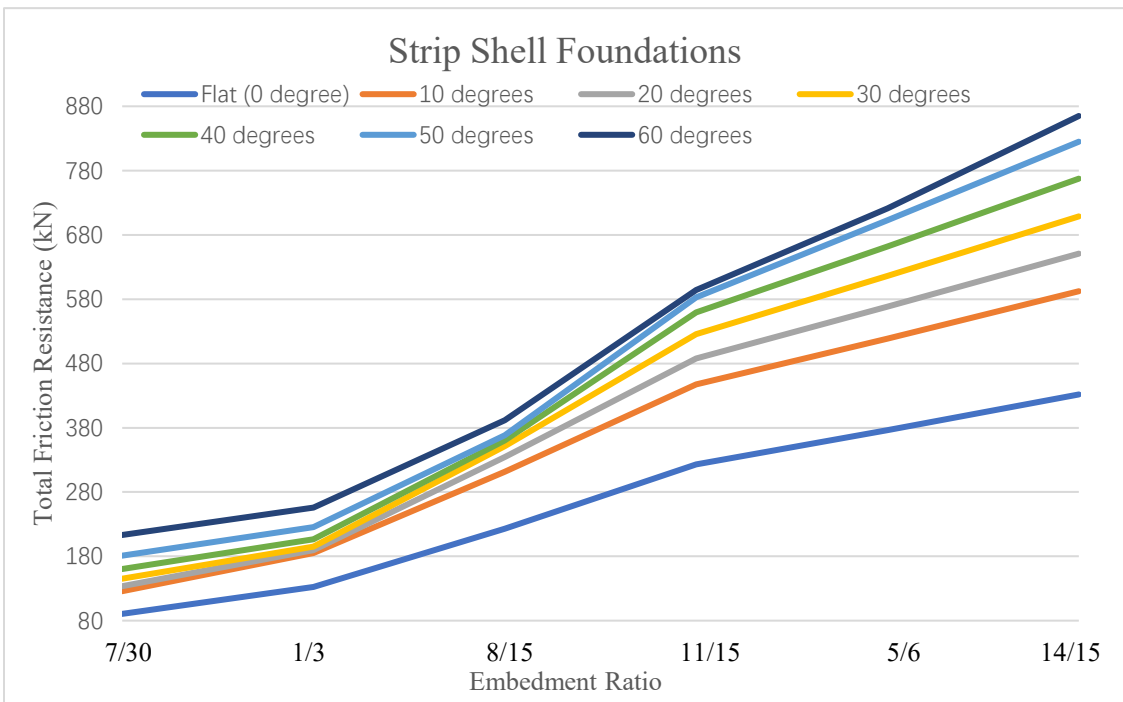


Figure 3-24. Total Lateral Friction Resistance of Strip Shell Foundations with Various Shell Angles in Different Embedment Ratio when $a > D$

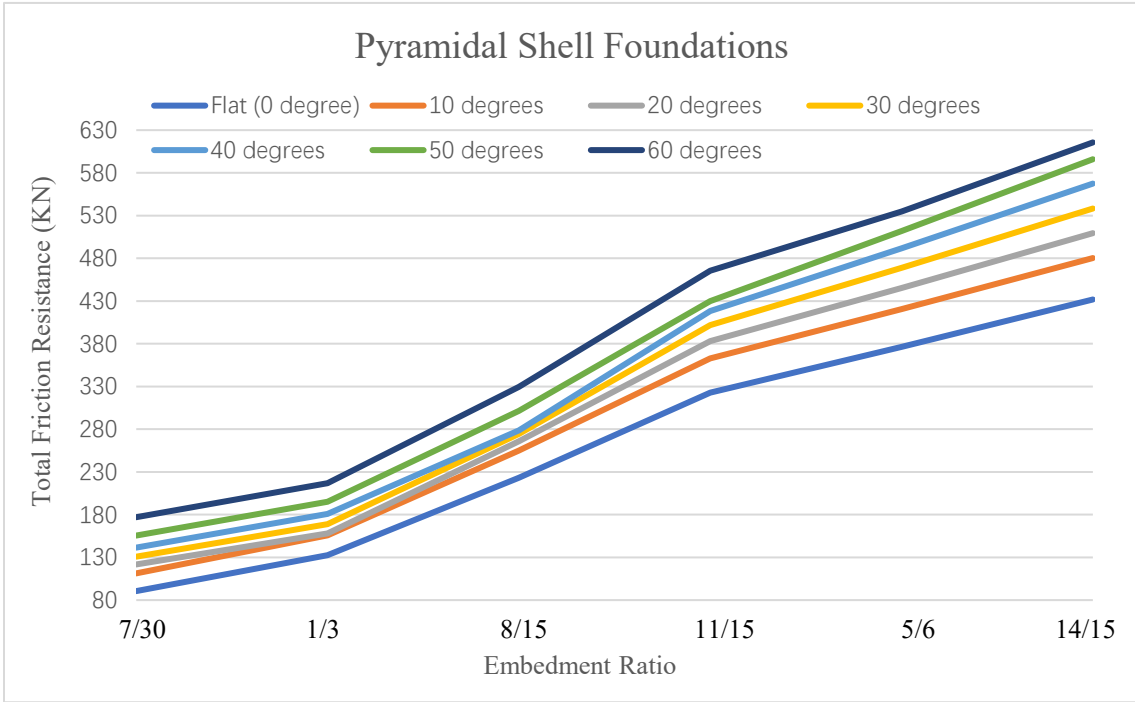


Figure 3-25. Total Lateral Friction Resistance of Pyramidal Shell Foundations with Various Shell Angles in Different Embedment Ratio when $a > D$

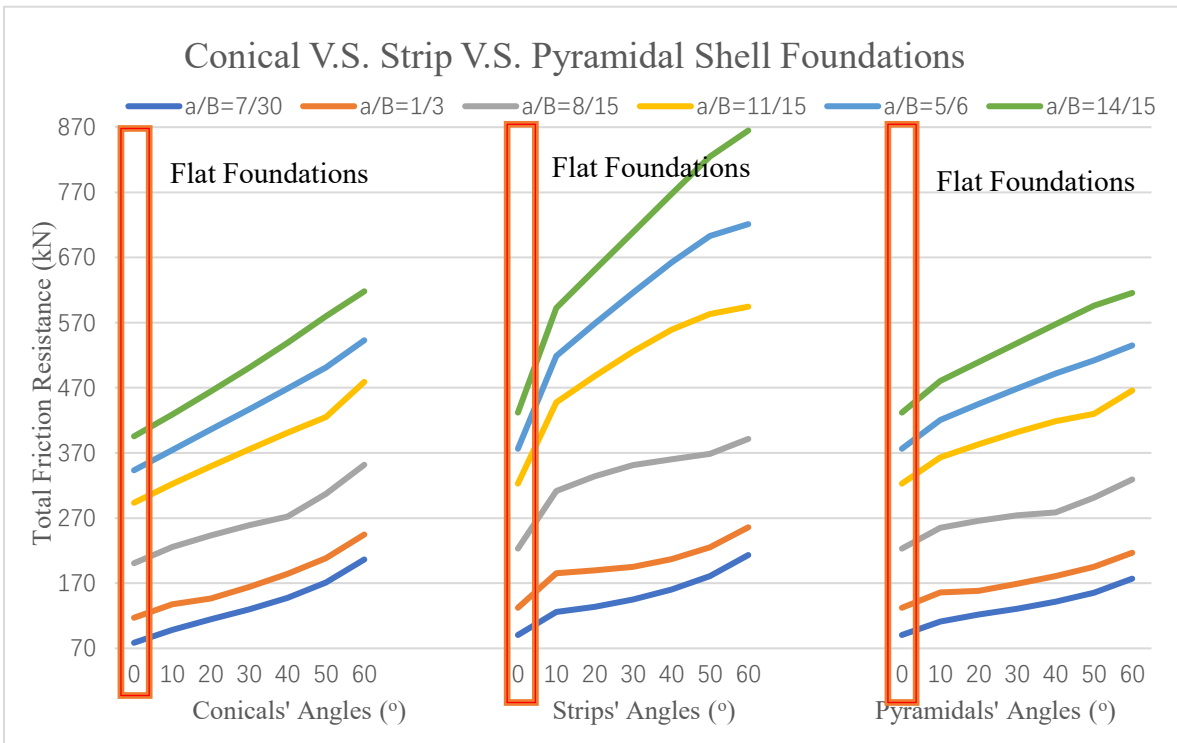


Figure 3-26. Total Lateral Friction of Conical/Strip/Pyramidal Shell Foundations with Various Shell Angles in Different Embedment Ratio when $a > D$ (0° Shell Foundations = Flat Foundations)

Referring to Figures 3-27 to 3-28, the overturning moment resistance caused by passive earth pressure raised with the increase of the embedment ratio. Compared with the strip shell foundation, the overturning moment resistance caused by passive earth pressure of flat foundations was always the lowest. Nevertheless, when the shell angle was less than 10 degrees, the anti-overturning moment caused by passive earth pressure of pyramidal and conical shell foundations were lower than that of flat foundations. It could be seen from these figures that the change in anti-overturning moment (caused by passive pressure) was dominated by the embedment ratio, especially when the buried ratio reached 11/15 or more.

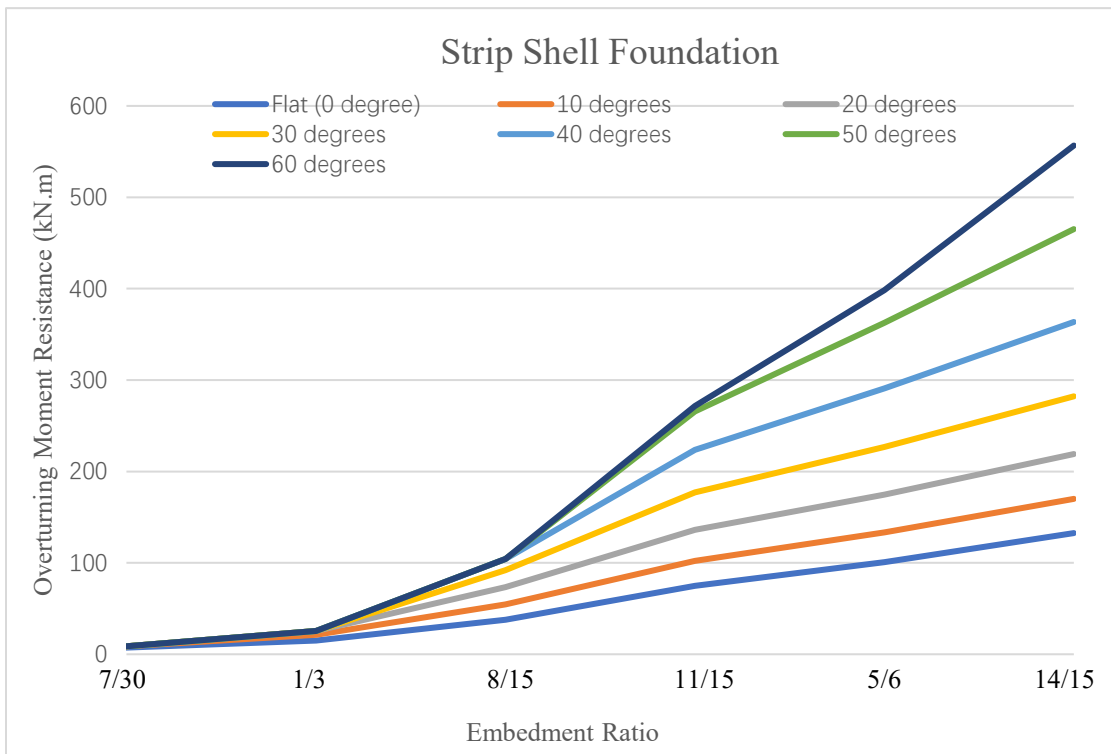


Figure 3-27. Overturning Moment due to Passive Earth Pressure for Strip Shell Foundations with Various Shell Angles in Different Embedment ratio when $a > D$

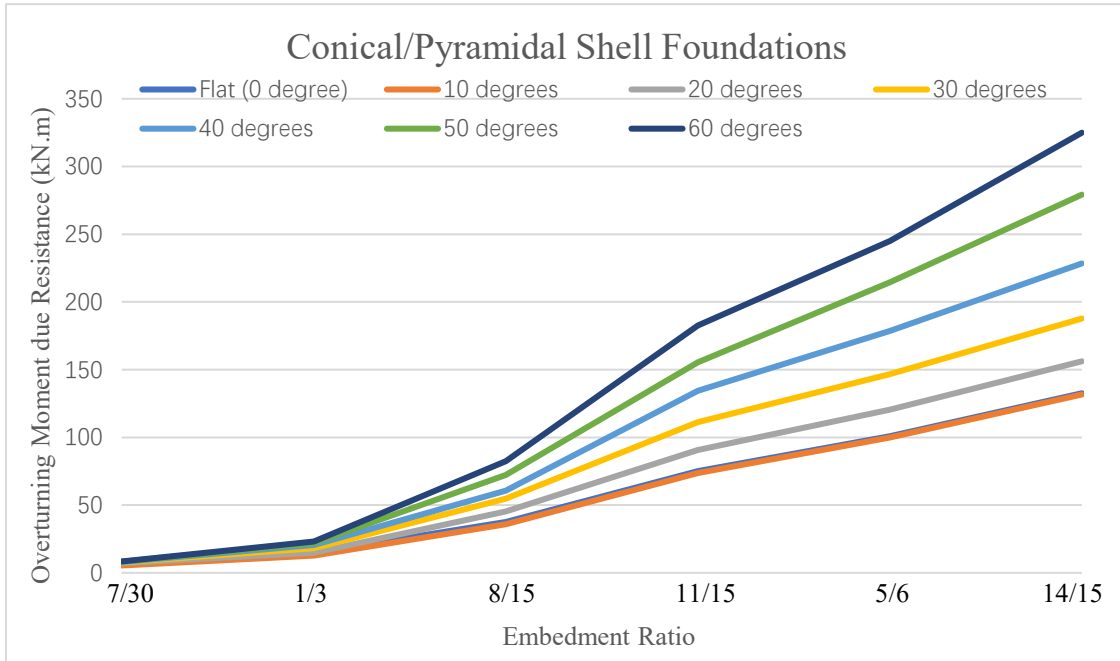


Figure 3-28. Overturning Moment due to Passive Earth Pressure for Conical/Pyramidal Shell Foundations with Various Shell Angles in Different Embedment Ratio when $a > D$

Figures 3-29 and 3-30 indicated that when the shell angle increased by 10 degrees, the anti-overturning moment, due to the passive pressure, for the strip, pyramidal, and conical would increase by approximately 16% to 22%, 14% to 18%, and 14% to 18%, respectively. In contrast, the overturning moment resistance, which caused by the self-weight (including the soil above the foundation), for the strip, pyramidal, and conical by increasing the shell angle by 10 degrees, would drop by approximately 4.8% to 18.6%, 5.1% to 11.4%, and 4.9% to 12.8%, respectively. Nevertheless, these rates of the increase of the anti-overturning moment (caused by passive pressure) and the rates of decrease of the anti-overturning moment (caused by the self-weight and the soil weight above the foundation) varied with the increase of the shell angle. Therefore, the total overturning moment resistance might decrease or increase as the rise of the shell angle, depending on the embedment ratio.

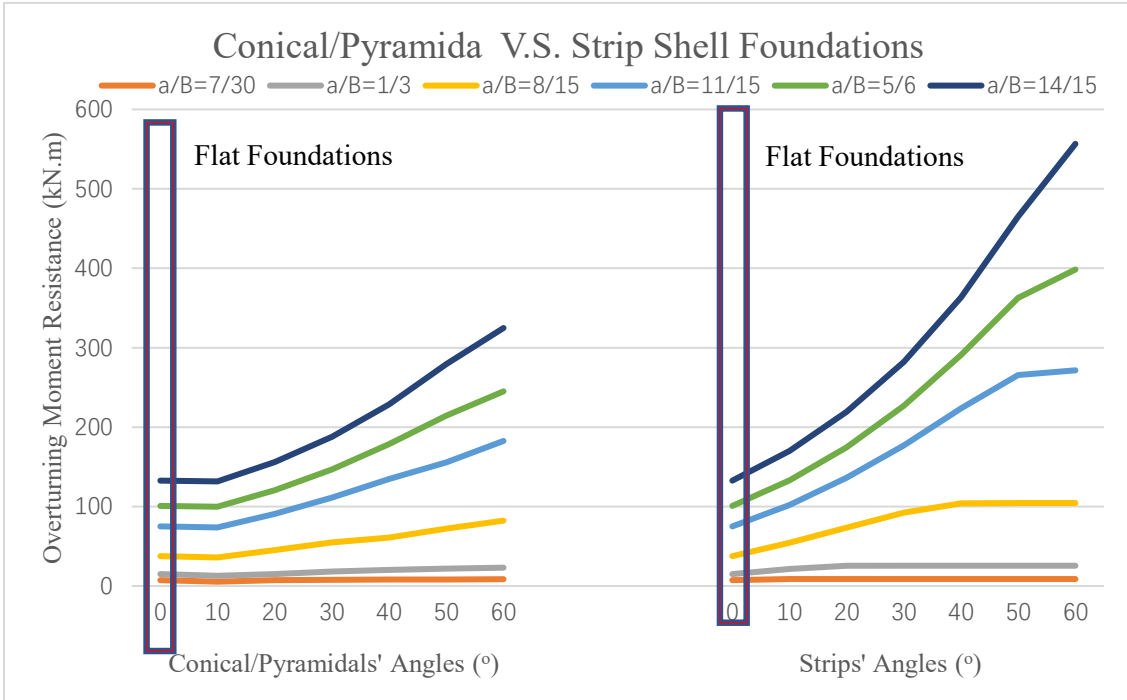


Figure 3-29. Overturning Moment due to Passive Earth Pressure for Conical/Pyramidal/Strip Shell Foundations with Various Shell Angles in Different Embedment Ratio when $a>D$ (0° Shell Foundations = Flat Foundations)

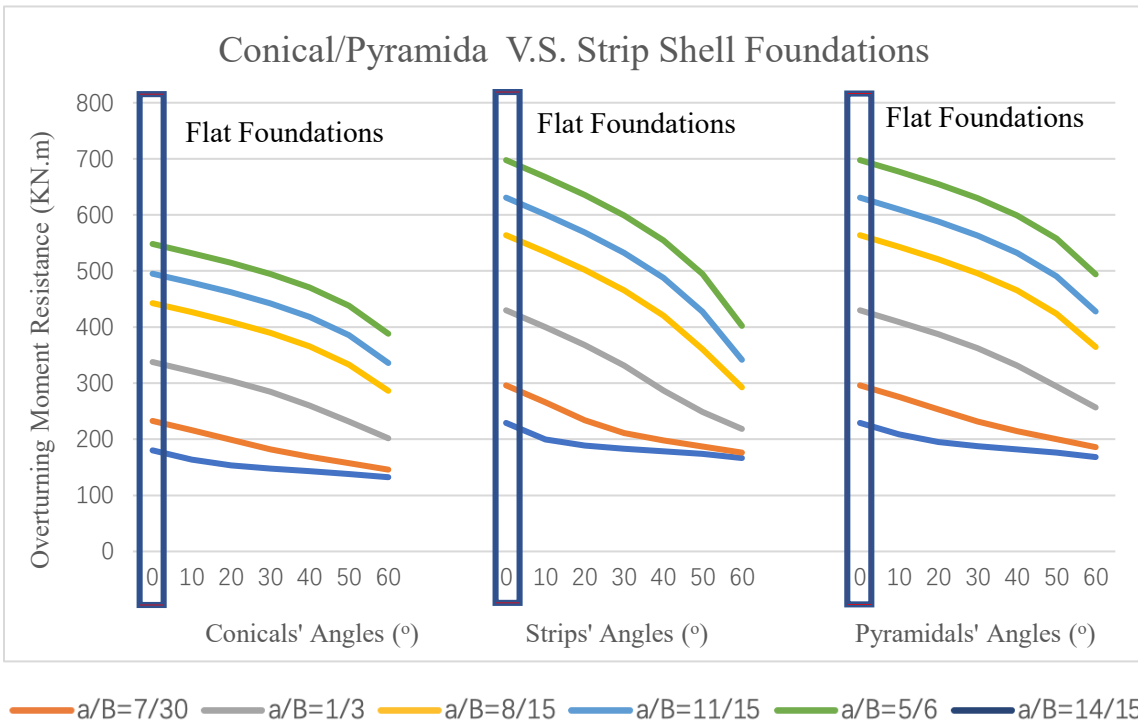


Figure 3-30. Overturning Moment due to Weight of Footings and Weight of Soil above Footings Conical/Pyramidal/Strip Shell Foundations with Various Shell Angles in Different Embedment Ratio when $a>D$ (0° Shell Foundations = Flat Foundations)

Figures 3-31 to 3-36 indicated that the total overturning moment increased with the increase of embedment ratio. Figures 3-32, 3-34, and 4-36 were enlarged views of Figures 3-31, 3-33, and 3-35 in the range of the embedment ratio from 11/15 to 14/15, respectively. According to these figures, for embedment ratio of the strip shell, conical and pyramid shapes foundations reach 11/15, 5/6, and 14/15 respectively, then the total moment resistance was greater than that of the flat foundation. Furthermore, as the embedment ratio increases, the increase in the total anti-overturning moment decreased. Taking a strip shell foundation with a shell angle of 10 degrees as an example, when the embedment ratio increased from 7/30 to 1/3, 13/30 to 8/15, and 5/6 to 14/15, the total moment resistance increased by about 26.1%, 14.3%, and 12.7%, respectively.

Figures 3-32 and 3-34 indicated that when shell angle increased from 10 to 40 degrees, total moment resistance of all embedment ratios was gradually increased. Nonetheless, total moment resistance dramatically decreased when the shell angle exceeded 50 degrees. It is because the weight of the soil above the shell foundation was significantly reduced in the higher shell angle as shown in Figure 3-40. The reduction in the weight of the soil above the shell foundation led to a reduction in moment resistance (due to weight of soil above footings) and moment resistance (due to passive earth pressure). Therefore, the total moment resistance of the strip/pyramidal/conical shell foundation decreased once the shell angle exceeds 50 degrees.

For embedment ratio less than 11/15, the total overturning moment was inversely proportional to the rise of shell angles. However, if embedment ratio reached 13/15, the total overturning moment rises with the increment of shell angle initially, but it drops again after the angle reaches 50 degrees, as shown in Figure 3-37.

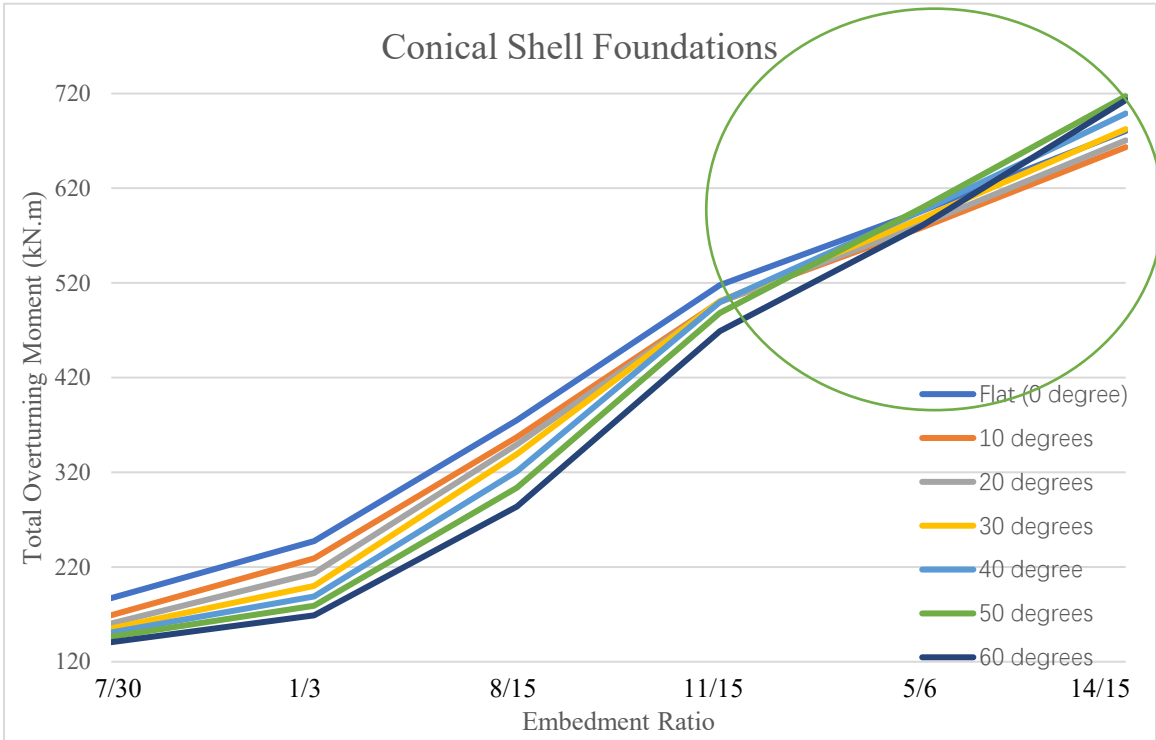


Figure 3-31. Total Overturning Moment Resistance for Conical Shell Foundations with Various Shell Angles in Different Embedment Ratio when $a > D$

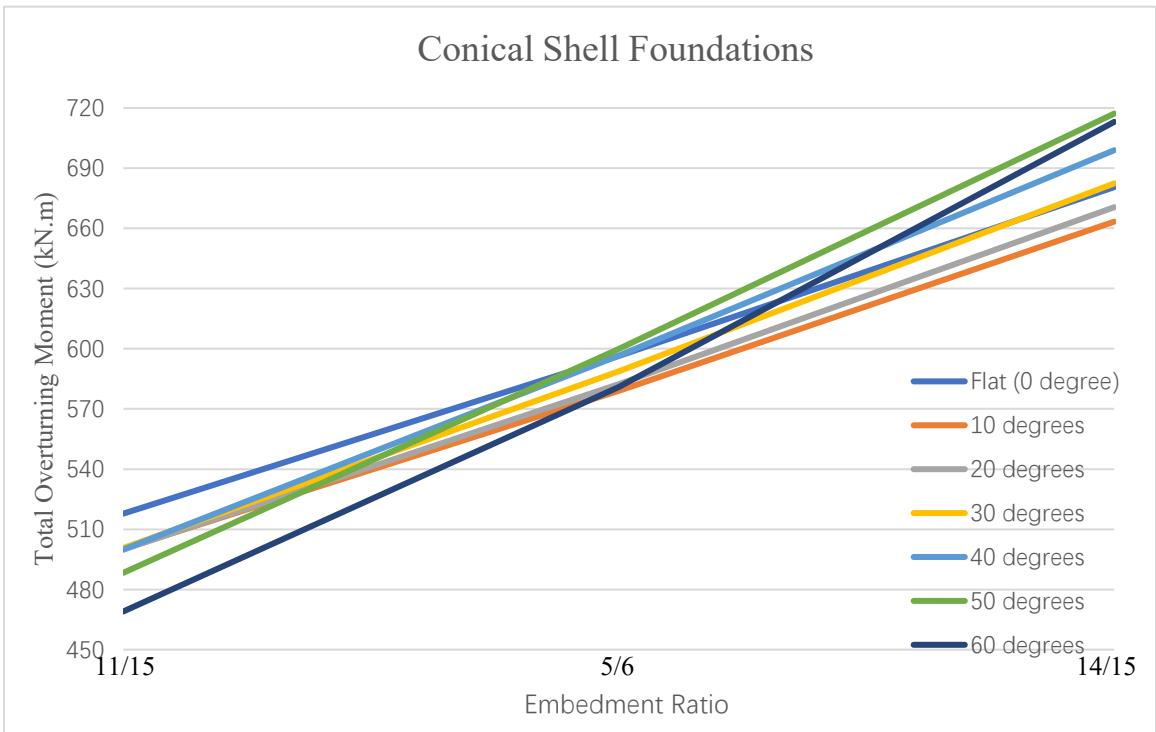


Figure 3-32. Total Overturning Moment Resistance for Conical Shell Foundations with Various Shell Angles in Embedment Ratio Between 11/15 to 14/15

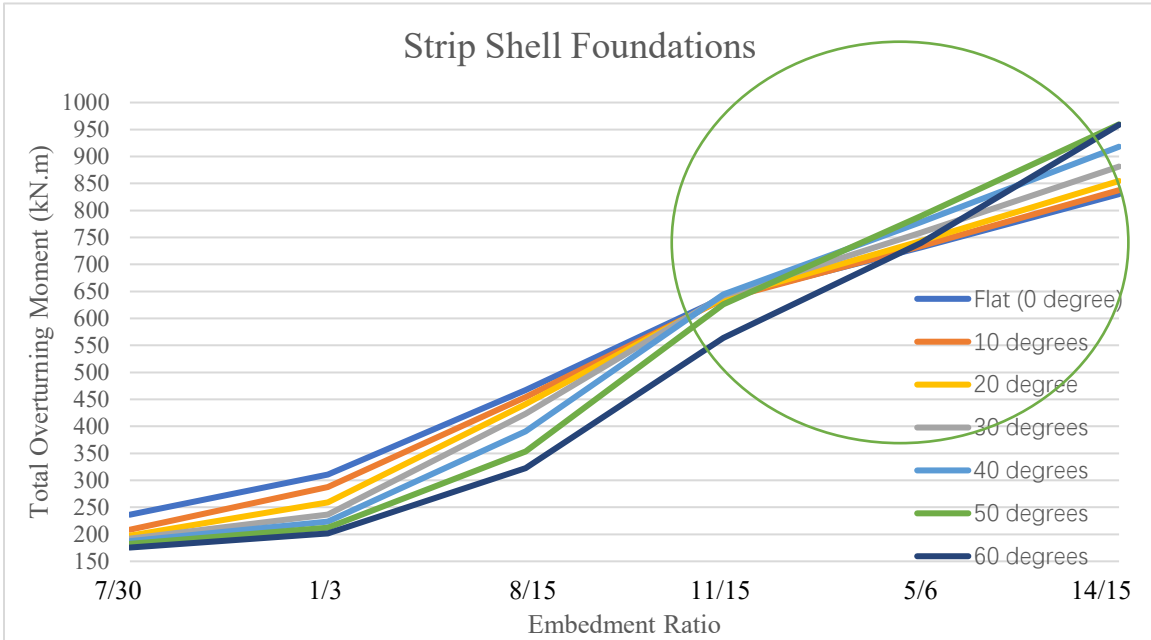


Figure 3-33. Total Overturning Moment Resistance for Strip Shell Foundations with Various Shell Angles in Different Embedment Ratio when $a > D$

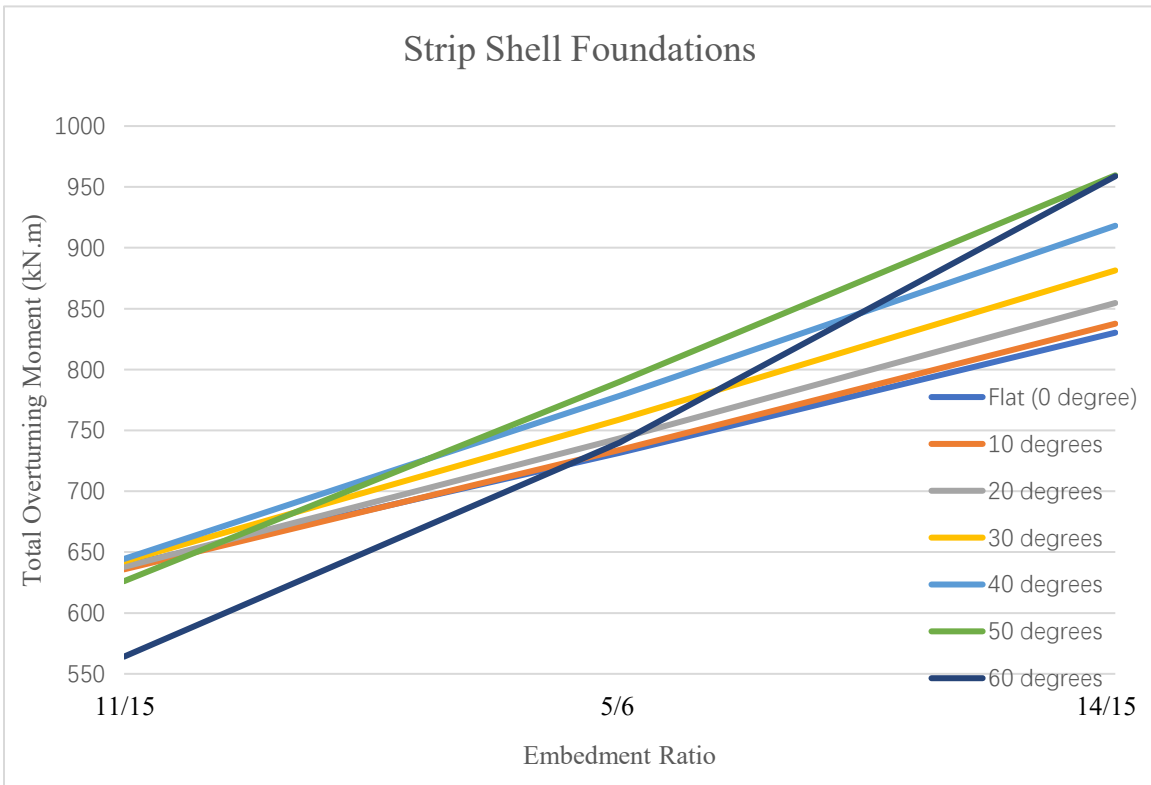


Figure 3-34. Total Overturning Moment Resistance for Strip Shell Foundations with Various Shell Angles in Embedment Ratio Between 11/15 to 14/15

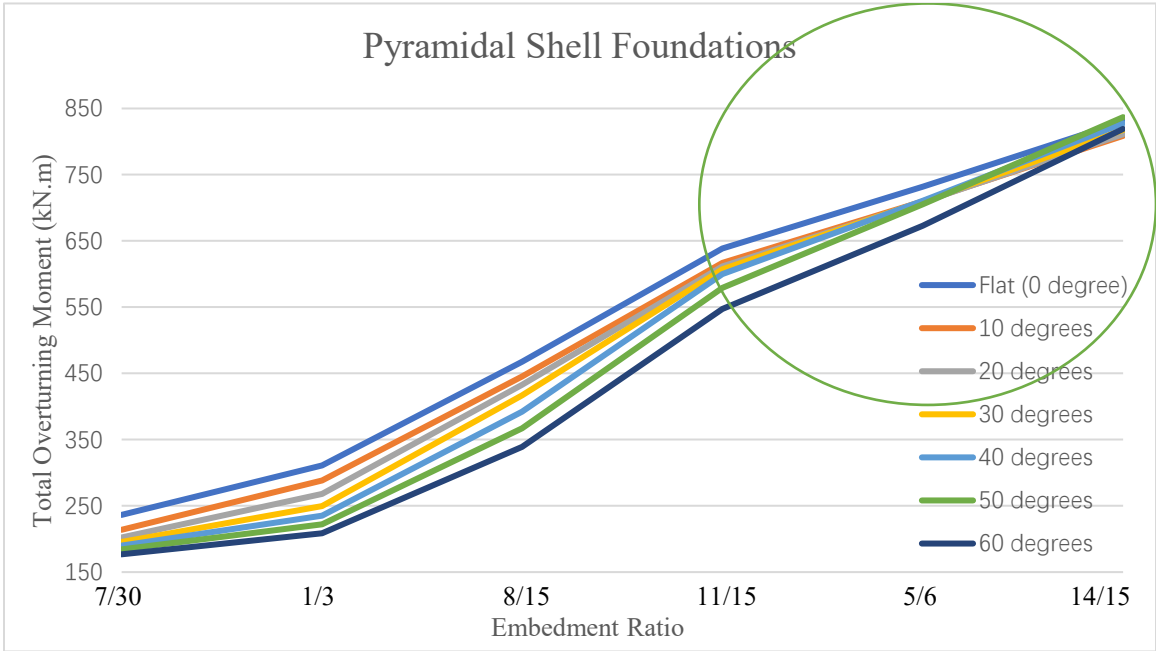


Figure 3-35. Total Overturning Moment Resistance for Pyramidal Shell Foundations with Various Shell Angles in Different Embedment Ratio when $a > D$

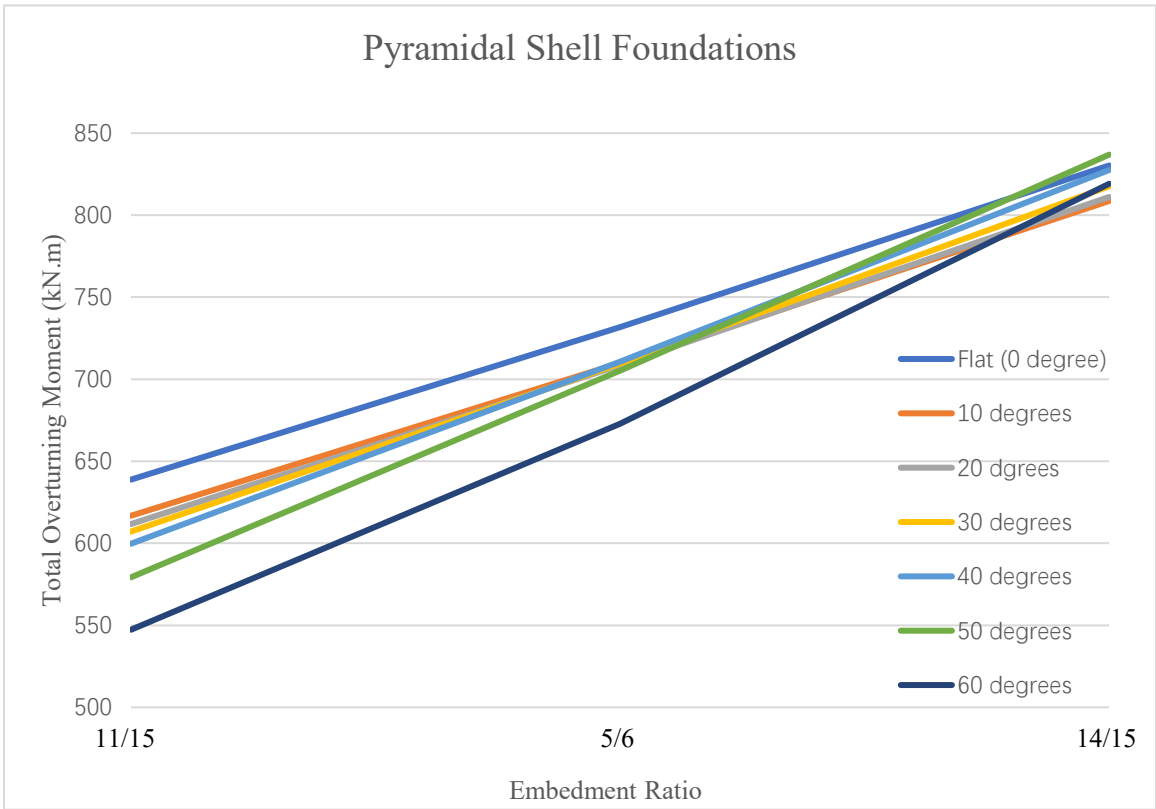


Figure 3-36. Total Overturning Moment Resistance for Pyramidal Shell Foundations with Various Shell Angles in Embedment Ratio Between 11/15 to 14/15

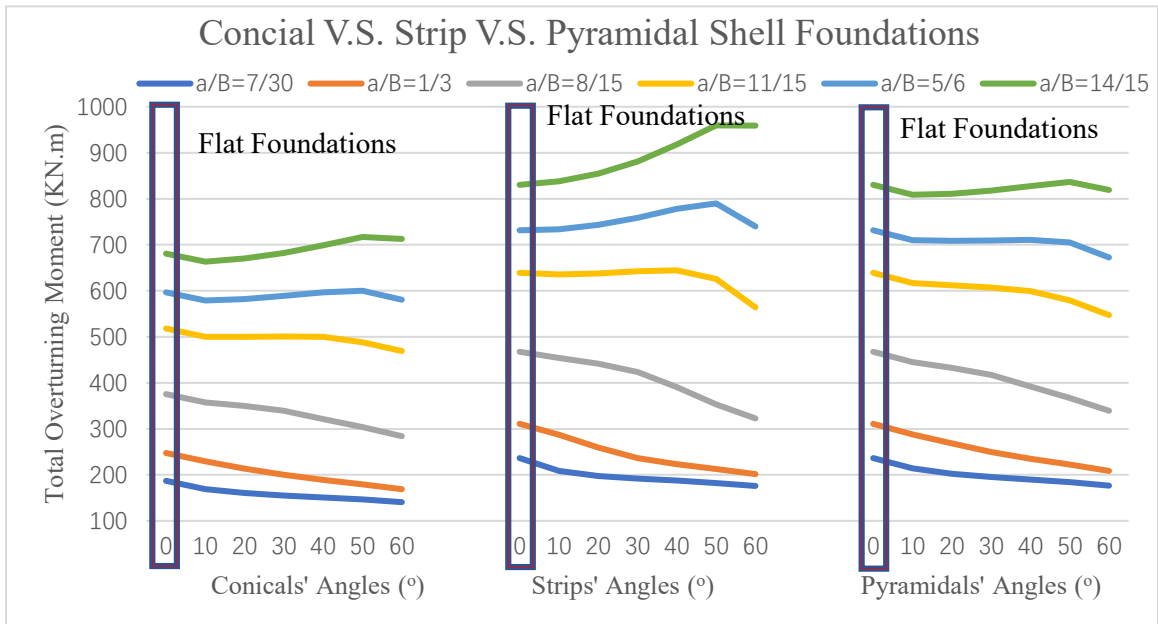


Figure 3-37. Total Overturning Moment Resistance for Conical/Strip/Pyramidal Shell Foundations with Various Shell Angles in Embedment Ratio Between 7/30 to 14/15 (0° Shell Foundations = Flat Foundations)

Figures 3-38 and 3-40 showed that the increased in the backfilled soil above footings/foundation's self-weight were inverse proportion to the rise of shell foundation angles. It could be seemed from these two figures that the flat foundation (0 degrees) has the most massive weight in aspects of self-weight and weight of soil above footings. This is why the anti-overturning moment (caused by the self-weight and the soil weight above the foundation) was greater than shell foundations, as shown in Figure 3-30.

Figure 3-39 showed that the increased in backfilled soil below the footing was proportional to the rise of shell angles. As the angle increases, the weight difference between the bottom of the cone-shaped shell foundation and the bottom of the pyramid-shaped shell foundation will increase. This is why the conical shell foundation had a lower sliding resistance (caused by self-weight) than the pyramidal shell foundation initially, but after the shell angle reached 30 degrees, the conical shell foundation had a higher sliding resistance than the pyramidal shell foundation, as shown in Figure 3-6.

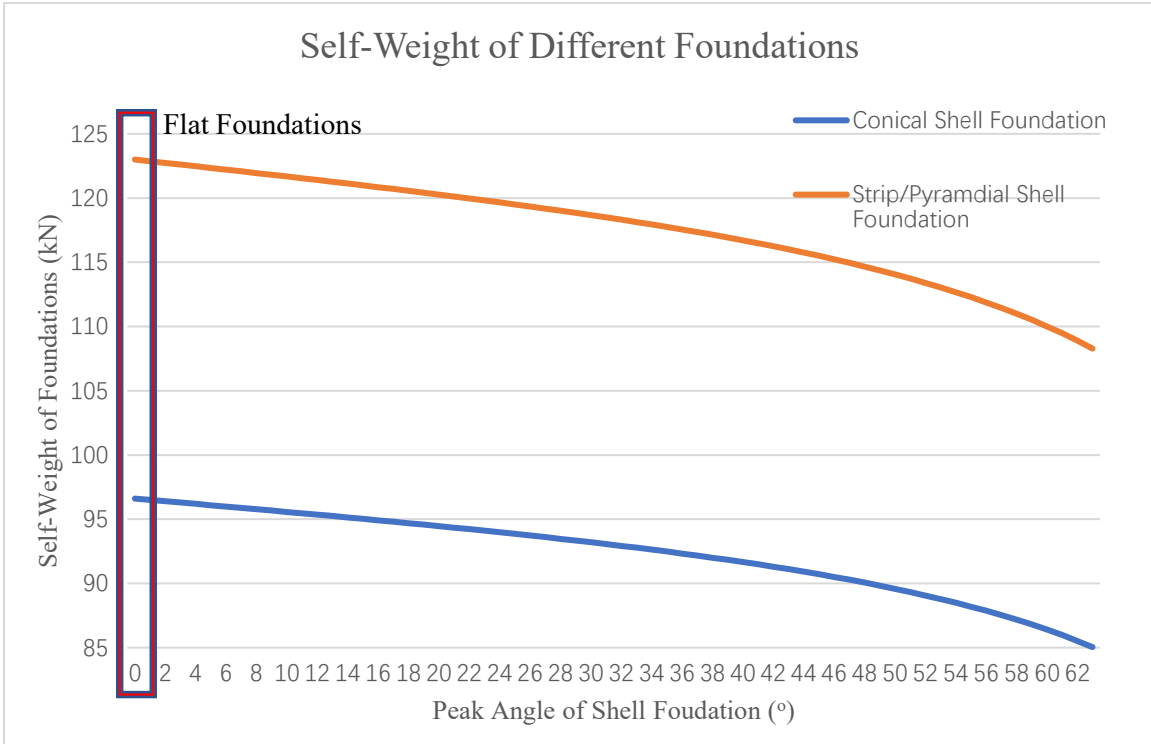


Figure 3-38. Self-Weight of Shell Foundations with Various Angles (0° Shell Foundations = Flat Foundations)

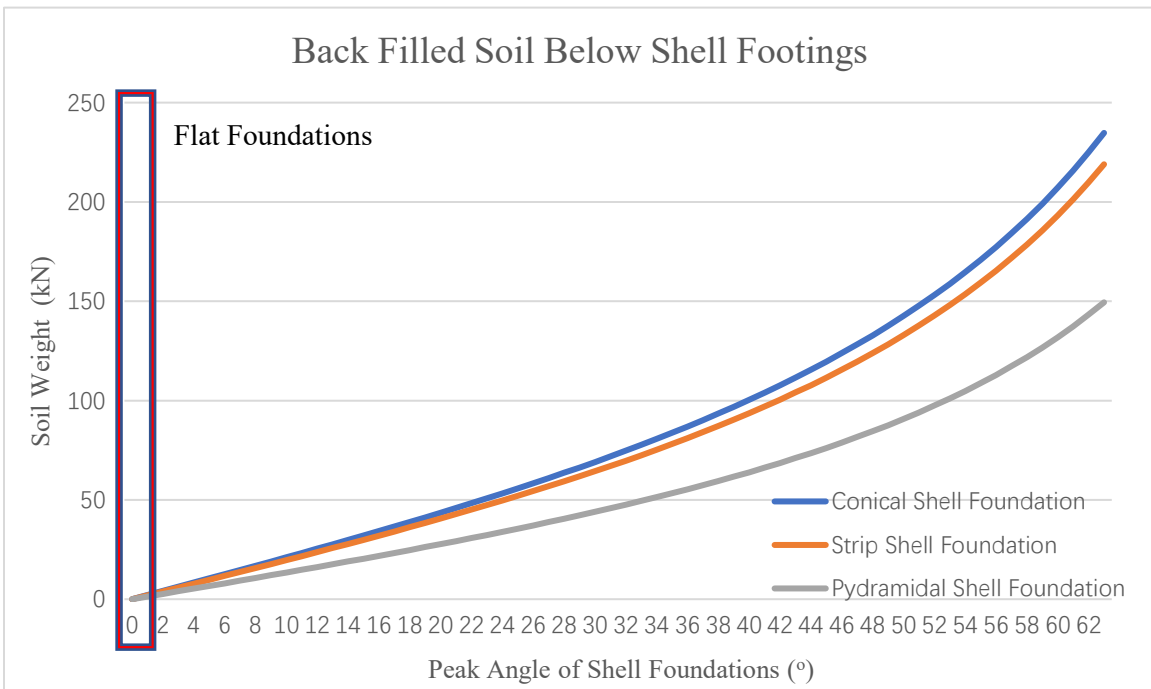


Figure 3-39. Weight of Back Filled Soil Below Footings with Various Angles (0° Shell Foundations = Flat Foundations)

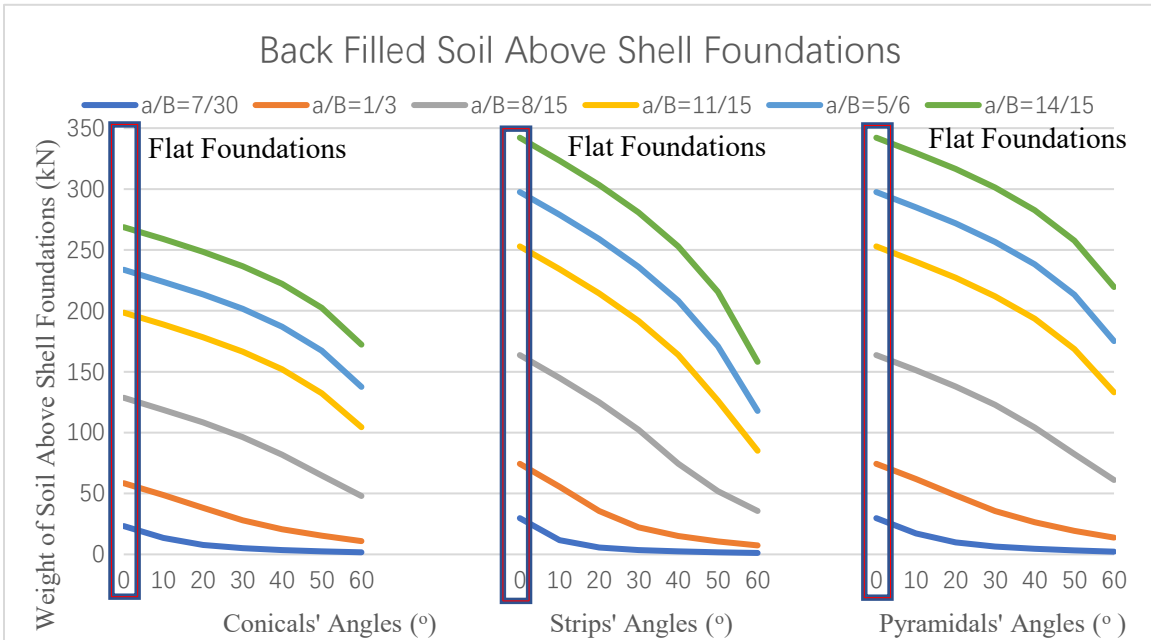


Figure 3-40. Weight of Back Filled Soil Above Footings with Various Angles (0° Shell Foundations = Flat Foundations)

CHAPTER 4

Numerical modeling

4.1 General

Plane-strain elastoplastic finite element model was developed to the cases of strip flat and shell footings with angle 21.8° and 38.66° using the commercial software PLAXIS 2-D Connect Edition V20. This analysis aimed to examine the failure mechanism of strip shells and conventional foundations. Mesh deformations, displacement vectors and failure points diagrams were recorded during the collapse.

The program 'PLAXIS' used the incremental tangent stiffness method in the analysis, in which the load was divided into multiple small increments, which were applied simultaneously. During each load increment, the stiffness characteristics suitable for the current stress level were used in the numerical analysis (Chekol, 2009).

4.2 Finite Element Model

Normally, since the geometry of the mesh for the plane-strain condition was axisymmetric about the centerline, the usual practice was to divide the footing into two halves and used the symmetry grid method to analyze only half of the footing. However, the present investigation involved modeling of the entire footing to compute the lateral collapse loads as showing in the following Figure 4-1, 4-2 and 4-3. The choice of the number of element and mesh design must reflect a compromise between an acceptable degree of accuracy and computing costs. The soil and the footing were modeled using 15-noded triangular element. Smaller size elements were selected near the footing of the soil, so that the changes in stress and strain are expected to be more significant. The total number of elements ranged between 2360 and 3148, depending on the geometrical parameters.

4.3 Properties of Soil and Footings

The soil in this analysis was modeled by the Mohr-Coulomb failure criteria. The model involved five parameters, viz Young's modulus, E , Poisson's ratio, ν , the cohesion, c , the friction angle, ϕ , and the dilatancy angle, ψ . The model of shell foundation was simulated as a linear elastic. Since the reinforced concrete foundation is completely rigid, the modulus of elasticity of the footings must be taken high enough to simulate the rigidity of concrete footings.

The properties of the adopted sand and shell foundation, which were simulated and defined in the program, were indicated in Table 4-1.

Table 4-1. Material Parameters for PLAXIS 2D

Material Parameters	Sand	Foundation (Concrete)
Material Model	Mohr-Coulomb	Linear elastic
Drainage type	Drained	Nonporous
γ_{unsat} [kN/m ³]	17	24
γ_{sat} [kN/m ³]	20	--
E [kN/m ²]	13e ³	26.6e ⁶
ν [-]	0.3	0.2
C [kN/m ²]	0	--
ϕ [°]	30	--
Ψ [°]	0	--

Dilatancy angle, $\psi = \phi - 30^\circ$ (Bolton, M. D., 1986).

Moreover, the Interface value, R_{inter} , had a significant impact on the bending moment. Thus, it was important to estimate a reasonable value for interface reduction factors. According to the research of Brinkgreve and Shen (2011) the interface strength, R_{inter} , between sand and concrete should range from 1 to 0.8. The R_{inter} of shell footing elements used in this investigation was taken as 0.8 since the lower the interface value results in the more massive the bending moment.

4.4 Boundary Conditions

In order to eliminate the influence of the boundary effect, the outer boundary should be placed as far away as possible from the region subjected to the largest change in the loading.

According to Lee, Jeong and Lee (2016), to avoid boundary effects, the radial boundaries of the mesh should have 6B width, and the base of the mesh should also be 6B deep below the footing. Therefore, various shell models with a size of 3m x 3m and a thickness of 0.5 m are embedded in a soil layer with a representative size of 39m x 20.5m.

4.5 Process Calculation

In this analysis, groundwater pressure was ignored. The loading scheme used in this study consisted of three main stages. In the first stage (Initial Condition), the lateral earth pressure coefficient K_0 was assigned to be 0 (Gouwt, 2014) to simulate the condition of the original soil body without any changes. The second stage was to activate all the structural elements and reset the displacement to zero. The third stage was to employ an external lateral point load to the footing. The point forces were concentrated and act on a geometry point at the center of shell footings. The input values of point forces were given in force per unit of length (kN/m). The applied point's value was taken according to the obtained value based on Equations (4-1) to (4-10).

$$W_{footing} = \gamma_{footing} \left[D(B - b) + b \left(H - \frac{B-b}{2} \tan\alpha - D \right) \right] \quad (4-1)$$

$$W_{soil\ below} = \gamma_{soil} \times \frac{B^2 - b^2}{4} \times \tan\alpha \quad (4-2)$$

When $0 < a < h'$,

$$W_{soil\ above} = \gamma_{soil} \times \frac{(a-D)^2}{\tan\alpha} \quad (4-3)$$

When $h' < a < H$

$$W_{soil\ above} = \gamma_{soil} \times (B - b) \times \left[(a - D) - \frac{1}{4}(B - b)\tan\alpha \right] \quad (4-4)$$

When $\alpha \neq 0$

$$F_w = (W_{footing} + W_{soil\ below} + W_{soil\ above}) \times \tan\phi \quad (4-5)$$

When $\alpha = 0$

$$F_w = (W_{footing} + W_{soil\ below} + W_{soil\ above}) \times \tan\left(\frac{2}{3}\phi\right) \quad (4-6)$$

$$P_{passive} = \frac{1}{2}\gamma_{soil} \times a^2 \times K_p \quad (4-7)$$

$$F_f = F_w + F_p \quad (4-8)$$

$$RM = P_{passive} \times \frac{1}{3}a \quad (4-9)$$

$$M_{total} = (W_{footing} + W_{soil\ above}) \times \frac{B}{2} + RM \quad (4-10)$$

4.6 Variables Considered

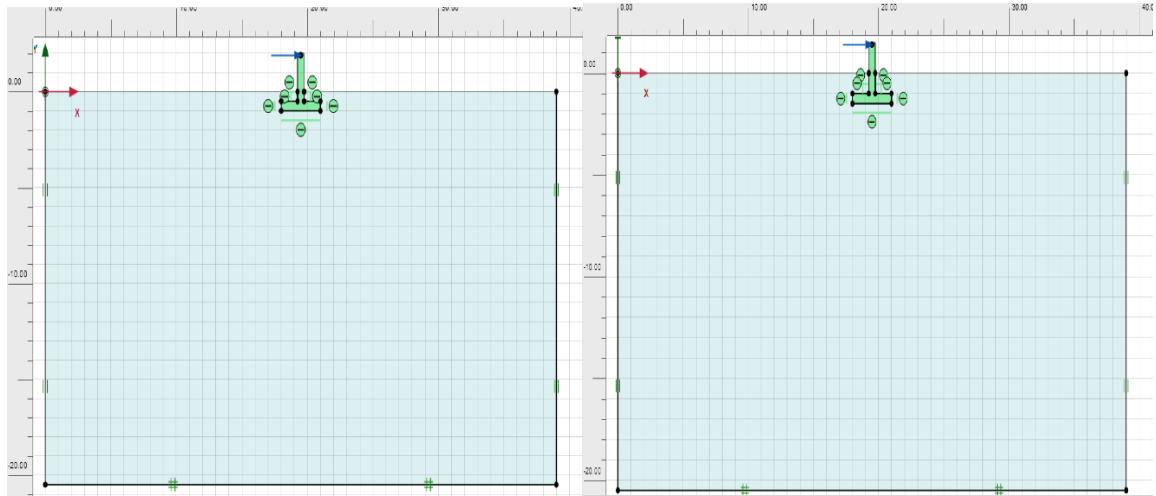
The following parameters were isolated in order to determine their effects on resisting the lateral loading on homogeneous soils:

4.6.1 Shell Angle (α)

In order to study the effect of the shell angle (α) on the resistance to lateral loading, model footings with shell angles of 0° , 21.8° , 38.66° were taken. Additionally, in order to facilitate drawing the shell footing in PLAXIS, the height of the shell (h) should be an integer. Thus, the shell angle is calculated by the equation $\alpha = \tan^{-1}\left(\frac{2h}{B-b}\right)$.

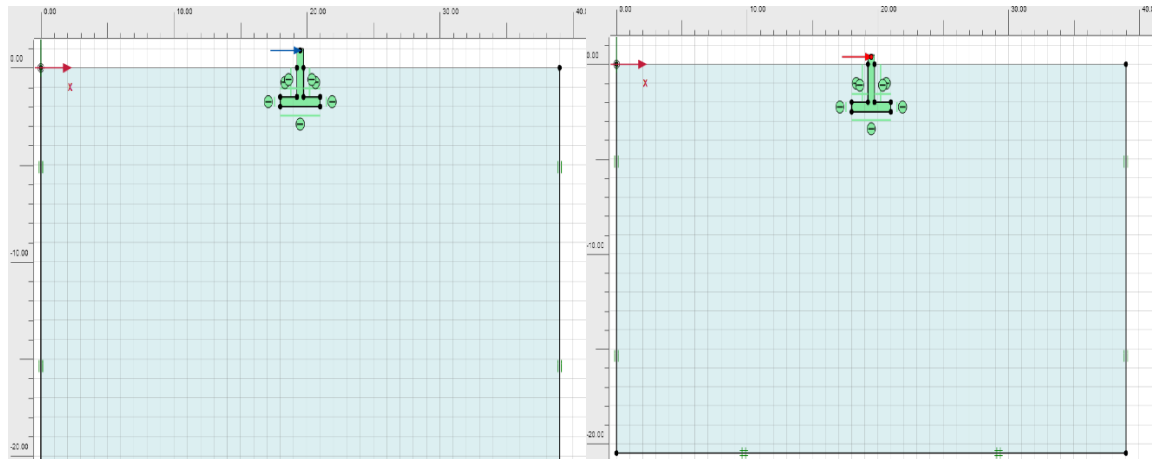
4.6.2 Embedment Ratio (a/D)

In order to study the effect of the embedment ratio on resisting the lateral loading, the models were buried in depths of 1m, 1.5m, 2m and 2.5m, respectively. Since the thickness of foundations was 0.5 meters, the embedment ratio (a/D) would be $1/3$, $1/2$, $2/3$ and $5/6$.



(a) Embedment Ratio=1/3

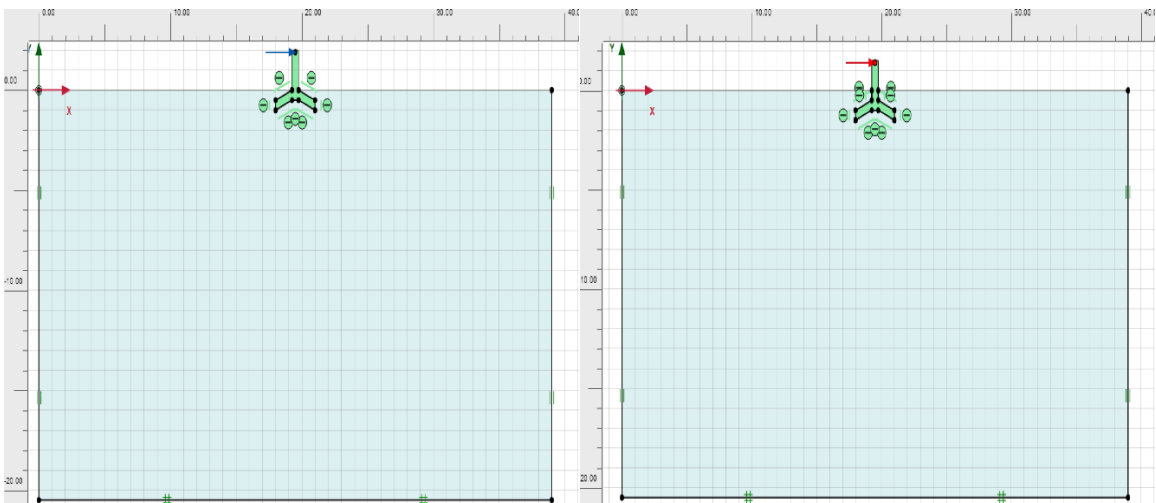
(b) Embedment Ratio=1/2



(c) Embedment Ratio=2/3

(d) Embedment Ratio=5/6

Figure 4-1. Finite Element Meshes for Flat Foundation with Various Embedment Ratio



(a) Embedment Ratio=1/3

(b) Embedment Ratio=1/2

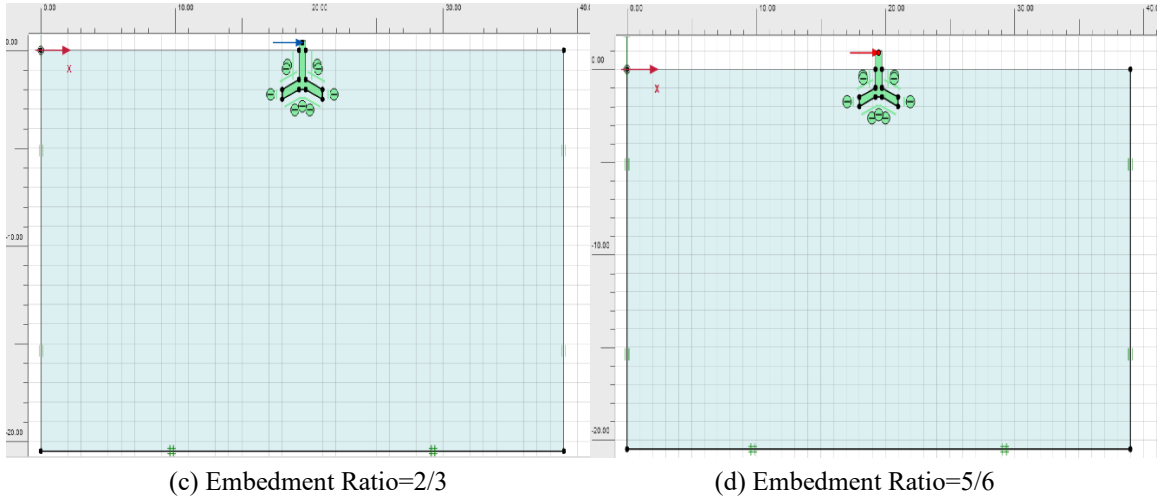


Figure 4-2. Finite Element Meshes for 21.8° Shell Foundation with Various Embedment Ratio

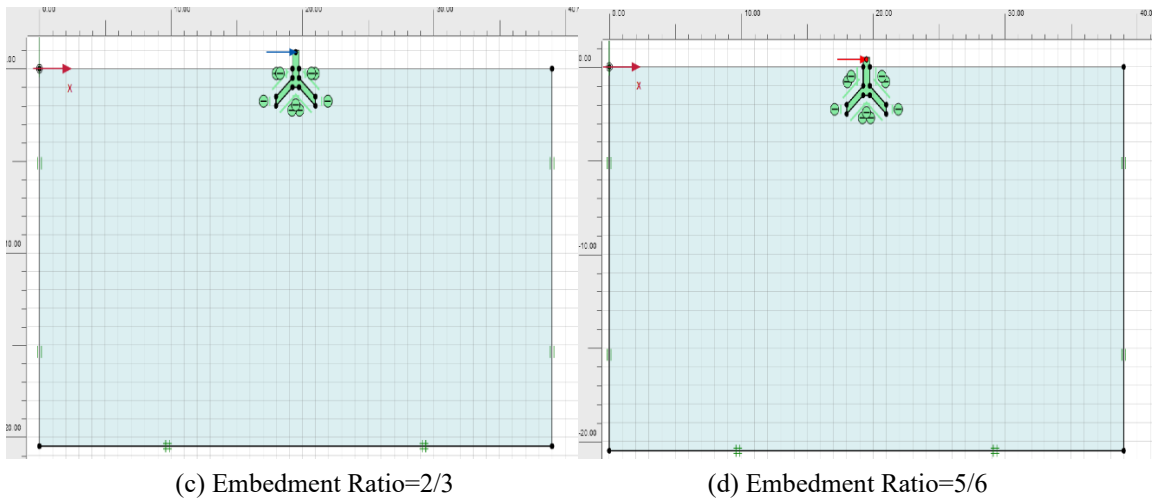
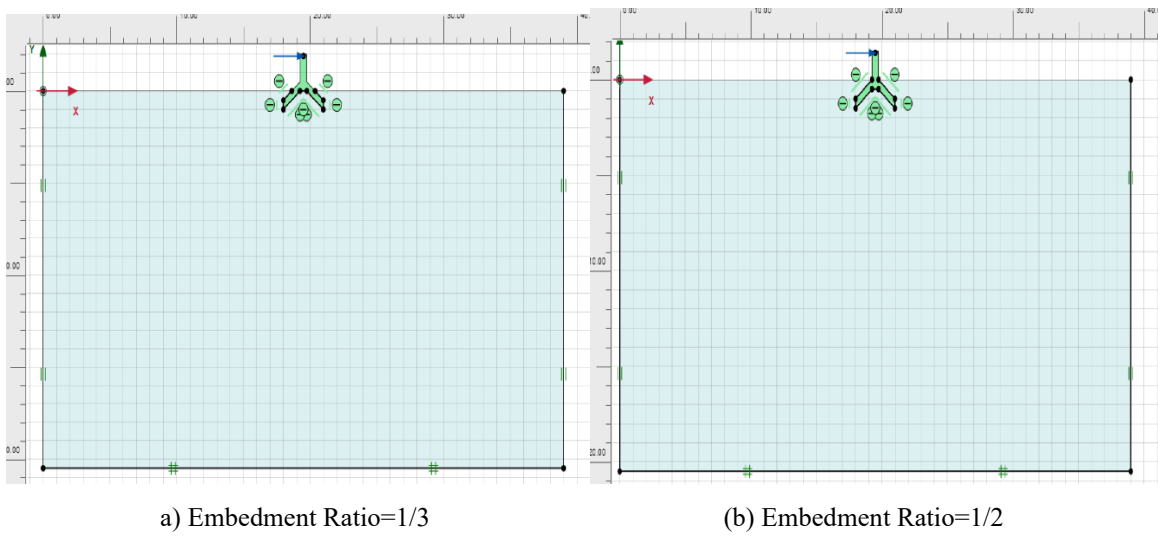


Figure 4-3. Finite Element Meshes for 38.66° Shell Foundation with Various Embedment Ratio

4.7 Verification of Finite Element Analysis

In this section, the comprehensive analytical results based on Equation 4-1 to 4-10 were compared with the finite element result obtained from the PLAXIS program. The comparison for the collapse lateral load between them was shown in Table 4-2 through 4-5 and Figure 4-4. These tables and the figure indicated that the results of the analytical models were consistent with the results of the numerical models, even though there was a little difference between them. The difference was in the range of 0.86% to 13.64%. The difference might be due to plain strain conditions and boundary effects. According to Figure 4-4, the finite element results were slightly higher than those of the numerical examples in the case of 28.1 degrees. On the other hand, the finite element results, and comprehensive analytical results were interlaced in the case of 0 and 38.66 degrees.

Furthermore, the collapse lateral load of flat foundations obtained from PLAXIS was greater than that of shell foundations, which was inconsistent with the analytical study. This was due to the numerical analysis used the two-dimensional in this research, but the three-dimensional model was studied in the analytical study. In two dimensions, the overturning moment caused by passive earth pressure of flat and shell foundations were consistent, but in three dimensions with deep embedment, the overturning moment due to the passive pressure of shell foundations was much larger than that of flat foundations.

Table 4-2. Load Resistance Between Analytical and Numerical Models when $a/B = 1/3$

2-D	F_f (kN)	Total M (kN.m)	Point load at 2.9m (kN)	Critical In PLAXIS (kN)	%
Angle 0°	57.26	130.38	130/2.9=45	51	11.76
Angle 21.8°	74.86	114.44	114/2.9=39.5	43	8.14
Angle 38.66°	76.92	97.47	97/2.9=33.6	36	6.67

Table 4-3. Load Resistance Between Analytical and Numerical Models when $a/B = 1/2$

2-D	F_f (kN)	Total M (kN.m)	Point load at 2.9m (kN)	Critical In PLAXIS (kN)	%
Angle 0°	96.87	191.44	191.44/2.9=66	70	5.71

Angle 21.8°	119.01	166.5	166.5/2.9=57	66	13.64
Angle 38.66°	118	141.56	141.56/2.9=49	51	3.92

Table 4-4 Load Resistance Between Analytical and Numerical Models when a/B = 2/3

2-D	F_f (kN)	Total M (kN.m)	Point load at 2.9m (kN)	Critical In PLAXIS (kN)	%
Angle 0°	149.23	262.63	262.63/2.9=91	92	1.09
Angle 21.8°	175.9	237.69	237.69/2.9=82	89	7.87
Angle 38.66°	174.89	212.75	212.75/2.9=73	71	2.82

Table 4-5. Load Resistance Between Analytical and Numerical Models, when a/B = 5/6

2-D	F_f (kN)	Total M (kN.m)	Point load at 2.9m (kN)	Critical In PLAXIS (kN)	%
Angle 0°	214.33	359.32	359.32/2.9=124	119	4.2
Angle 21.8°	245.54	334.38	334.38/2.9=115	116	0.86
Angle 38.66°	244.53	309.44	309.44/2.9=107	103	3.88

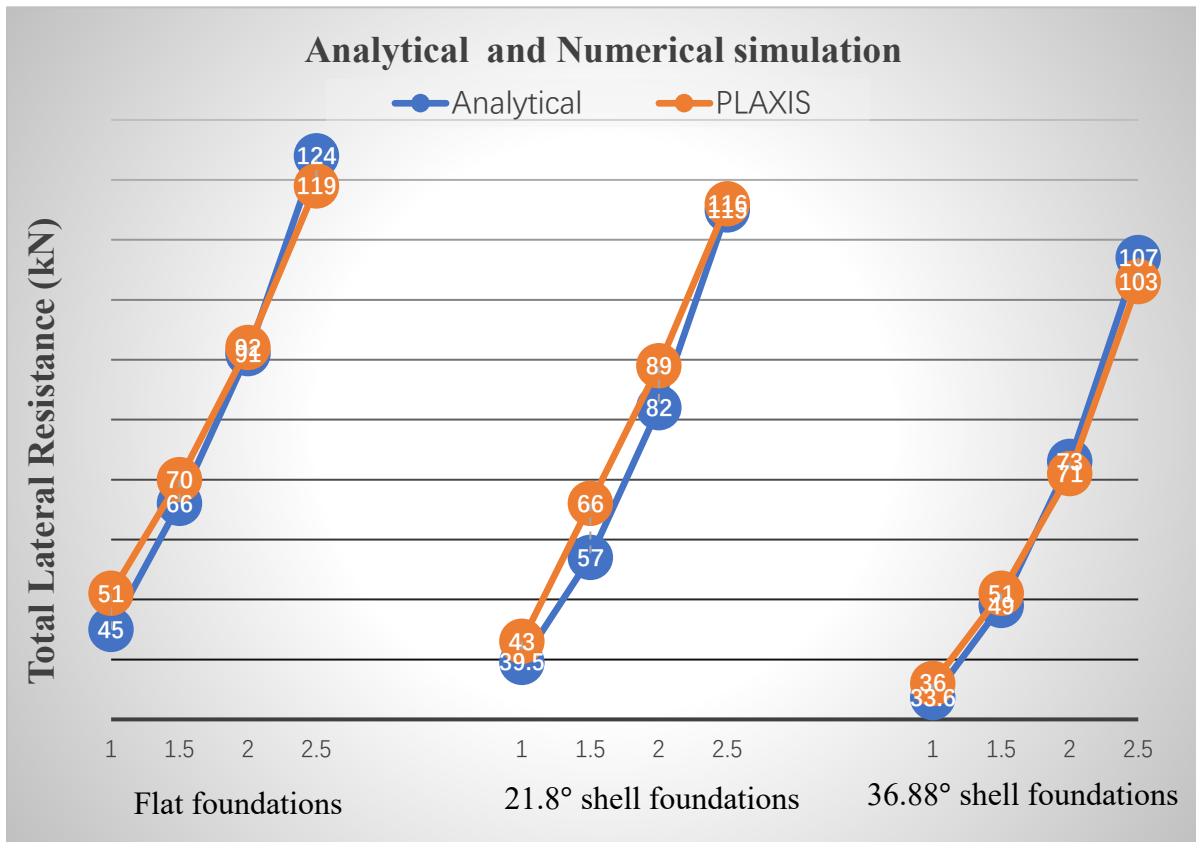
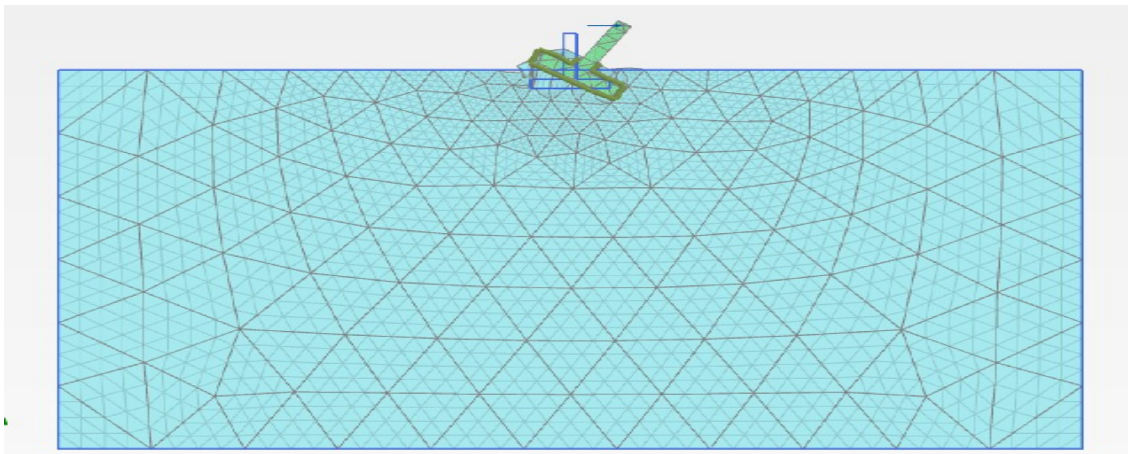


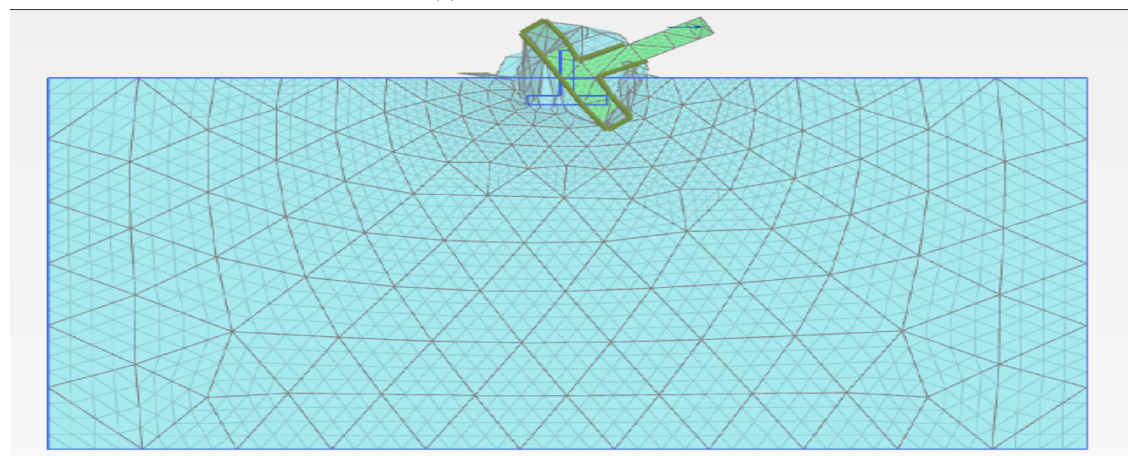
Figure 4-4. The Comparison Between Analytical and Numerical Models

The deformed meshes were presented in Figures 4-5 through 4-7. These figures showed that all footings suffered a massive overturning moment during the collapse. The results of the numerical examples in Chapter 3 seemed to confirm the prediction, which overturning moment resistance was the leading cause of foundations collapse.

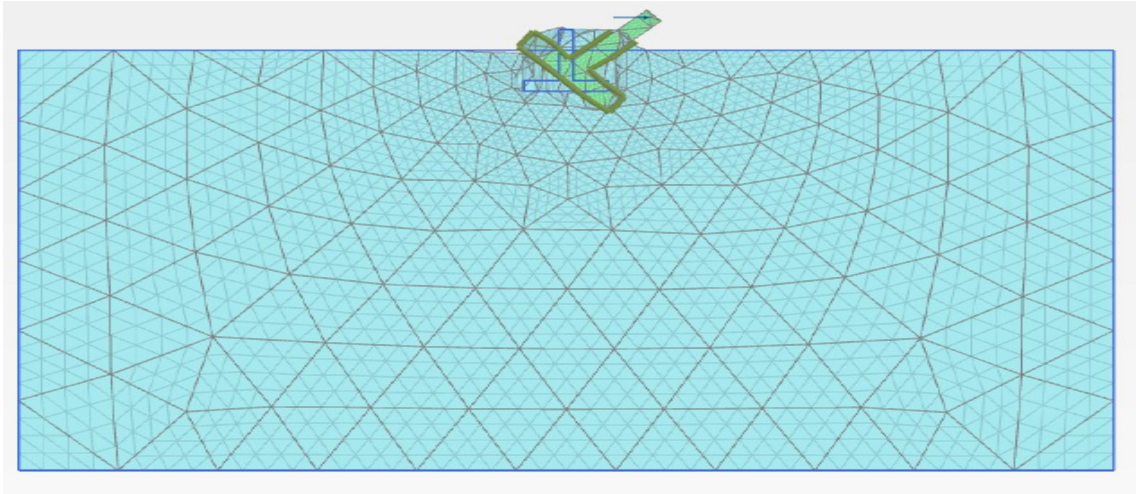
During the collapse, the flat foundation made the soil heave significantly along each side as shown in Figure 4-5 (a), (b) and (c). In addition, Figure 4-6 (a), (b) and (c) indicated that there was a trivial soil heave along each side of the shell. However, the soil had downward deformation alongside the footing, as shown in Figures 4-7, 4-6 (d) and 4-5 (d). Thus, increase the embedment ratio and shell angle might be beneficial to resist the overturning moments.



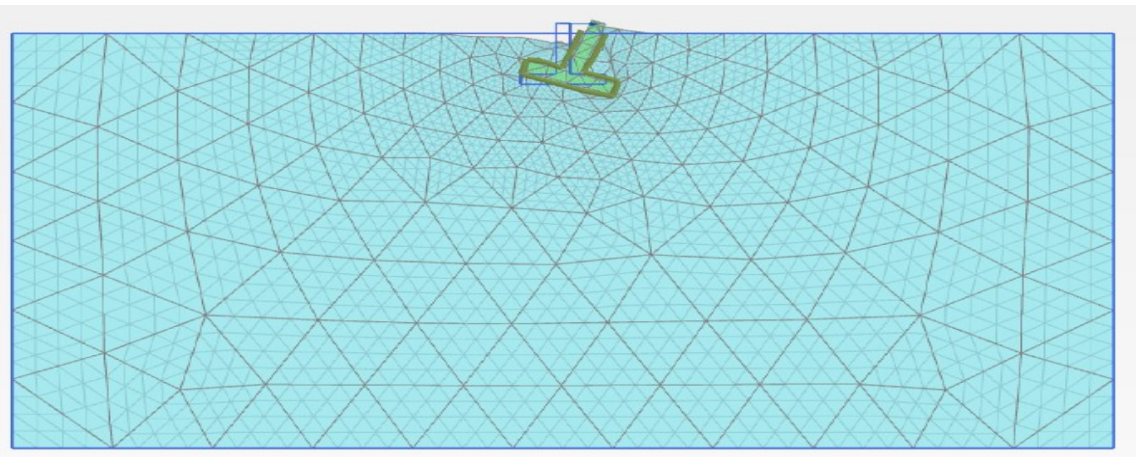
(a) Embedment Ratio=1/3



(b) Embedment Ratio=1/2

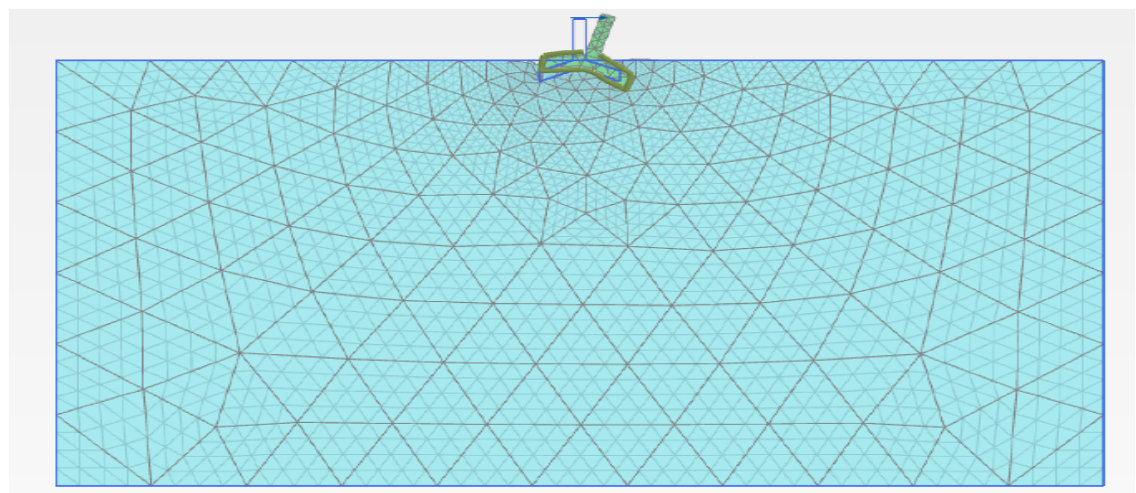


(c) Embedment Ratio= $2/3$

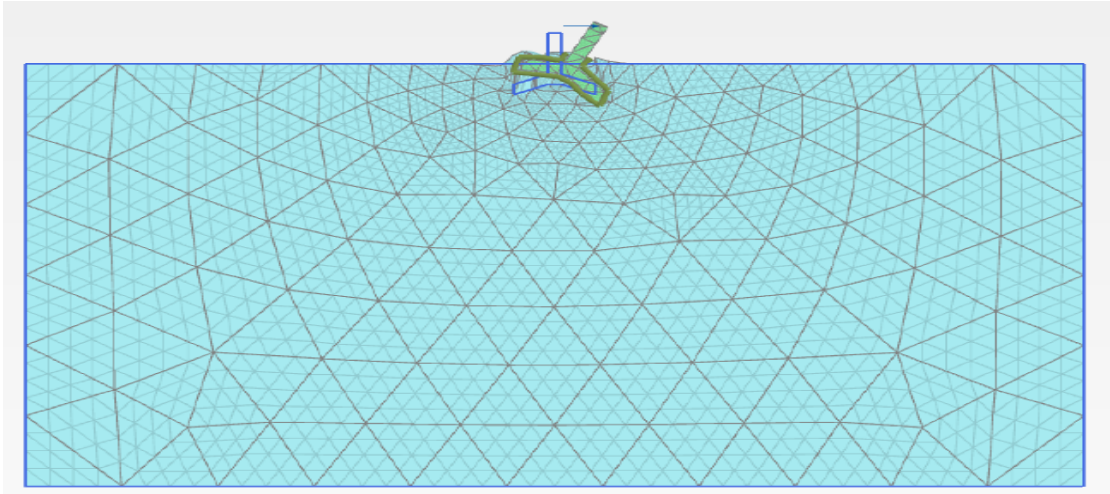


(d) Embedment Ratio= $5/6$

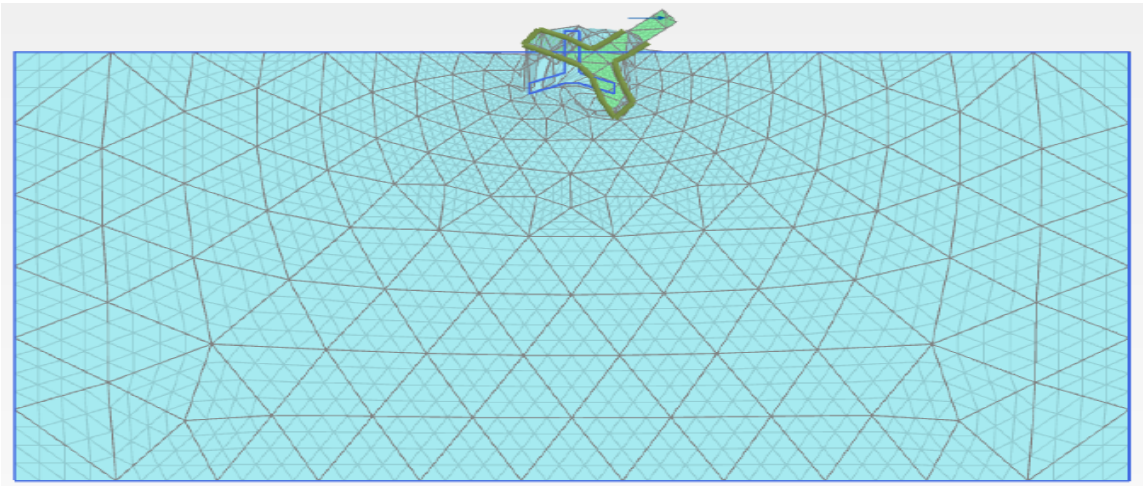
Figure 4-5. Finite Element Displacement Vectors for Flat Foundations with Various Embedment Ratio



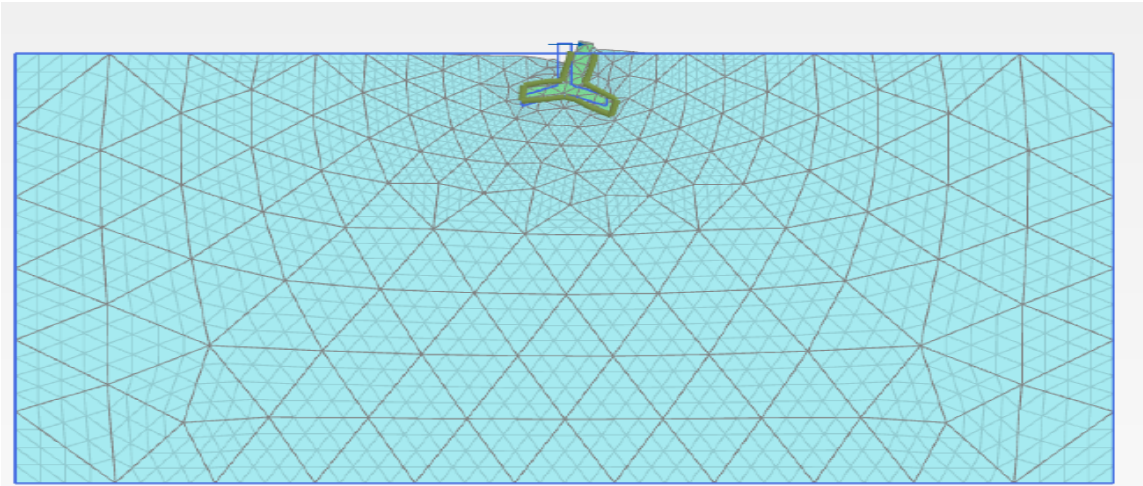
(a) Embedment Ratio= $1/3$



(b) Embedment Ratio=1/2

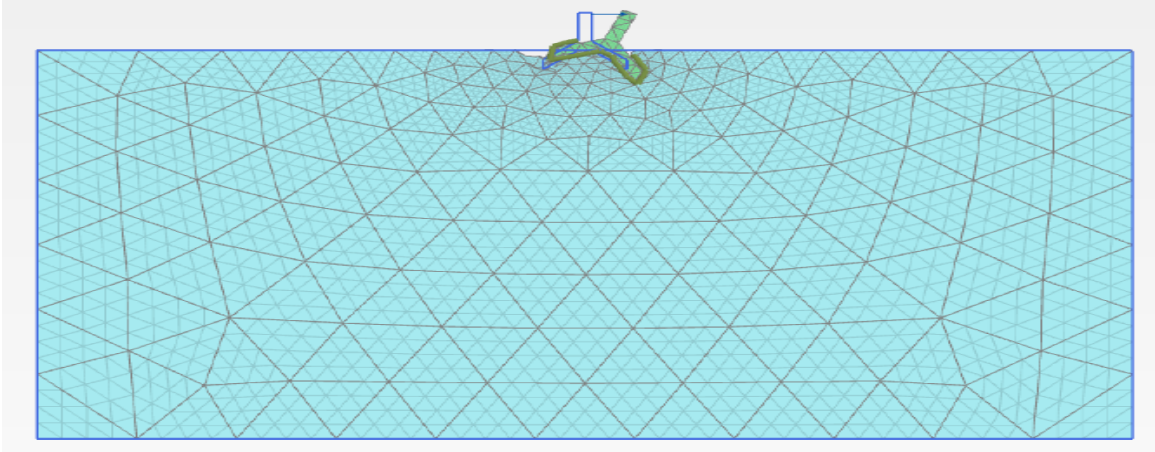


(c) Embedment Ratio=2/3

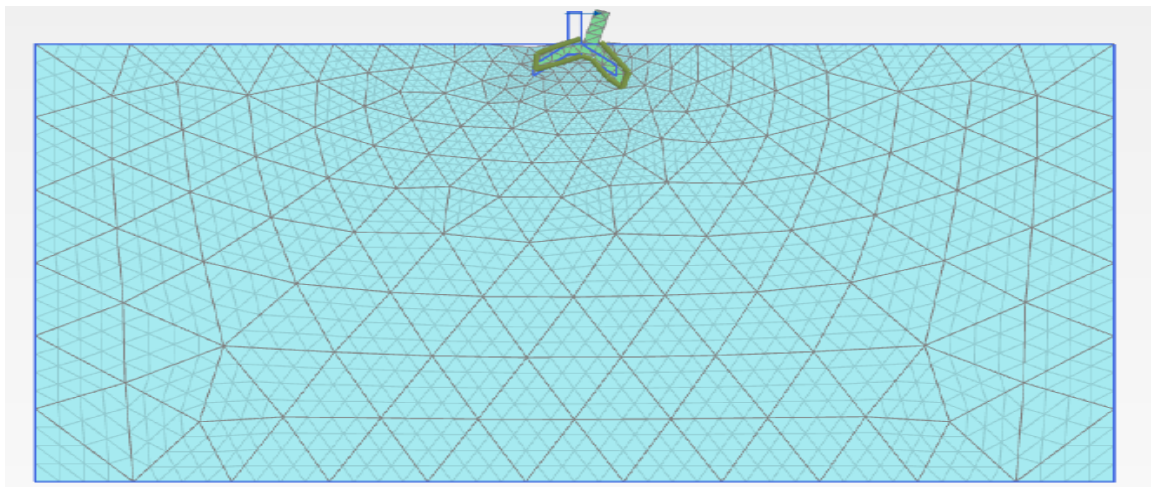


(d) Embedment Ratio=5/6

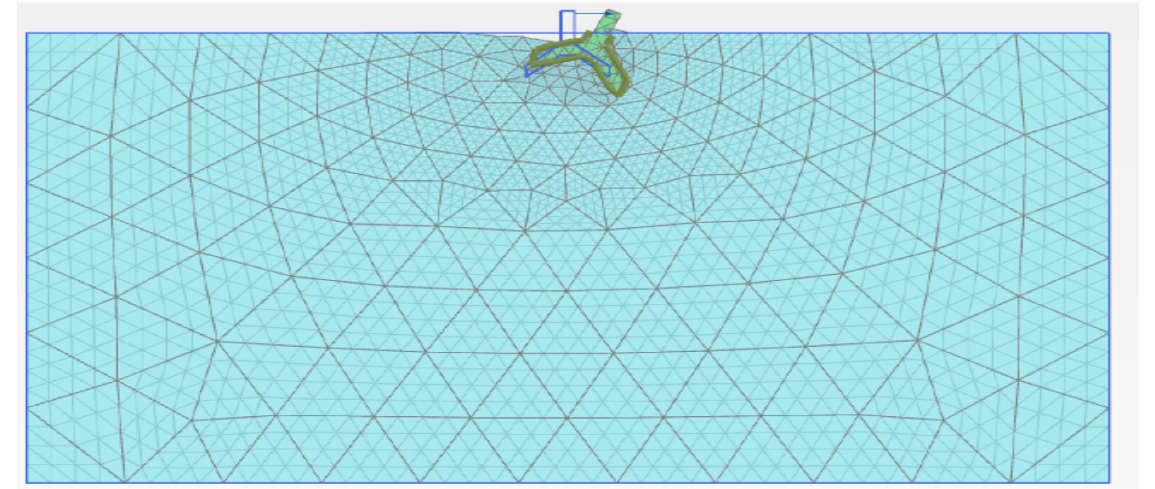
Figure 4-6. Finite Element Displacement Vectors for 21.8° Shell Foundation with Various Embedment Ratio



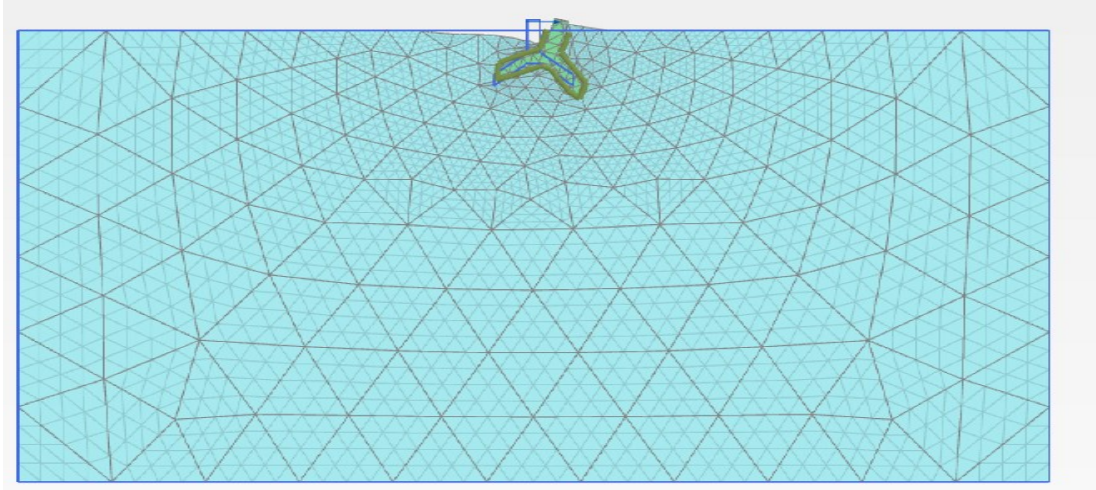
(a) Embedment Ratio=1/3



(b) Embedment Ratio=1/2



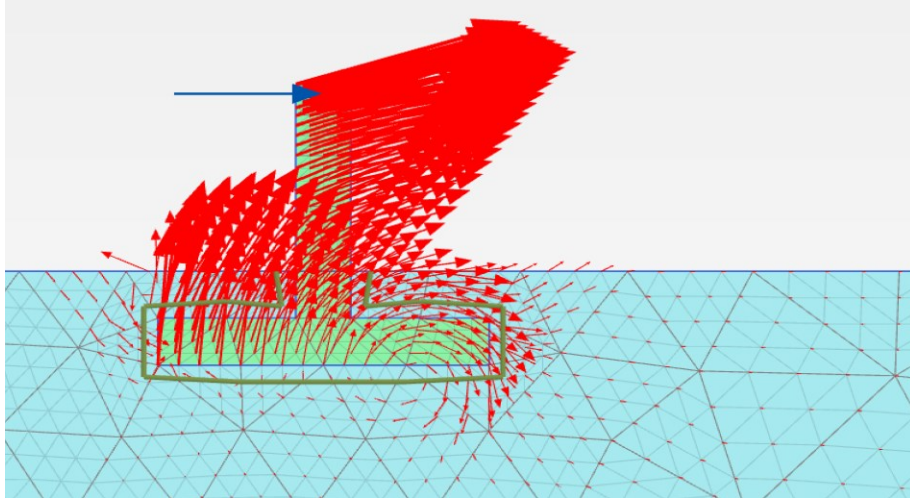
(c) Embedment Ratio=2/3



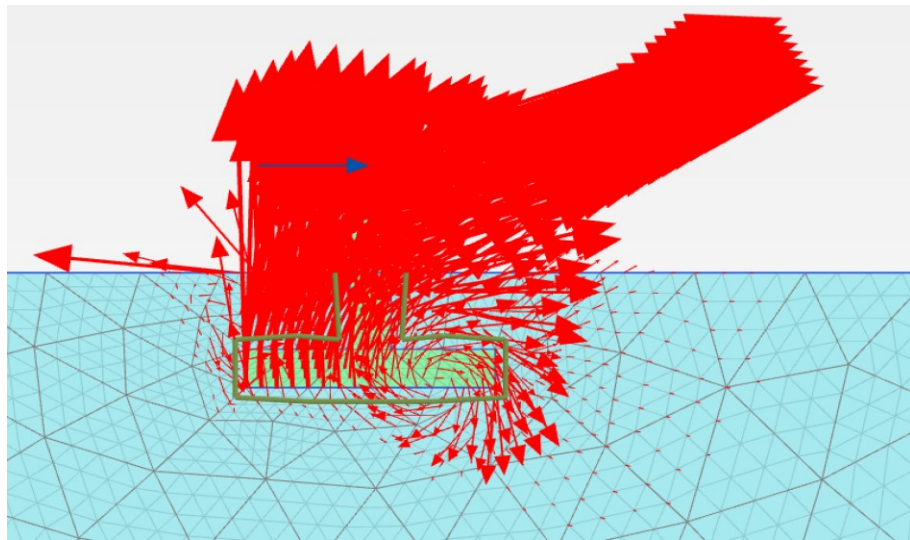
(d) Embedment Ratio=5/6

Figure 4-7. Finite Element Displacement Vectors for 38.66° Shell Foundation with Various Embedment Ratio

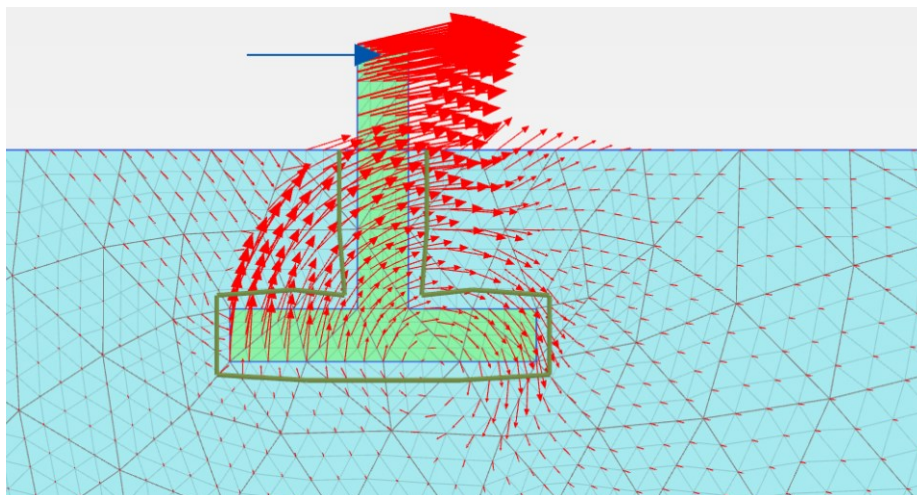
The total displacement vectors diagrams, Figures 4-8 to 4-10, revealed the flow of the soil particles for strip flat, 21.8°, and 38.66° shell footings. Observing these figures, the soil outside the footing on the left-hand side, especially near the ground surface, tended to move downwards to the foundations. On the other hand, the soil outside the footing on the right-hand side for those near the ground surface tended to move upwards trivially and tended to move horizontally for those away from the footing. There was a trivial upward deformation at the left-hand side under the footing, but downwards deformation at the right-hand side under the footings. The soil above the foundation was overturning clockwise with the foundation. It seemed to have the same configuration as the one provided by Ntritsos, Anastasopoulos and Gazetas (2015), which was shown in Figure 4-11. Nonetheless, the subtle difference between Figure 4-8 and 4-10 was that the tipping point of this study was slightly to the right, rather than the midpoint shown in the research of Ntritsos et al. (2015). Additionally, Figure 4-9 (d) and 4-10 (d) indicated that with a steeper shell angle or a larger embedment ratio, the overturning point moved to the back-fill soil which below the shell foundation. Generally, the comparison between flat and shell foundations indicated that the shell footing's rupture surface was more profound than that for the strip flat counterpart, as shown in Figure 4-12.



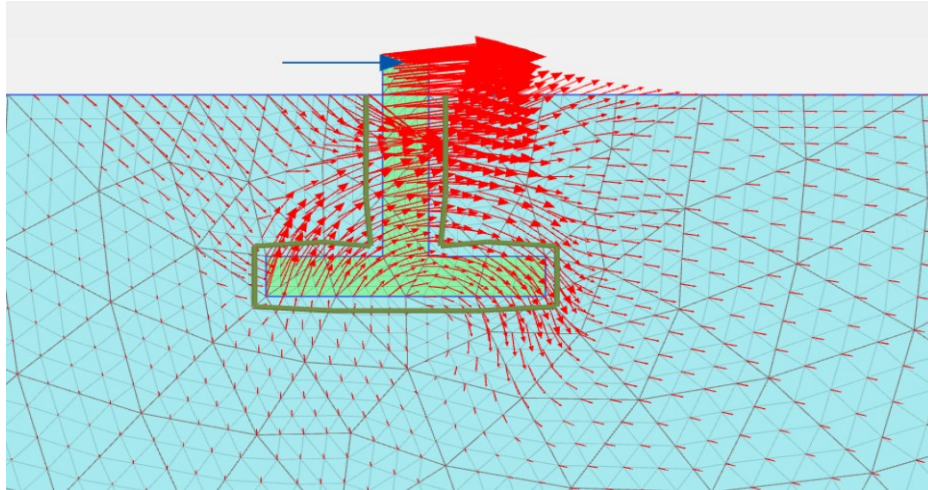
(a) Embedment Ratio=1/3



(b) Embedment Ratio=1/2

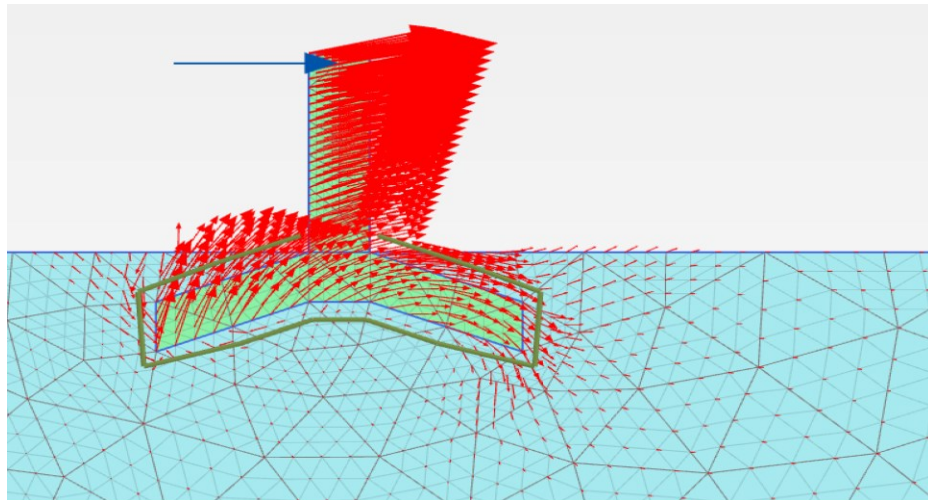


(c) Embedment Ratio=2/3

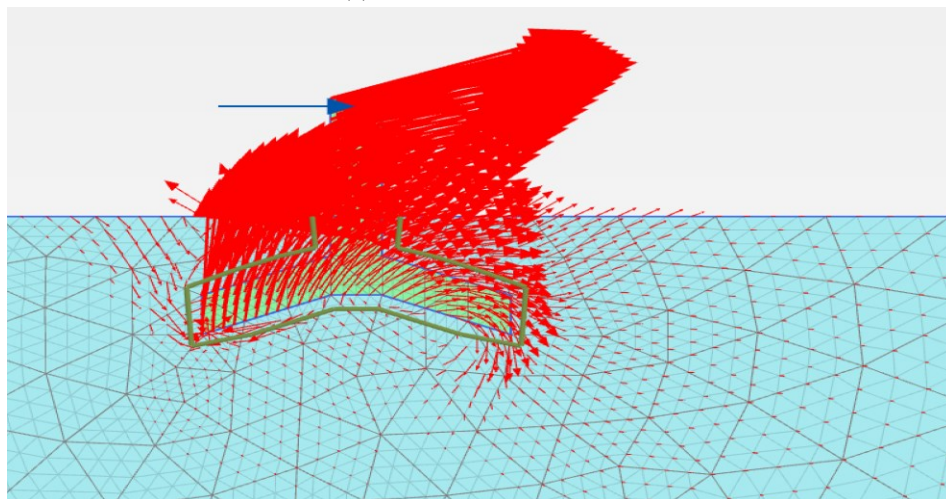


(d) Embedment Ratio=5/6

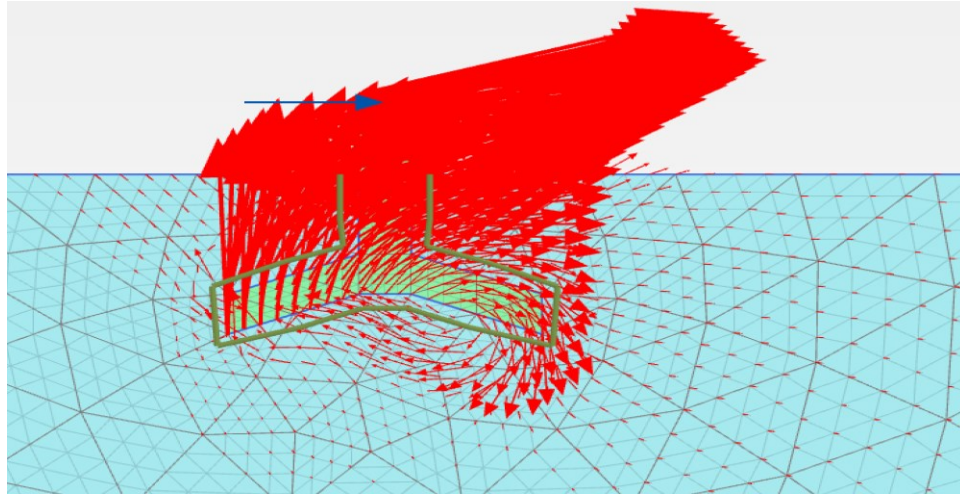
Figure 4-8. Finite Element Displacement Vectors for Flat Foundations with Various Embedment Ratio



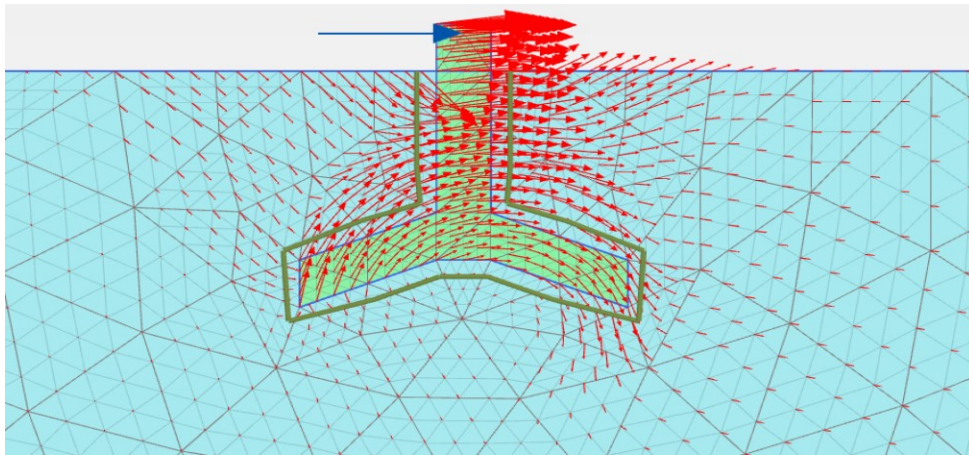
(a) Embedment Ratio=1/3



(b) Embedment Ratio=1/2

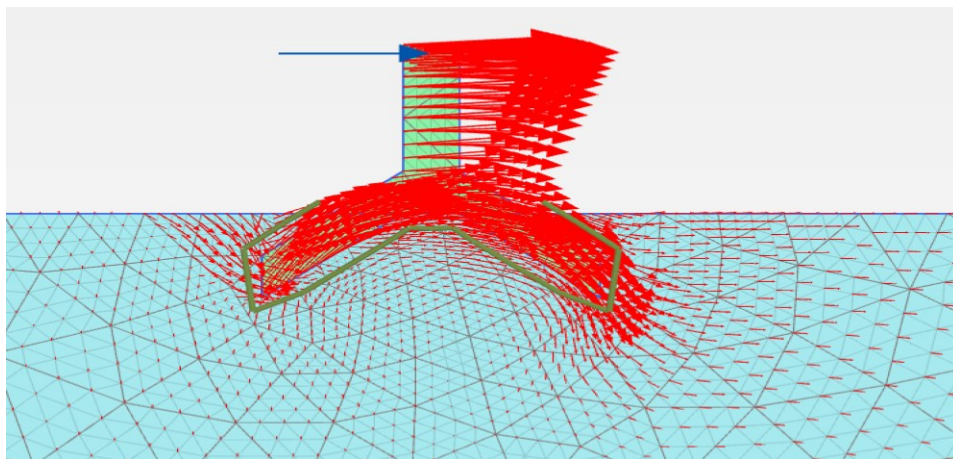


(c) Embedment Ratio=2/3

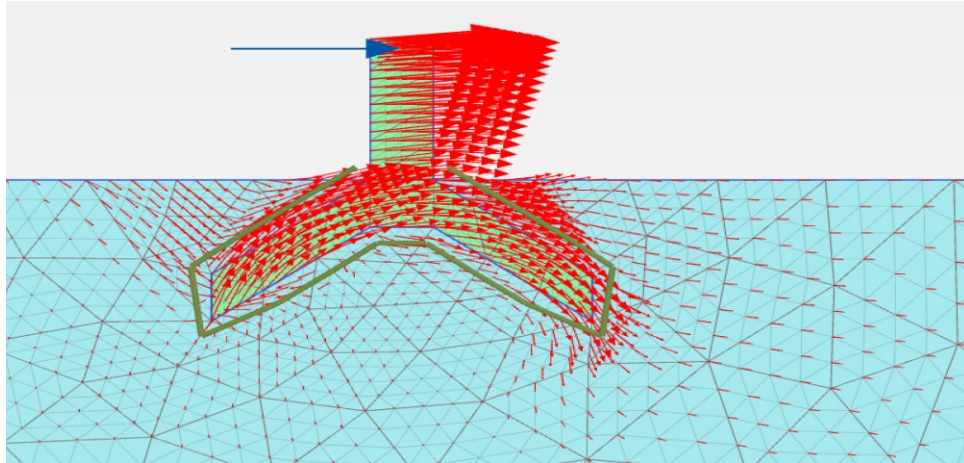


(d) Embedment Ratio=5/6

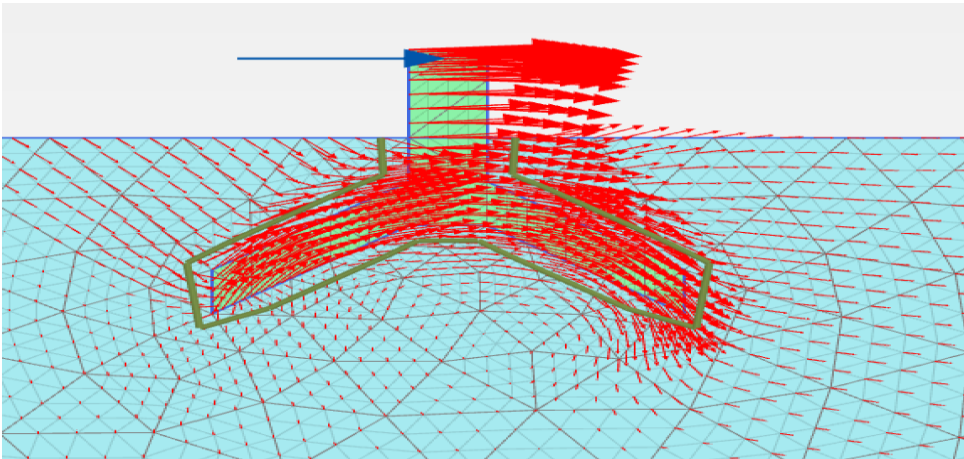
Figure 4-9. Finite Element Displacement Vectors for 21.8° Shell Footings with Various Embedment Ratio



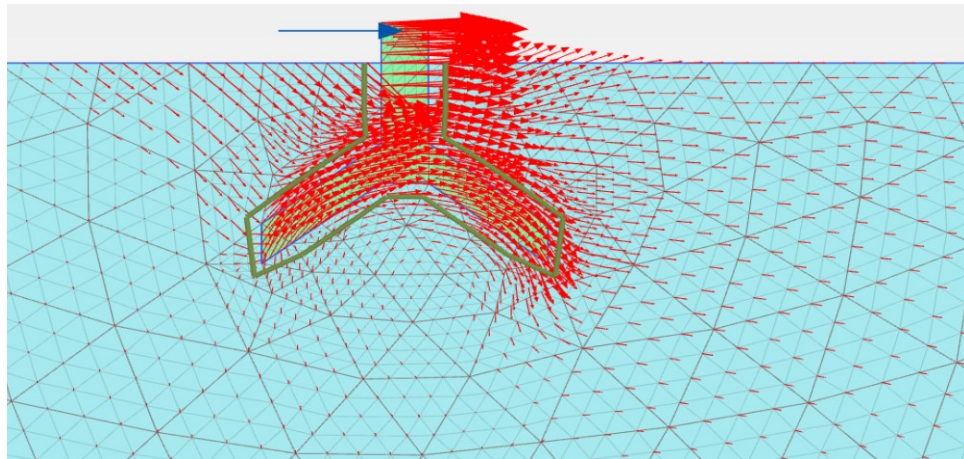
(a) Embedment Ratio=1/3



(b) Embedment Ratio=1/2



(c) Embedment Ratio=2/3



(d) Embedment Ratio=5/6

Figure 4-10. Finite Element Displacement Vectors for 38.66° Shell Footing with Various Embedment Ratio

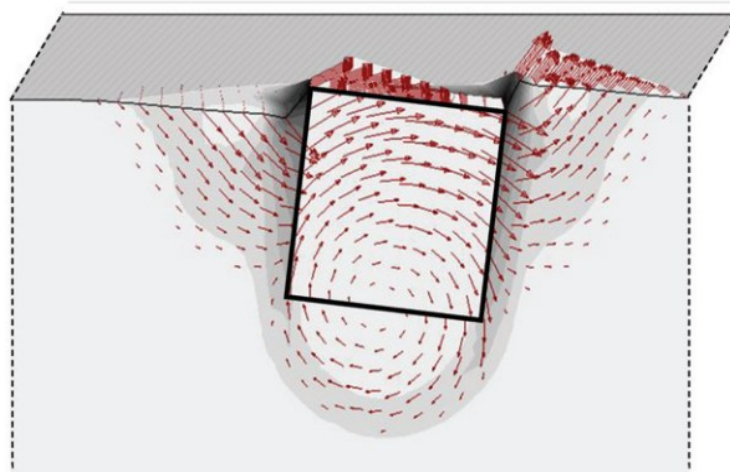
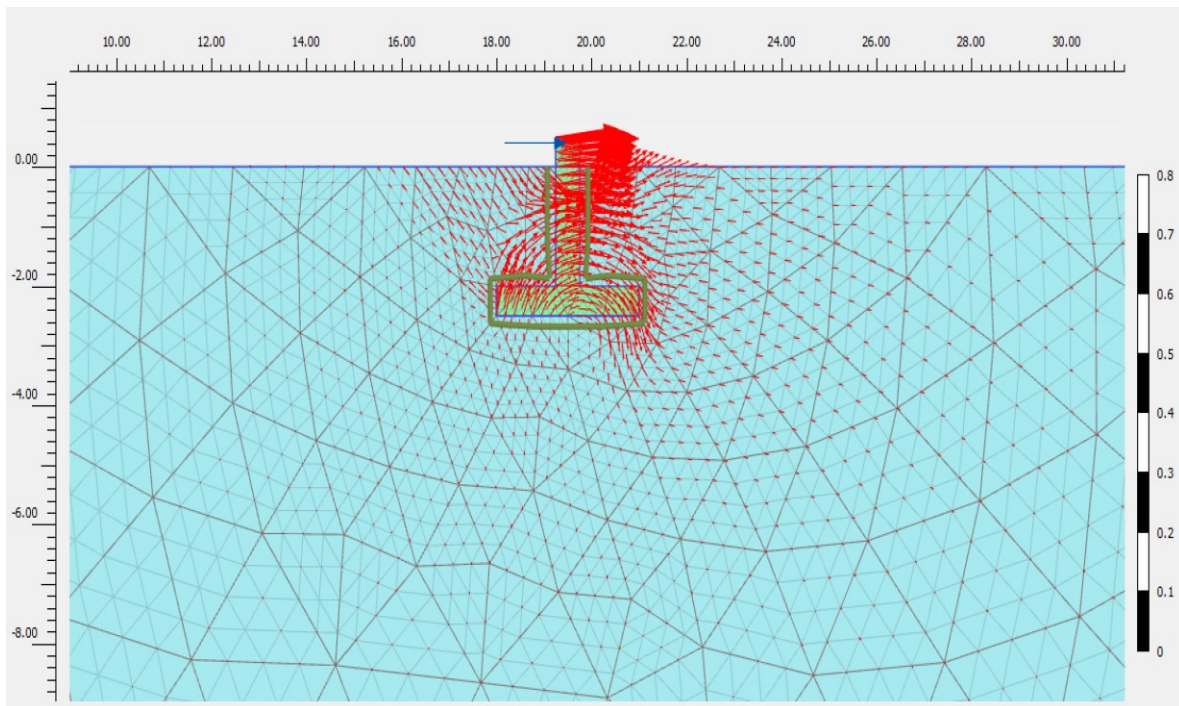
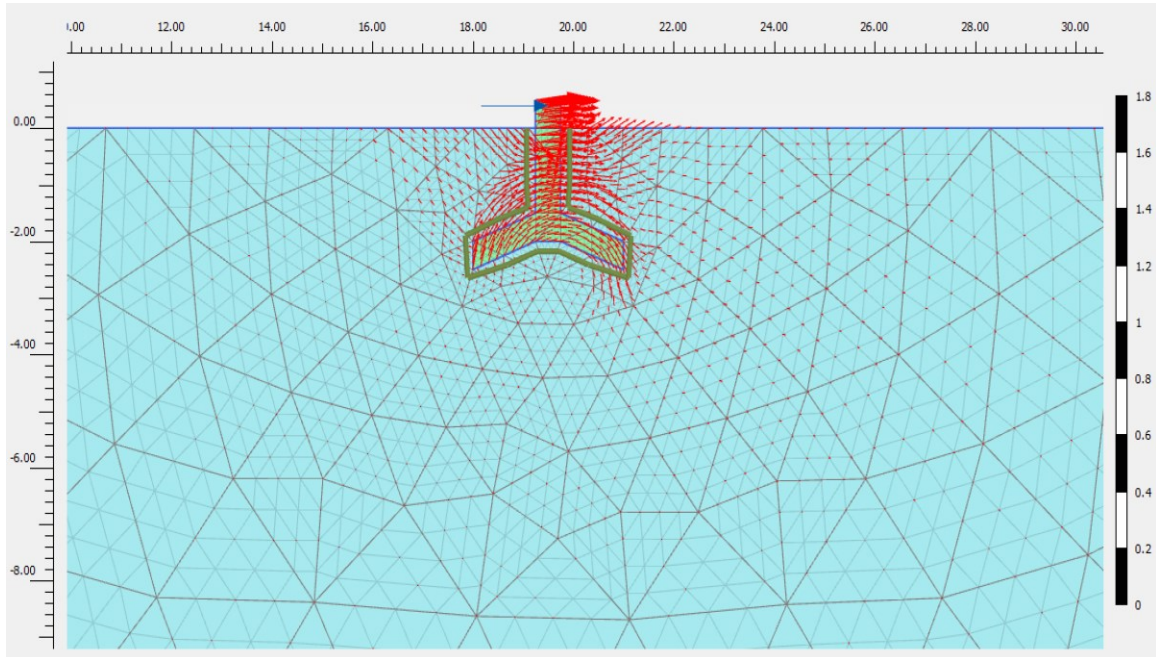


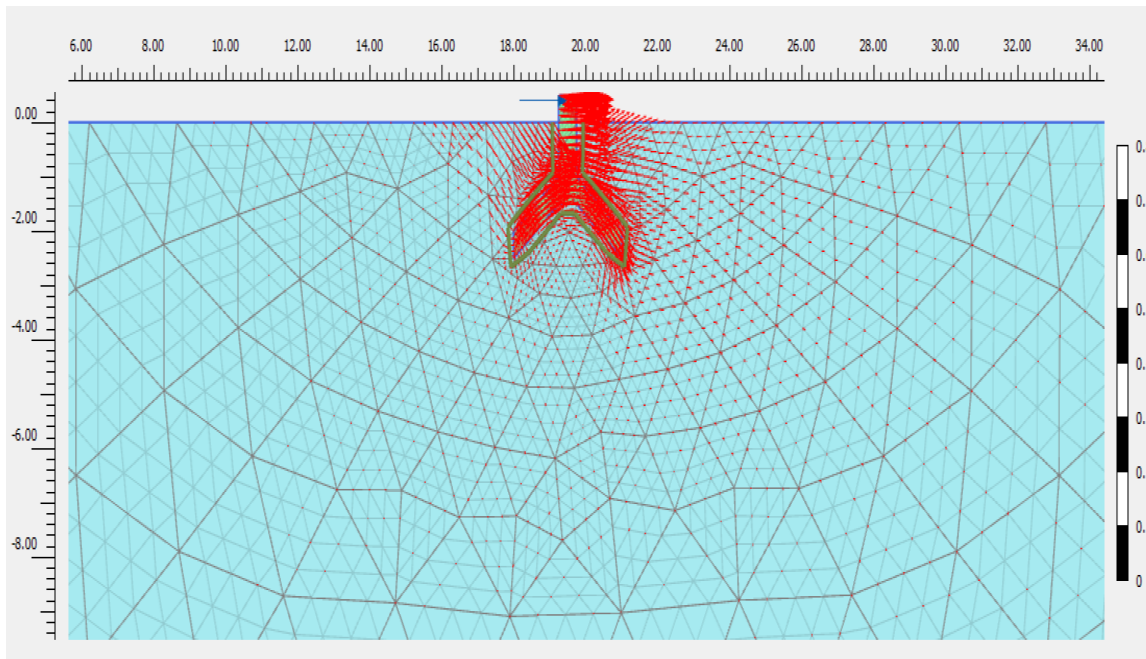
Figure 4-11. Displacement Vectors at Failure Load (M_{max}) with Zero Horizontal Displacement. (Ntritsos, Anastasopoulos & Gazetas, 2015)



(a) Flat Foundation



(b) 21.8° Shell Foundation



(c) 38.66° Shell Foundation

Figure 4-12. Finite Element Total Displacement Vectors for Various Footings with Embedment Ratio=5/6

The red point shown in Figures 4-13 to 4-15 was denoted as a plastic failure point that was currently on the failure envelope, such as the Mohr-Coulomb envelope. Besides the white point shown in those figures was represented as tension cut-off points.

Observing Figures 4-13 to 4-15, except for shell foundations when embedment ratio was $1/3$ (as shown in Figures 4-14 (a) and 4-15 (a)), not only were most of the failure and tension cut off points found around the foundation, but some of them also were extended to the soil at the bottom right of the foundation with a certain depth. Additionally, the shell footing's rupture surface was more profound than that for the strip flat counterpart.

Furthermore, to reduce the soil failure, reinforced the soil or added the edge beams at the bottom of the footing might work, as mentioned in the Literature review.

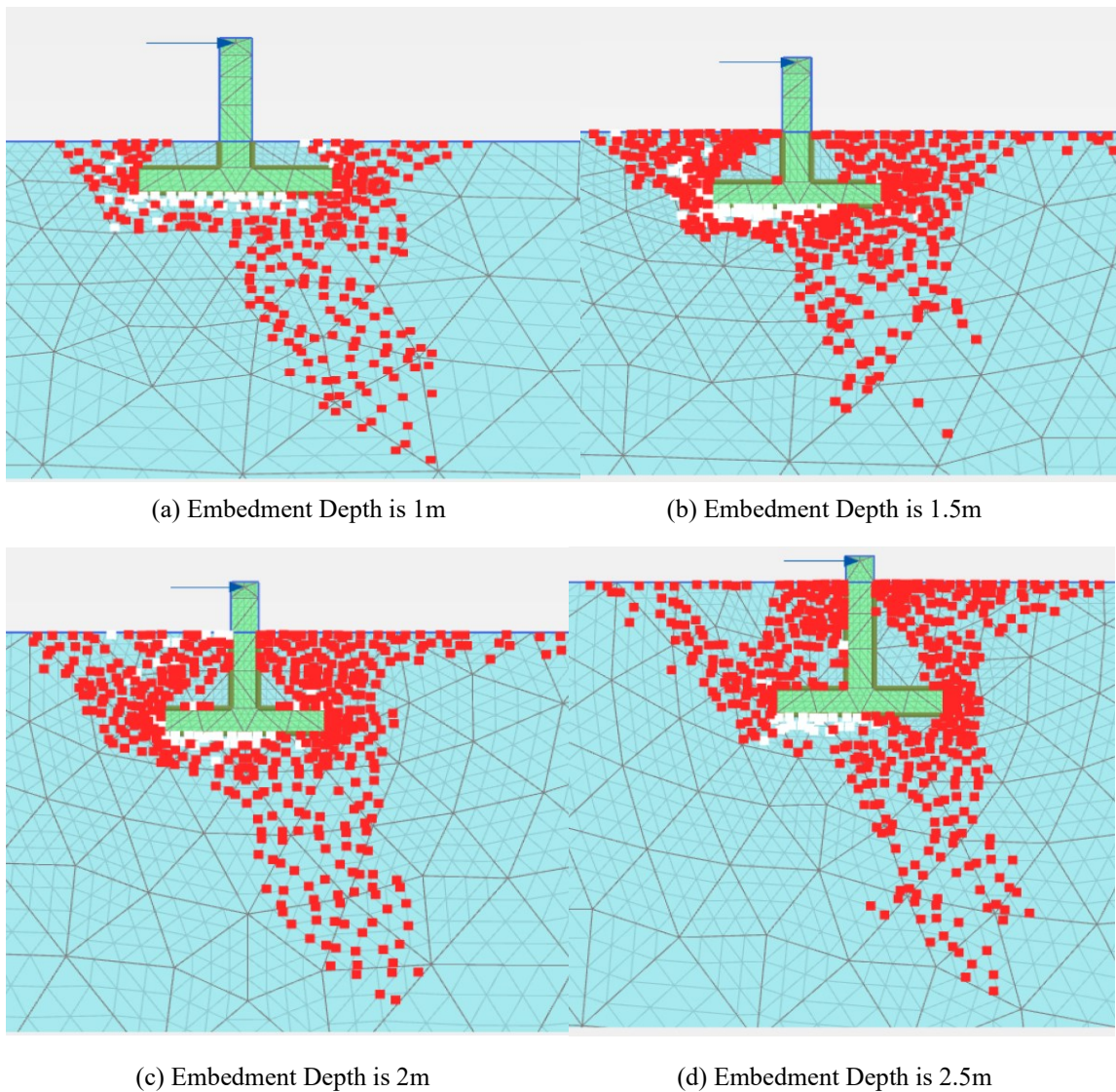
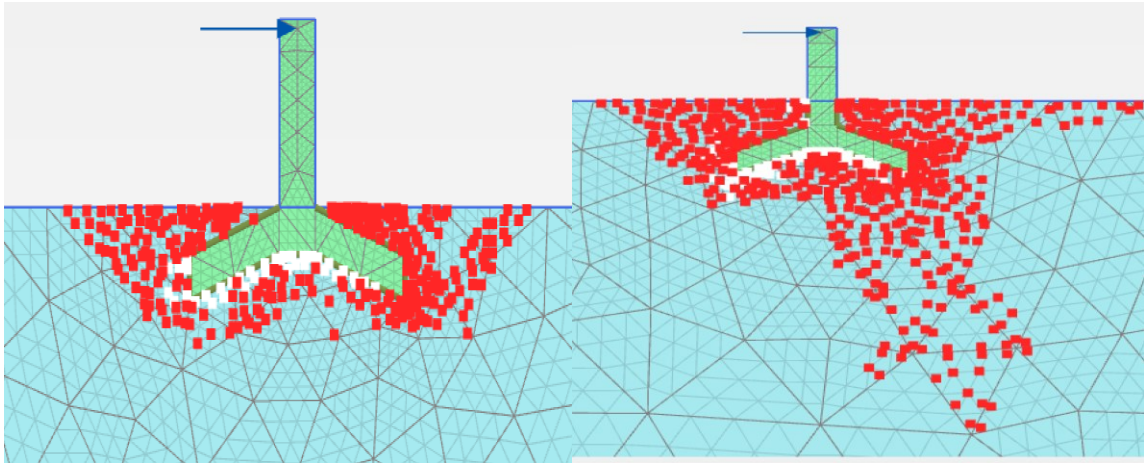
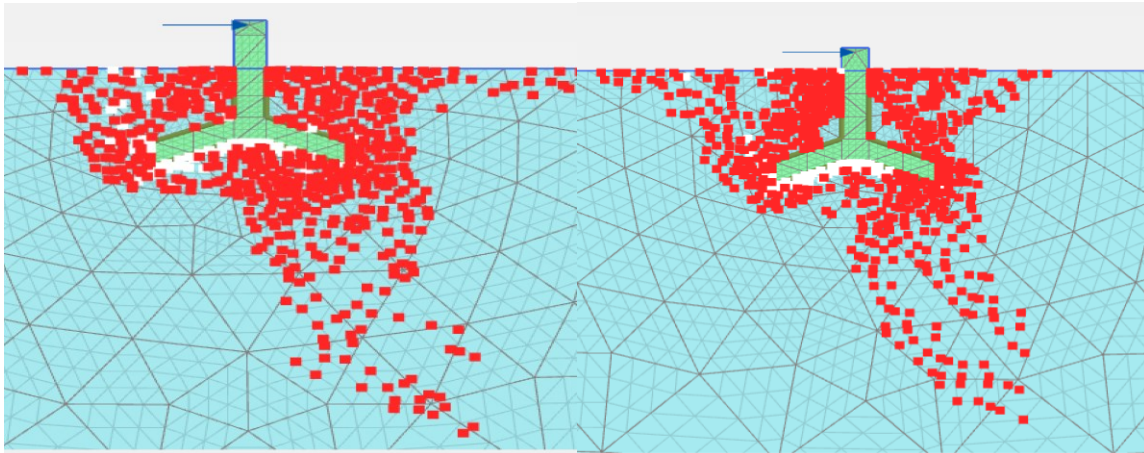


Figure 4-13. Finite Element Displacement Vectors for Flat Foundations with Various Embedment Ratio



(a) Embedment Depth is 1m

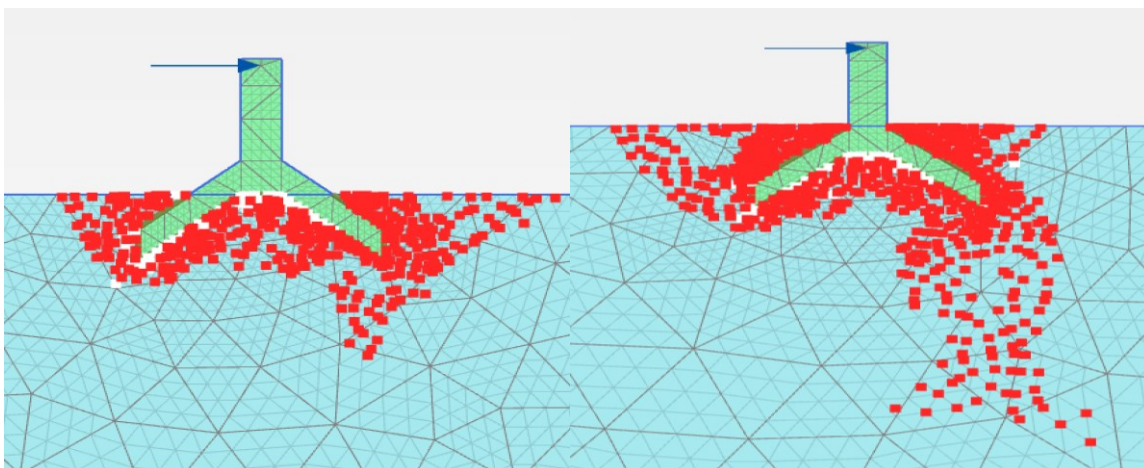
(b) Embedment Depth is 1.5m



(c) Embedment Depth is 2m

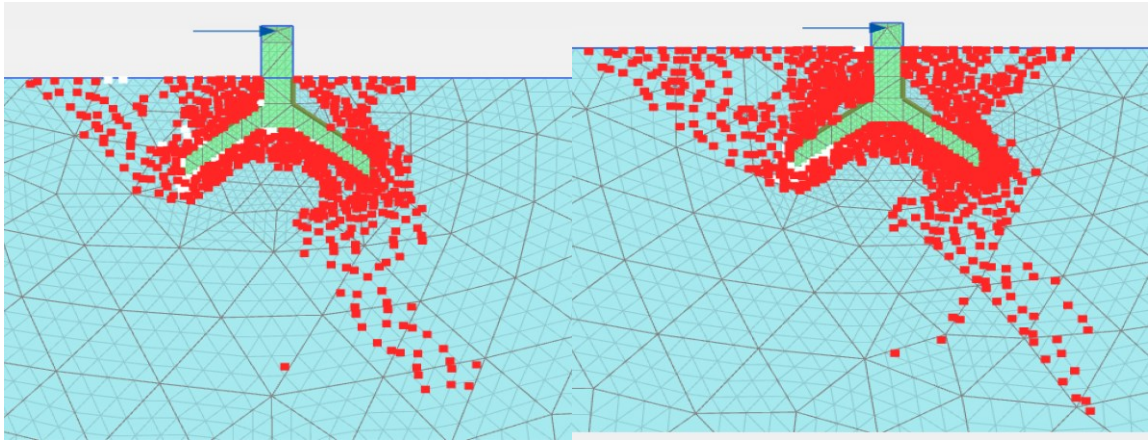
(d) Embedment Depth is 2.5m

Figure 4-14. Finite Element Displacement Vectors for 21.8° Shell Footing with Various Embedment Ratio



(a) Embedment Depth is 1m

(b) Embedment Depth is 1.5m



(c) Embedment Depth is 2m

(d) Embedment Depth is 2.5m

Figure 4-15. Finite Element Displacement Vectors for 38.66° Shell Footing with Various Embedment Ratio

CHAPTER 5

Conclusion and Discussion

5.1 Conclusions

The lateral force resistance for shell foundation with diverse shell geometry and embedment depths in sand was investigated and compared with its counterpart the flat one. In general shell footings resist higher lateral load as compare to the conventional footings in terms of resisting sliding and overturning moment. The following was concluded:

1. Shell foundations are superior to resist sliding than that of flat foundations. Besides the resistance varies with the shell shape (pyramidal and conical shell footings), shell angle and embedment ratio.
2. For surface footing, for a shell angle increase by one degree, the total friction resistance for strip, pyramidal, and conical will increase by approximately 1.4% to 2.6%, 1% to 2.1%, and 1.9% to 2.9%, respectively.
3. For embedment foundation, increasing the shell angle by one degree, will increase the rate of the friction resistance due to passive pressure decreases from a maximum of 2% to near 0%.
4. The embedment ratio has a significant effect on the friction resistance of shell foundations. For a shell foundation with a shell angle of 10 degrees, if the embedment ratio increases from 7/30 to 1/3, the friction resistance due to the passive pressure increases by about 44%, while the total friction resistance increases by about 28%.
5. To the contrary, shell foundations are not always superior to resist overturning moment than that of flat foundations because flat foundation provide higher resistance for overturning moment, which is caused by self-weight as compared to the shell ones. For surface foundation, increasing the shell angle by one degree, the total moment resistance for strip, pyramidal, and conical will decrease by approximately 0.1% to 0.6%.

6. For embedded foundation, when shell angle increases by 10 degrees, the overturning moment resistance, due to the passive pressure, for the strip, pyramidal, and conical will increase by approximately 16% to 22%, 14% to 18%, and 14% to 18%, respectively.
7. In contrast, the moment resistance, which caused by the self-weight (including the soil above the foundation), for the strip, pyramidal, and conical by increasing the shell angle by 10 degrees, will drop by approximately 4.8% to 18.6%, 5.1% to 11.4%, and 4.9% to 12.8%, respectively. Therefore, the total moment resistance will increase as the rise of the shell angle in this case.
8. Nevertheless, these rates of the increase of the moment resistance (caused by passive pressure) and the rates of decrease of the moment resistance (caused by the self-weight and the soil weight above the foundation) varies with the increase of shell angle. Therefore, the total moment resistance may decrease or increase as the rise of the shell angle, depending on the embedment ratio.
9. For embedment ratio less than $11/30$, the total overturning moment is inversely proportional to the rise of shell angles. However, if embedment ratio reaches $13/15$, the total moment resistance rises with the increment of shell angle initially, but it drops again after the angle reaches 50 degrees.
10. For embedment ratio of the strip shell, conical and pyramid shapes foundations reach $11/15$, $5/6$, and $14/15$ respectively, then the total moment resistance is greater than the flat foundation.
11. For a shell foundation with a shell angle of 10 degrees, when the embedment ratio increases from $7/30$ to $1/3$, the moment resistance caused by passive pressure increases by about 61%, while the total moment resistance increases by about 26%.
12. Conical shell foundation has lower friction resistance than the pyramidal shell foundation for shell angle less than 30 degrees. But when shell angle reaches to certain degrees, conical shell foundation provided higher friction resistance than the pyramidal

shell foundation.

13. The numerical model developed herein using the elastic perfectly plastic soil model of Mohr-Coulomb's yield criterion was capable to produce realistic representation of the behavior of cohesionless soil.
14. Numerical models in general and in particular for the present case provide an economical alternative to field data. The comparison of the lateral resistance between the 2-D numerical results with the analytical models showed good agreement. The difference is in the range of 0.86% to 13.64%.
15. In analyzing shell and conventional foundation cases subjected to vertical and horizontal loading, shell foundation will be more efficient to withstand lateral force as compared to the conventional foundation.
16. Based on the results obtained in this investigation, shell foundations will provide higher resistance to seismic and earthquake condition as compared to its counterpart the flat one.
17. Shell foundation should be superior to resist dynamic lateral force, such as wind and seismic loading.

5.2 Recommendation

In order to enhance the knowledge of the anti-lateral loading performance of shell foundations, future research should be directed to the following:

1. In this study, the lateral force resistance for strip shell footing was only considered in y axis direction. If the lateral force applies on x axis direction, it may have much lower lateral force resistance.
2. Study other shapes of shell foundations which may provide a better lateral resistance.
3. Examine and develop the theoretical models or empirical formulas when shell foundation is resisting dynamic lateral force, such as wind and earthquakes loading.

4. Simulate the preformation of shell foundation in resisting static and dynamic lateral force in 3-D condition.
5. Full scale testing and field data are needed to validate further the theories developed.

Reference

1. Abdel-Rahman, M. M. & Hanna, A. M., (2003). Contact Pressure Distribution under Shell Foundations. Proceedings of the 10th International Colloquium for Structural and Geotechnical Engineering, Faculty of Engineering, Ain Shams University, 22-25 April 2003, CAIRO, Egypt, Paper No. F03GE22.
2. Aziz, R. J., Al-Azzwai, A. A. & Al-Ani, A. A., (2011). Finite Element Elastic Analysis of Hypar Shells on Winkler Foundation. *Journal of the Serbian Society for Computational Mechanics*, Vol 5, pp.1-18. Retrieved 11 October 2020.
3. Azzam, W. & Nasr, A. M. A. (2015). Bearing Capacity of Shell Strip Footing on Reinforced Sand. *Journal of Advanced Research*, 6(5), 727-737.
<https://doi.org/10.1016/j.jare.2014.04.003>
4. Bohnhoff, D. R. (2015). Lateral Strength and Stiffness of Post and Pier Foundations. ASABE. Retrieved 12 October 2020, From. <https://www.nfba.org/view/download.php/resources/technical/lateral-strength-and-stiffness-of-post--pier-foundations>
5. Bolton, M. D. (1986). The Strength and Dilatancy of Sands. *Geotechnique* 36(1):65–78
6. Brinkgreeve, R. B. J. & Shen, R. F. (2011). Structural Elements & Modelling Excavations in PLAXIS, Power Point Presentation File, DELF, the Netherlands.
7. Chekol, E. T. (2009). A Study on the Design and Advantage of Conical Type Shell Foundation Using Analytical and FEM. [Online] Semantic Scholar.org. Available at: <<https://www.semanticscholar.org/paper/A-Study-on-the-Design-and-Advantage-of-Conical-Type-Taye/a178a4c621a6aac623d1836ed44ac259ad2c87b6>> [Accessed 20 November 2020].
8. Clough, G. W. & Duncan, J. M. (1991) “Earth Pressures”. In: Foundation Engineering Handbook

9. Das, B. (2007). *Principles of Foundation Engineering* (6th ed.), Chapter 8: Retaining Wall, pp. 358.
10. Das, B. (2007). *Principles of Foundation Engineering* (6th ed.), Chapter 8: Retaining Wall, pp. 359.
11. Esmaili, D. & Hataf, N. (2008). Experimental and Numerical Investigation of Ultimate Load Capacity of Shell Foundations on Reinforced and Unreinforced Sand. *Iranian Journal of Science & Technology, Transaction B, Engineering, Vol. 32*(No. B5), 491-500. Retrieved 12 October 2020.
12. Fattah, M. Y., Waryosh, W. A. & Al-Hamdani, M. A. E., (2015). Investigation on the Behavior of Conical Shell Foundations Composed of Reactive Powder Concrete Embedded on Sandy Soil. *Advances in Structural Engineering, 18*(11), 1859-1873. <https://doi.org/10.1260/1369-4332.18.11.1859>
13. Fattah, M. Y., Waryosh, W. A. & Al-Hamdani, M. A. E. (2015). Experimental and Theoretical Study on Bearing Capacity of Conical Shell Foundations Composed of Reactive Powder Concrete. *ACTA Geodynamica et Geomaterialia*, 411-426. <https://doi.org/10.13168/agg.2015.0037>
14. Gadre, A., & Dobry, R. (1998). Lateral Cyclic Loading Centrifuge Tests on Square Embedded Footing. *Journal of Geotechnical and Geoenvironmental Engineering*. Retrieved 30 November 2020.
15. Gouwt, T. L. (2014). Common Mistakes on the Application of PLAXIS 2D in Analyzing Excavation Problems. *International Journal of Applied Engineering Research*, 9(21), pp.8291-8311.
16. Hanna, A. M. & Abdel-Rahman, M. M., (1998). Experimental Investigation of Shell Foundations on Dry Sand. *Canadian Geotechnical Journal, 35*(5), 847-857. <https://doi.org/10.1139/t98-049>
17. Hanna, A. M. & El-Rahman, M. A. (1990). Ultimate Bearing Capacity of Triangular Shell Strip Footings on Sand. *Journal of Geotechnical Engineering, 116*(12), 1851-1863. [https://doi.org/10.1061/\(asce\)0733-9410\(1990\)116:12\(1851\)](https://doi.org/10.1061/(asce)0733-9410(1990)116:12(1851))

18. Hassan, S. A., Al-Soud, M. S. & Mohammed, S. A. (2018). Behavior of Pyramidal Shell Foundations on Reinforced Sandy Soil. *Geotechnical and Geological Engineering*, 37(4), 2437-2452. <https://doi.org/10.1007/s10706-018-00767-z>
19. Huat, B. B. K. & Mohammed, T. A. (2006). Finite Element Study Using FEM Code (PLAXIS) on the Geotechnical Behavior of Shell Footings. *Journal of Computer Science*, 2(1), pp.104-108.
20. Krishnan A. V., Sivapriya S. V. & Nagarajan, V. (2017). Finite Element Analysis of Hyper Shell Footings with Variation in Edge Beam Dimensions and Embedment Ratio. *International Journal of Earth Sciences and Engineering*, 10(02), pp.150-154.
21. Lee, J. K., Jeong, S. & Lee, S. (2016). Undrained Bearing Capacity Factors for Ring Footings in Heterogeneous Soil. *Computers and Geotechnics*, 75.
22. Luebkehan, C. H. and Peting, D. Lecture 18: Lateral Load, Copyright © 1995,1996, Available at, http://web.mit.edu/4.441/1_lectures/1_lecture18/1_lecture18.html (Retrieved 11 October 2020).
23. McManus, K. J. & Burdon, N. R. R. (2001). Lateral Resistance of Shallow Foundations. *NZSEE Conferences*. Retrieved 11 October 2020.
24. Minami, J. K. (n.d.). Shell Type Foundation Construction for Earthquake Resistance.
25. Mohammed, M. F., Singh, B. K. & Pandey, V. K. (2018). Structural Efficiency and Economy of Shells Foundations. *International Journal of Trend in Scientific Research and Development*, Volume-2(issue-3), pp.2125-2129.
26. Ntritsos, N., Anastasopoulos, I. & Gazetas, G., 2015. Static and Cyclic Undrained Response of Square Embedded Foundations. *Géotechnique*, 65(10), pp.805-823.
27. Rinaldi, R., Abdel-Rahman, M. & Hanna, A. M. (2017). Experimental Investigation on Shell Footing Models Employing High-Performance Concrete. *Sustainable Civil Infrastructures*, 373–390. DOI:10.1007/978-3-319-61914-9_29

28. Shoukath, S. & Rajesh, A. K. (2017). Seismic Performance of Hyperbolic Paraboloid and Inverted Spherical Shell Foundation. *International Research Journal of Advanced Engineering and Science*, Vol 2.
29. Thilakan, S. & Naik, N. P. (2015). Geotechnical Behavior of Shell Foundations. *50th Indian Geotechnical Conference*.
30. *Unit Weights and Densities of soil, Mathalino*. Retrieved 30 November 2020, From <https://mathalino.com/reviewer/geotechnical-engineering/unit-weights-and-densities-soil>.

APPENDIX

MatLab code for Strip shell Foundation from 1 degree to 90 degree

```
% strip
clear all;
clc;
syms Pa Kp RM
a=24; % a=unit weight of concrete
s=17; % s=unit weight of soil
c=0:1*pi/180:90*pi/180; % c=the angle of shell footing
C=30*pi/180; % C=the friction angle of soil
B=3; % B=width of the foundation
D=0.5; % D=thickness of the foundation
H=3; % H=the height of the foundation
b=0.5; % b=width of the column on the foundation
height=H-(B-b)/2*tan(c)-D;
A=2.5; % A=embedded depth
Kp=(1+sin(C))/(1-sin(C)); % Kp=passive earth pressure
if A>0 & A<=D
    Pa=1/2*s*A^2*Kp*B; % Pa=friction due to earth pressure
    RM=Pa*1/3*A; % RM=moment due to earth pressure
    % for strip shell footing
    result=find(height>=0); % find value that height>0
    height(result); % 63 values of height
    tanc=(H-height(result)-D)/((B-b)/2); % 63 value of tan(c) that won't let height<0
    result1=find(tanc>0);
    tanc(result1);
    wfs=a*((B^2)*D+((H-(B-b)/2*tanc(result1)-D)*b^2));
    % weight of strip shell foundation itself
    wss=s*tanc(result1)*B*(B^2-b^2)/4; % weight of soil below the footing
    Fs=(wfs+wss)*tan(C); % friction resistance on footing base
    Fts=Fs+Pa; % total friction resistance
    Ms=wfs*B/2; % overturning moment due Weight
    Mts=Ms+RM; % total overturning moment
    % for square flat foundation
    result2=find(tanc==0);
    tanc(result2);
    wff=a*((B^2)*D+((H-(B-b)/2*tanc(result2)-D)*b^2));
    % weight of square shallow foundation itself
    wsf=s*tanc(result2)*B*(B^2-b^2); % weight of soil below the footing
    Ff=(wff+wsf)*tan(2/3*C);
    Ftf=Ff+Pa;
```

```

Mf=wff*B/2;
Mtf=Mf+RM;
fprintf('Strip Vs. Flat foundation');
fprintf('Results are arranged in sequence from 0 to 90, with an interval of 1;');
fprintf('Weight of foundation is equal to\n');
Wfooting=[wff wfs]
fprintf('Weight of soil below the footing is equal to\n');
Wsoil=[wsf wss]
fprintf('Friction resistance on footing base is equal to\n');
Fw=[Ff Fs]
fprintf('Friction resistance due to passive earth pressure is equal to\n');
disp(Pa);
fprintf('Total friction resistance is equal to\n');
Ft=[Ftf Fts]
fprintf('Overturning moment due Weight is equal to\n');
Mfooting=[Mf Ms]
fprintf('Overturning moment due to passive earth pressure is equal to\n');
disp(RM);
fprintf('Total overturning moment is equal to\n');
Mt=[Mtf Mts]
else if A>0 & A>D & A>=3
    disp('Answer incorrect, because embedded should not exceed 3m')
else if A>0 & A>D & A<3
    % for strip shell footing
    result=find(height>=0); % find value that height>0
    height(result); % 63 values of height
    tanc=(H-height(result)-D)/((B-b)/2); % 63 value of tan(c) that wont let height<0
    result1=find(tanc>0);
    tanc(result1);
    h1=(B-b)/2*tanc(result1)+D; % h1=h'
% calculate the moment & friction resistance when z>=0
z=A-h1; % z=a-h'
result2=find(z>=0); % find value that z>=0
z(result2); % 38 values of z which z>0
tancs1=(A-D-z(result2))/((B-b)/2);
% recalculate the 38 value of tan(c) that won't let z<0
Z1=(A-(B-b)/2*tancs1-D); % renamed Z1 as a-h'
H1=(B-b)/2*tancs1+D; % renamed H1 as h'
wfs1=a*((B^2)*D+((H-(B-b)/2*tancs1-D)*b^2)); % weight of strip foundation itself
wss1=s*tancs1*B*(B^2-b^2)/4; % weight of soil below the footing
wsas1=s*(((1/4*(B-b)^2)*tancs1*B)+(B^2-b^2)*Z1);

```

```

% soil above the strip shell foundation
  Msas1=wsas1*B/2; % moment due to soil above
  F11=1/2*s*Kp*b*Z1'.^2'; % friction due to earth pressure
  RM11=1/6*s*Kp*b*Z1'.^3'+1/2*s*Kp*b*(A^2*H1-2*A*H1'.^2'+H1'.^3');
% moment due to earth pressure
  F21=1/2*s*B*Kp*(2*A*H1-H1'.^2'); % friction due to earth pressure
  RM21=1/6*s*B*Kp*(3*A*H1'.^2'-2*H1'.^3'); % moment due to earth pressure
  Fs1=(wfs1+wss1+wsas1)*tan(C); % friction resistance on footing base
  F1=F11+F21; % total friction resistance due to earth pressure
  Fts1=Fs1+F11+F21; % total friction resistance
  Mfs1=wfs1*B/2; % overturning moment due Weight
  Ms1=Mfs1+Msas1; % overturning moment
  RM1=RM11+RM21; % total overturning moment due to earth pressure
  Mts1=Ms1+RM11+RM21; % total overturning moment
% calculate the moment & friction resistance when z<0
  result4=find(z<0); % find value that z<0
  z(result4); % 38 values of z which z<0
  tancs2=(A-D-z(result4))/((B-b)/2);
% recalculate the 38 value of tan(c) that won't let z<0
  wfs2=a*((B^2)*D+((H-(B-b)/2*tancs2-D)*b^2)); % weight of strip foundation itself
  wss2=s*tancs2*B*(B^2-b^2)/4; % weight of soil below the footing
  wsas2=s*B*(A-D)^2*tancs2'.^(-1)'; % soil above the strip shell foundation
  Msas2=wsas2*B/2; % moment due to soil above
  F12=1/2*s*A^2*Kp*B; % friction due to earth pressure
  RM12=F12*1/3*A; % moment due to earth pressure
  Fs2=(wfs2+wss2+wsas2)*tan(C); % friction resistance on footing base
  F2=F12; % total friction resistance due to earth pressure
  Fts2=Fs2+F12; % total friction resistance
  RM2=RM12; % total moment due to earth pressure
  Mfs2=wfs2*B/2; % overturning moment due Weight
  Ms2=Mfs2+Msas2; % overturning moment
  Mts2=Ms2+RM12; % total overturning moment
% for square flat foundation
  result6=find(tanc==0);
  tanc(result6);
  Z2=(A-(B-b)/2*tanc(result6)-D); % renamed Z2 as a-h'
  H2=(B-b)/2*tanc(result6)+D; % renamed H2 as h'
  wff=a*((B^2)*D+((H-(B-b)/2*tanc(result6)-D)*b^2));
  wsf=s*tanc(result6)*B*(B^2-b^2);
  wsaf=s*(1/4*(B-b)^2*tanc(result6)*B+(B^2-b^2)*Z2);
  Msaf=wsaf*1/2*B;

```

```

Ff1=1/2*s*Kp*b*Z2'.^2';
RMf1=1/6*s*Kp*b*Z2'.^3'+1/2*s*Kp*b*(A^2*H2-2*A*H2'.^2'+H2'.^3');
Ff2=1/2*s*B*Kp*(2*A*H2-H2'.^2');
RMf2=1/6*s*B*Kp*(3*A*H2'.^2'-2*H2'.^3');
Ff=(wff+wsf+wsaf)*tan(2/3*C);
Ftf=Ff+Ff1+Ff2;
Fft=Ff1+Ff2;
Mf=(wff+wsaf)*B/2;
RMt=RMf2+RMf1;
Mtf=Mf+RMf1+RMf2;
fprintf('Strip Vs. Flat foundation');
fprintf('Results are arranged in sequence from 0;ãto 90;ã, with an interval of 1;ã\n');
fprintf('Weight of foundation is equal to\n');
Wfooting=[wff wfs1 wfs2]
fprintf('Weight of soil below the footing is equal to\n');
Wsoil=[wsf wss1 wss2]
fprintf('Weight of soil above the footing is equal to\n');
Wsoilabove=[wsaf wsas1 wsas2]
fprintf('Friction resistance on footing base is equal to\n');
Fw=[Ff Fs1 Fs2]
fprintf('Friction resistance due to passive earth pressure is equal to\n');
Pa=[Fft F1 F2]
fprintf('Total friction resistance is equal to\n');
Ft=[Ftf Fts1 Fts2]
fprintf('Overturning moment due Weight is equal to\n');
Mfooting=[Mf Ms1 Ms2]
fprintf('Overturning moment due to passive earth pressure is equal to\n');
RM=[RMt RM1 RM2]
fprintf('Total overturning moment is equal to\n');
Mt=[Mtf Mts1 Mts2]
else
    Pa=0;
    RM=0;
    % for strip shell footing
    result=find(height>=0);           % find value that height>0
    height(result);                   % 63 values of height
    tanc=(H-height(result)-D)/((B-b)/2); % 63 value of tan(c) that won't let height<0
    result1=find(tanc>0);
    tanc(result1);
    wfs=a*((B^2)*D+((H-(B-b)/2*tanc(result1)-D)*b^2));
% weight of strip shell foundation itself

```

```

wss=s*tanc(result1)*B*(B^2-b^2)/4;    % weight of soil below the footing
Fs=(wfs+wss)*tan(C);                 % friction resistance on footing base
Fts=Fs+Pa;                           % total friction resistance
Ms=wfs*B/2;                          % overturning moment due Weight
Mts=Ms+RM;                           % total overturning moment
% for square flat foundation
result2=find(tanc==0);
tanc(result2);
wff=a*((B^2)*D+((H-(B-b)/2*tanc(result2)-D)*b^2));
wsf=s*tanc(result2)*B*(B^2-b^2);
Ff=(wff+wsf)*tan(2/3*C);
Ftf=Ff+Pa;
Mf=wff*B/2;
Mtf=Mf+RM;
fprintf('Strip Vs. Flat foundation');
fprintf('Results are arranged in sequence from 0 to 90, with an interval of 1\n');
fprintf('Weight of foundation is equal to\n');
Wfooting=[wff wfs]
fprintf('Weight of soil below the footing is equal to\n');
Wsoil=[wsf wss]
fprintf('Friction resistance on footing base is equal to\n');
Fw=[Ff Fs]
fprintf('Friction resistance due to passive earth pressure is equal to\n');
disp(Pa);
fprintf('Total friction resistance is equal to\n');
Ft=[Ftf Fts]
fprintf('Overturning moment due Weight is equal to\n');
Mfooting=[Mf Ms]
fprintf('Overturning moment due to passive earth pressure is equal to\n');
disp(RM);
fprintf('Total overturning moment is equal to\n');
Mt=[Mtf Mts]
end
    end
end
MatLab code for Pyramidal shell Foundation from 1 degree to 90 degree
% Pyramidal
clear all;
clc;
syms Pa Kp RM
a=24;                                % a=unit weight of concrete

```

```

s=17; % s=unit weight of soil
c=0:1*pi/180:90*pi/180; % c=the angle of shell footing
C=30*pi/180; % C=the friction angle of soil
B=3; % B=width of the foundation
D=0.5; % D=thickness of the foundation
H=3; % H=the height of the foundation
b=0.5; % b=width of the column on the foundation
height=H-(B-b)/2*tan(c)-D;
A=2.9; % A=embedded depth
Kp=(1+sin(C))/(1-sin(C)); % Kp=passive earth pressure
if A>0 & A<=D
    Pa=1/2*s*A^2*Kp*B; % Pa=friction due to earth pressure
    RM=Pa*1/3*A; % RM=moment due to earth pressure
    % for pyramidal shell footing
    result=find(height>=0); % find value that height>0
    height(result); % 63 values of height
    tanc=(H-height(result)-D)/((B-b)/2); % 63 value of tan(c) that wont let height<0
    result1=find(tanc>0);
    tanc(result1);
    wfp=a*((B^2)*D+((H-(B-b)/2*tanc(result1)-D)*b^2));
% weight of pyramidal shell foundation itself
    wsp=1/6*s*tanc(result1)*(B^3-b^3); % weight of soil below the footing
    Fp=(wfp+wsp)*tan(C); % friction resistance on footing base
    Ftp=Fp+Pa; % total friction resistance
    Mp=wfp*B/2; % overturning moment due Weight
    Mtp=Mp+RM; % total overturning moment
% for square flat foundation
    result2=find(tanc==0);
    tanc(result2);
    wff=a*((B^2)*D+((H-(B-b)/2*tanc(result2)-D)*b^2));
    wsf=s*tanc(result2)*B*(B^2-b^2);
    Ff=(wff+wsf)*tan(2/3*C);
    Ftf=Ff+Pa;
    Mf=wff*B/2;
    Mtf=Mf+RM;
    fprintf('Pydramidal Vs. Flat foundation');
    fprintf('Results are arranged in sequence from 0;ãto 90;ã, with an interval of 1;ã\n');
    fprintf('Weight of foundation is equal to\n');
    Wfooting=[wff wfp]
    fprintf('Weight of soil below the footing is equal to\n');
    Wsoil=[wsf wsp]

```

```

fprintf('Friction resistance on footing base is equal to\n');
Fw=[Ff Fp]
fprintf('Friction resistance due to passive earth pressure is equal to\n');
disp(Pa);
fprintf('Total friction resistance is equal to\n');
Ft=[Ftf Ftp]
fprintf('Overturning moment due Weight is equal to\n');
Mfooting=[Mf Mp]
fprintf('Overturning moment due to passive earth pressure is equal to\n');
disp(RM);
fprintf('Total overturning moment is equal to\n');
Mt=[Mtf Mtp]
else if A>0 & A>D & A>=3
    disp('Answer incorrect,because embedded should not excess 3m');
else if A>0 & A>D & A<3
% for Pydramidal shell footing
    result=find(height>=0);           % find value that height>0
    height(result);                   % 63 values of height
    tanc=(H-height(result)-D)/((B-b)/2); % 63 value of tan(c) that wont let height<0
    result1=find(tanc>0);
    tanc(result1);
    h1=(B-b)/2*tanc(result1)+D;       % h1=h'
% calculate the moment & friction resistance when z>=0
    z=A-h1;                           % z=a-h'
    result2=find(z>=0);                % find value that z>=0
    z(result2);                        % 38 values of z which z>0
    tancs1=(A-D-z(result2))/((B-b)/2);
% recalculate the 38 value of tan(c) that won't let z<0
    Z1=(A-(B-b)/2*tancs1-D);           % renamed Z1 as a-h'
    H1=(B-b)/2*tancs1+D;               % renamed H1 as h'
    wfp1=a*((B^2)*D+((H-(B-b)/2*tancs1-D)*b^2)); % weight of strip foundation itself
    wsp1=1/6*s*tancs1*(B^3-b^3);       % weight of soil below the footing
    wsap1=s*((1/6*(2*B^3-3*B^2*b+b^3)*tancs1)+(B^2-b^2)*Z1);
% soil above the strip shell foundation
    Msap1=wsap1*B/2;                  % moment due to soil above
    F11=1/2*s*Kp*b*Z1'.^2;            % friction due to earth pressure
    RM11=1/6*s*Kp*b*Z1'.^3'+1/2*s*Kp*b*(A^2*H1-2*A*H1'.^2'+H1'.^3');
% moment due to earth pressure
    F21=1/4*s*(B+b)*Kp*(2*A*H1-H1'.^2'); % friction due to earth pressure
    RM21=1/12*s*(B+b)*Kp*(3*A*H1'.^2'-2*H1'.^3'); % moment due to earth pressure
    Fp1=(wfp1+wsp1+wsap1)*tan(C);    % friction resistance on footing base

```

```

F1=F11+F21; % total friction resistance due to earth pressure
Ftp1=Fp1+F11+F21; % total friction resistance
Mfp1=wfp1*B/2; % overturning moment due Weight
Mp1=Mfp1+Msap1; % overturning moment
RM1=RM11+RM21; % total overturning moment due to earth pressure
Mtp1=Mp1+RM11+RM21; % total overturning moment
% calculate the moment & friction resistance when z<0
result4=find(z<0); % find value that z<0
z(result4); % 38 values of z which z<0
tancs2=(A-D-z(result4))/((B-b)/2);
% recalculate the 38 value of tan(c) that won't let z<0
wfp2=a*((B^2)*D+((H-(B-b)/2*tancs2-D)*b^2)); % weight of strip foundation itself
wsp2=1/6*s*tancs2*(B^3-b^3); % weight of soil below the footing
wsap2=s^2*B*(A-D)^2*tancs2'.^(-1)-4/3*s*(A-D)^3*tancs2'.^(-2);
% soil above the strip shell foundation
Msap2=wsap2*B/2; % moment due to soil above
F12=1/2*s*A^2*Kp*(B-(A-D)*tancs2'.^(-1)); % friction due to earth pressure
RM12=F12*1/3*A; % moment due to earth pressure
Fp2=(wfp2+wsp2+wsap2)*tan(C); % friction resistance on footing base
Ftp2=Fp2+F12; % total friction resistance
F2=F12; % total friction resistance due to earth pressure
RM2=RM12; % total moment due to earth pressure
Mfp2=wfp2*B/2; % overturning moment due Weight
Mp2=Mfp2+Msap2; % overturning moment
Mtp2=Mp2+RM2; % total overturning moment
% for square flat foundation
result6=find(tanc==0);
tanc(result6);
Z2=(A-(B-b)/2*tanc(result6)-D); % renamed Z2 as a-h'
H2=(B-b)/2*tanc(result6)+D; % renamed H2 as h'
wff=a*((B^2)*D+((H-(B-b)/2*tanc(result6)-D)*b^2));
wsf=s*tanc(result6)*B*(B^2-b^2);
wsaf=s*(1/4*(B-b)^2*tanc(result6)*B+(B^2-b^2)*Z2);
Msaf=wsaf*1/2*B;
Ff1=1/2*s*Kp*b*Z2'.^2';
RMf1=1/6*s*Kp*b*Z2'.^3'+1/2*s*Kp*b*(A^2*H2-2*A*H2'.^2'+H2'.^3');
Ff2=1/2*s*B*Kp*(2*A*H2-H2'.^2');
RMf2=1/6*s*B*Kp*(3*A*H2'.^2'-2*H2'.^3');
Ff=(wff+wsf+wsaf)*tan(2/3*C);
Fft=Ff1+Ff2;
Ftf=Ff+Ff1+Ff2;

```

```

Mf=(wff+wsaf)*B/2;
RMt=RMf1+RMf2;
Mtf=Mf+RMf1+RMf2;
fprintf('Pyramidal Vs. Flat foundation');
fprintf('Results are arranged in sequence from 0;ãto 90;ã, with an interval of 1;ã\n');
fprintf('Weight of foundation is equal to\n');
Wfooting=[wff wfp1 wfp2]
fprintf('Weight of soil below the footing is equal to\n');
Wsoil=[wsf wsp1 wsp2]
fprintf('Weight of soil above the footing is equal to\n');
Wsoilabove=[wsaf wsap1 wsap2]
fprintf('Friction resistance on footing base is equal to\n');
Fw=[Ff Fp1 Fp2]
fprintf('Friction resistance due to passive earth pressure is equal to\n');
Pa=[Fft F1 F2]
fprintf('Total friction resistance is equal to\n');
Ft=[Ftf Ftp1 Ftp2]
fprintf('Overturning moment due Weight is equal to\n');
Mfooting=[Mf Mp1 Mp2]
fprintf('Overturning moment due to passive earth pressure is equal to\n');
RM=[RMt RM1 RM2]
fprintf('Total overturning moment is equal to\n');
Mt=[Mtf Mtp1 Mtp2]
else
    Pa=0;
    RM=0;
    % for pyramidal shell footing
    result=find(height>=0);          % find value that height>0
    height(result);                 % 63 values of height
    tanc=(H-height(result)-D)/((B-b)/2); % 63 value of tan(c) that wont let height<0
    result1=find(tanc>0);
    tanc(result1);
    wfp=a*((B^2)*D+((H-(B-b)/2*tanc(result1)-D)*b^2));
    % weight of pyramidal shell foundation itself
    wsp=1/6*s*tanc(result1)*(B^3-b^3); % weight of soil below the footing
    Fp=(wfp+wsp)*tan(C);             % friction resistance on footing base
    Ftp=Fp+Pa;                       % total friction resistance
    Mp=wfp*B/2;                      % overturning moment due Weight
    Mtp=Mp+RM;                       % total overturning moment
    % for square flat foundation
    result2=find(tanc==0);

```

```

tanc(result2);
wff=a*((B^2)*D+((H-(B-b)/2*tanc(result2)-D)*b^2));
wsf=s*tanc(result2)*B*(B^2-b^2);
Ff=(wff+wsf)*tan(2/3*C);
Ftf=Ff+Pa;
Mf=wff*B/2;
Mtf=Mf+RM;
fprintf('Pyramidal Vs. Flat foundation');
fprintf('Results are arranged in sequence from 0 to 90, with an interval of 1;');
fprintf('Weight of foundation is equal to\n');
Wfooting=[wff wfp]
fprintf('Weight of soil below the footing is equal to\n');
Wsoil=[wsf wsp]
fprintf('Friction resistance on footing base is equal to\n');
Fw=[Ff Fp]
fprintf('Friction resistance due to passive earth pressure is equal to\n');
disp(Pa);
fprintf('Total friction resistance is equal to\n');
Ft=[Ftf Ftp]
fprintf('Overturning moment due Weight is equal to\n');
Mfooting=[Mf Mp]
fprintf('Overturning moment due to passive earth pressure is equal to\n');
disp(RM);
fprintf('Total overturning moment is equal to\n');
Mt=[Mtf Mtp]
end
end
end

```

MatLab code for Conical shell Foundation from 1 degree to 90 degree

```

% Conical
clear all;
clc;
syms Pa Kp RM
a=24; % a=unit weight of concrete
s=17; % s=unit weight of soil
c=0:1*pi/180:90*pi/180; % c=the angle of shell footing
C=30*pi/180; % C=the friction angle of soil
B=3; % B=width of the foundation
D=0.5; % D=thickness of the foundation
H=3; % H=the height of the foundation
b=0.5; % b=width of the column on the foundation

```

```

height=H-(B-b)/2*tan(c)-D;
A=2.5; % A=embedded depth
Kp=(1+sin(C))/(1-sin(C)); % Kp=passive earth pressure
if A>0 & A<=D
    Pa=1/2*s*A^2*Kp*B; % Pa=friction due to earth pressure
    RM=Pa*1/3*A; % RM=moment due to earth pressure
% for conical shell footing
result=find(height>=0); % find value that height>0
height(result); % 63 values of height
tanc=(H-height(result)-D)/((B-b)/2); % 63 value of tan(c) that wont let height<0
result1=find(tanc>0);
tanc(result1);
wfc=1/4*a*pi*((B^2)*D+((H-(B-b)/2*tanc(result1)-D)*b^2));
% weight of conical foundation itself
wsc=1/12*s*pi*tanc(result1)*(B^3-b^3); % weight of soil below the footing
Fc=(wfc+wsc)*tan(C); % friction resistance on footing base
Ftc=Fc+Pa; % total friction resistance
Mc=wfc*B/2; % overturning moment due Weight
Mtc=Mc+RM; % total overturning moment
% for circular flat foundation
result2=find(tanc==0);
tanc(result2);
wff=1/4*a*pi*((B^2)*D+((H-(B-b)/2*tanc(result2)-D)*b^2));
wsf=1/12*s*pi*tanc(result2)*(B^3-b^3);
Ff=(wff+wsf)*tan(2/3*C);
Ftf=Ff+Pa;
Mf=wff*B/2;
Mtf=Mf+RM;
fprintf('Conical Vs. Flat foundation');
fprintf('Results are arranged in sequence from 0;ãto 90;ã, with an interval of 1;ã\n');
fprintf('Weight of foundation is equal to\n');
Wfooting=[wff wfc]
fprintf('Weight of soil below the footing is equal to\n');
Wsoil=[wsf wsc]
fprintf('Friction resistance on footing base is equal to\n');
Fw=[Ff Fc]
fprintf('Friction resistance due to passive earth pressure is equal to\n');
disp(Pa);
fprintf('Total friction resistance is equal to\n');
Ft=[Ftf Ftc]
fprintf('Overturning moment due Weight is equal to\n');

```

```

Mfooting=[Mf Mc]
fprintf('Overturning moment due to passive earth pressure is equal to\n');
disp(RM);
fprintf('Total overturning moment is equal to\n');
Mt=[Mtf Mtc]
else if A>0 & A>D & A<3
% for conical shell footing
result=find(height>=0);           % find value that height>0
height(result);                   % 63 values of height
tanc=(H-height(result)-D)/((B-b)/2); % 63 value of tan(c) that won't let height<0
result1=find(tanc>0);
tanc(result1);
h1=(B-b)/2*tanc(result1)+D;       % h1=h'
% calculate the moment & friction resistance when z>=0
z=A-h1;                           % z=a-h'
result2=find(z>=0);               % find value that z>=0
z(result2);                       % 38 values of z which z>0
tancc1=(A-D-z(result2))/((B-b)/2);
% recalculate the 38 value of tan(c) that won't let z<0
wfc1=1/4*a*pi*((B^2)*D+((H-(B-b)/2*tancc1-D)*b^2));
% weight of conical foundation itself
wsc1=1/12*s*pi*tancc1*(B^3-b^3); % weight of soil below the footing
wsac1=1/12*s*pi*(((B-b)/2)*tancc1)*(2*B^2-B*b-b^2)+1/4*s*pi*(A-(B-
b)/2*tancc1-D)*(B^2-b^2);        % soil above the conical shell foundation
Msac1=wsac1*B/2;                 % moment due to soil above
Z1=(A-(B-b)/2*tancc1-D);         % renamed Z1 as a-h'
H1=(B-b)/2*tancc1+D;            % renamed H1 as h'
F11=1/2*s*Kp*b*Z1.^2;           % friction due to earth pressure
RM11=1/6*s*Kp*b*Z1.^3+1/2*s*Kp*b*(A^2*H1-2*A*H1.^2+H1.^3);
% momnet due to earth pressure
F21=1/4*s*(B+b)*Kp*(2*A*H1-H1.^2); % friction due to earth pressure
RM21=1/12*s*(B+b)*Kp*(3*A*H1.^2-2*H1.^3); % moment due to earth pressure
Fc1=(wfc1+wsc1+wsac1)*tan(C);   % friction resistance on footing base
F1=F11+F21;                      % total friction resistance due to earth pressure
Ftc1=Fc1+F11+F21;               % total friction resistance
Mfc1=wfc1*B/2;                  % overturning moment due Weight
Mc1=Mfc1+Msac1;                 % overturning moment
RM1=RM11+RM21;                  % total overturning moment due to earth pressure
Mtc1=Mc1+RM11+RM21;            % total overturning moment
% caluculate the moment & friction resistance when z>=0
result4=find(z<0);              % find value that z<0

```

```

z(result4); % 38 values of z which z<0
tancc2=(A-D-z(result4))/((B-b)/2);
% recalculate the 38 value of tan(c) that won't let z<0
wfc2=1/4*a*pi*((B^2)*D+((H-(B-b)/2*tancc2-D)*b^2));
% weight of conical foundation itself
wsc2=1/12*s*pi*tancc2*(B^3-b^3); % weight of soil below the footing
wsac2=(1/2*s*pi*B*((A-D)^2*tancc2'.^(-1))-(1/3*s*pi*((A-D)^3)*tancc2'.^(-2)));
% soil above the conical shell foundation
Msac2=wsac2*B/2; % moment due to soil above
F12=1/2*s*A^2*Kp*(B-(A-D)*tancc2'.^(-1)); % friction due to earth pressure
RM12=F12*1/3*A; % moment due to earth pressure
Fc2=(wfc2+wsc2+wsac2)*tan(C); % friction resistance on footing base
F2=F12; % total friction resistance due to earth pressure
Ftc2=Fc2+F12; % total friction resistance
RM2=RM12; % total moment due to earth pressure
Mfc2=wfc2*B/2; % overturning moment due Weight
Mc2=Mfc2+Msac2; % overturning moment
Mtc2=Mc2+RM12; % total overturning moment
% for circular flat foundation
result6=find(tanc==0);
tanc(result6);
wff=1/4*a*pi*((B^2)*D+((H-(B-b)/2*tanc(result6)-D)*b^2));
wsf=1/12*s*pi*tanc(result6)*(B^3-b^3);
wsaf=1/4*s*pi*(B^2-b^2)*(A-D);
Msaf=wsaf*1/2*B;
Ff1=1/2*s*(A-D)^2*Kp*b;
RMf1=Ff1*(D+(A-D)/3);
Ff2=1/2*s*Kp*D*B*(2*A-D);
RMf2=1/6*s*Kp*B*D^2*(3*A-2*D);
Ff=(wff+wsf+wsaf)*tan(2/3*C);
Ftf=Ff+Ff1+Ff2;
Fft=Ff1+Ff2;
Mf=(wff+wsaf)*B/2;
RMt=RMf2+RMf1;
Mtf=Mf+RMf1+RMf2;
fprintf('Conical Vs. Flat foundation');
fprintf('Results are arranged in sequence from 0;ãto 90;ã, with an interval of 1;ã\n');
fprintf('Weight of foundation is equal to\n');
Wfooting=[wff wfc1 wfc2]
fprintf('Weight of soil below the footing is equal to\n');
Wsoil=[wsf wsc1 wsc2]

```

```

fprintf('Weight of soil above the footing is equal to\n');
Wsoilabove=[wsaf wsac1 wsac2]
fprintf('Friction resistance on footing base is equal to\n');
Fw=[Ff Fc1 Fc2]
fprintf('Friction resistance due to passive earth pressure is equal to\n');
Pa=[Fft F1 F2]
fprintf('Total friction resistance is equal to\n');
Ft=[Ftf Ftc1 Ftc2]
fprintf('Overturning moment due Weight is equal to\n');
Mfooting=[Mf Mc1 Mc2]
fprintf('Overturning moment due to passive earth pressure is equal to\n');
RM=[RMt RM1 RM2]
fprintf('Total overturning moment is equal to\n');
Mt=[Mtf Mtc1 Mtc2]
else if A>0 & A>D & A>=3
    disp('Answer incorrect,because embedded should not excess 3m')
else
    Pa=0;
    RM=0;
    % for conical shell footing
    result=find(height>=0); % find value that height>0
    height(result); % 63 values of height
    tanc=(H-height(result)-D)/((B-b)/2); % 63 value of tan(c) that won't let height<0
    result1=find(tanc>0);
    tanc(result1);
    wfc=1/4*a*pi*((B^2)*D+((H-(B-b)/2*tanc(result1)-D)*b^2));
    % weight of conical foundation itself
    wsc=1/12*s*pi*tanc(result1)*(B^3-b^3); % weight of soil below the footing
    Fc=(wfc+wsc)*tan(C); % friction resistance on footing base
    Ftc=Fc+Pa; % total friction resistance
    Mc=wfc*B/2; % overturning moment due Weight
    Mtc=Mc+RM; % total overturning moment
% for circular flat foundation
result2=find(tanc==0);
tanc(result2);
wff=1/4*a*pi*((B^2)*D+((H-(B-b)/2*tanc(result2)-D)*b^2));
wsf=1/12*s*pi*tanc(result2)*(B^3-b^3);
Ff=(wff+wsf)*tan(2/3*C);
Ftf=Ff+Pa;
Mf=wff*B/2;
Mtf=Mf+RM;

```

```

fprintf('Conical Vs. Flat foundation');
fprintf('Results are arranged in sequence from 0 to 90, with an interval of 15');
fprintf('Weight of foundation is equal to\n');
Wfooting=[wff wfc]
fprintf('Weight of soil below the footing is equal to\n');
Wsoil=[wsf wsc]
fprintf('Friction resistance on footing base is equal to\n');
Fw=[Ff Fc]
fprintf('Friction resistance due to passive earth pressure is equal to\n');
disp(Pa);
fprintf('Total friction resistance is equal to\n');
Ft=[Ftf Ftc]
fprintf('Overturning moment due Weight is equal to\n');
Mfooting=[Mf Mc]
fprintf('Overturning moment due to passive earth pressure is equal to\n');
disp(RM);
fprintf('Total overturning moment is equal to\n');
Mt=[Mtf Mtc]
end
end
end

```